NASA-CR-159215
19800024984

NASA CONTRACTOR REPORT 159215

CARBON FIBER PLUME SAMPLING FOR LARGE-SCALE FIRE TESTS AT DUGWAY PROVING GROUND

A. R. Chovit, P. Lieberman,
D. E. Freeman, W. C. Beggs,
and W. A. Millavec

TRW DEFENSE AND SPACE SYSTEMS GROUP
Redondo Beach, CA 90278

CONTRACT NAS 1-15465
March 1980

NASA
National Aeronautics and
Space Administration

Langley Research Center
Hampton, Virginia 23665

CONTENTS

TABLES

TABLES

FIGURES

FIGURES

FIGURES

CARBON FIBER PLUME SAMPLING FOR LARGE-SCALE FIRE TESTS AT DUGWAY PROVING GROUND

Albert R. Chovit, Paul Lieberman, Donald E. Freeman,
William C. Beggs and William A. Millavec

TRW Defense and Space Systems Group

SUMMARY

As a participant in the NASA-sponsored large-scale fire tests at Dugway Proving Ground, TRW developed and fielded two types of carbon fiber sampling instruments. These were first, passive collectors made of sticky bridal veil mesh, and second, active instruments using a light-emitting diode (LED) source. Both of these fiber collecting or sensing instruments measured the number or number-rate of carbon fibers released from carbon/graphite composite material when the material was burned in a 10.7 m (35-ft) dia JP-4 pool fire for approximately 20 minutes.

Both types of instruments were placed in an array suspended from a 305 m (1000 ft) by 305 m (1000 ft) "Jacob's Ladder" net held vertically aloft by balloons and oriented cross-wind approximately 140 metres downwind of the pool fire. The "Jacob's Ladder" was also developed, fabricated, installed, and operated by TRW as part of this program.

The LED fiber detectors were first checked out and calibrated at NSWC in a series of tests in the "shock tube" facility. Three large-scale tests were conducted at Dugway Proving Ground during October and November 1979 during which released carbon fiber data was acquired. These data were subsequently reduced and analyzed to obtain the characteristics of the released fibers including their spatial and size distributions and estimates of the number and total mass of fibers released.

The results of the data analyses showed that 2.5 to 3.5 x 10^8 single carbon fibers were released during the 20-minute burn of 30 to 50 kg mass of initial, unburned carbon fiber material. The mass released as single carbon fibers was estimated to be between 0.1 and 0.2% of the initial, unburned fiber mass. The average length of the released fibers was approximately 3.2 mm. Excellent correlation of the results was obtained among all three tests.

1. INTRODUCTION

The potential advantages of carbon/graphite fiber-reinforced composite material for aircraft parts has led to an increasing use of this material for commercial aircraft. However, it has been recognized that the accidental crash of an aircraft containing carbon/graphite composite materials followed by a fire results in the release of carbon fibers in the smoke plume. These carbon fibers are electrically conductive, transport downward and downwind with the plume, can penetrate facilities and equipment, and can degrade circuit performance if they come to rest on critical portions of a circuit. When the fiber bridges two points in a circuit that has a voltage difference between the two points, logic upset and/or circuit burnout becomes possible. This potentially hazardous phenomenon has spurred an ongoing investigative program into the problem of such aircraft crashes and subsequent fires.

Consequently, during the months of October and November 1979, NASA conducted a series of field tests at Dugway Proving Ground (ref. 1) to simulate, with a controlled JP fuel fire, the accidental burning of aircraft parts that are constructed of fiber-reinforced carbon/graphite composites. The main test objective was to systematically collect or sense the released fibers in the immediate vicinity of the fire and downwind. The data yielded by the tests were to be reduced and analyzed for information on the fraction of carbon fiber released, the physical characteristics of the fibers, the transport phenomenology, and the downwind fiber-dispersion characteristics.

As a participant in the program, TRW was asked to develop, field, and operate two types of fiber-collecting or -sensing instruments. The first type was a passive collector made by fastening bridal veil netting on a standard vugraph frame. Before a test, a sticky adhesive was sprayed on the bridal veil. For each test, a large number of these vugraphs was attached approximately every 15 m (50-ft) on a "Jacob's Ladder" net held vertically aloft by balloons, and oriented cross-wind approximately 140 metres downwind of the pool fire. As the released fibers were transported downwind to the net by ambient wind currents, the airborne fibers were intercepted and collected on the vugraphs, thus producing a permanent record of the total fiber exposure at each vugraph location.

The second type of instrumentation was a detector with a light-emitting diode source. This active sensor instrument measures a number-rate of particles passing through a light beam and causing a shadow on a detector. This number-rate can be converted to fiber concentration by introducing the wind velocity and LED beam dimensions. Four of these LED instruments were used on three tests of the series. Two of the instruments were newly developed, flight weight, airborne instruments that were attached to and lofted by the Jacob's Ladder; and two were ground-based instruments developed proviously for similar Air Force field tests and located at ground level under the Jacob's Ladder.

The extent of the TRW assistance in these field test experiments included the design, development, fabrication, field installation, and operation of the Jacob's Ladder; the provision and fielding of the passive vugraph fiber

collectors; the design, development, and fabrication of the airborne LED instruments; the fielding and operation of the four active LED instruments; and the reduction, analysis, and evaluation of the data obtained from both the passive collectors and the active instrumentation for each of the three tests in which this instrumentation was used.

This report, which describes the TRW test activity, has been organized so that the reader can focus directly on any of three primary areas of information: (1) the design, development, and operation of the test equipment, (2) the operational conditions and layout of the test equipment in the field environments, and (3) the results of the data analyses and evaluations. Thus, in reverse order, Section 5 presents a comprehensive discussion and graphic representation of the results obtained from the reduction, analysis, and evaluation of the collected data including descriptions of the data reduction techniques that may influence the interpretation or use of the results. Section 4 lists the ambient and controlled test conditions and the physical layouts of the instrumentation and equipment for each of the tests, as well as other test observations and operational conditions that are pertinent to the reduction and analysis of the acquired data. Section 3 documents the details of the design, development, and operation of the Jacob's Ladder and airborne LED instruments, and supplies background information for the vugraph collectors and ground-based LED instruments.

Section 2 lists the symbols and abbreviations used in this report.

Section 6 restates concisely the major findings of the investigations. These are concerned principally with the results obtained from the data analyses and evaluations. Appendixes B and C contain the fabrication and operational procedures and plans that were developed for the Jacob's Ladder. Appendix A summarizes the results of the static load analysis performed for wind velocities from 0 to 10 m/s (0 to 22.5 miles/hour).

The use of specific commercial products, brand name items, etc., on this program or mention of these items in this document does not imply an endorsement of these products by NASA.

2. SYMBOLS AND UNITS

SYMBOLS

M	Fiber mass released from burned composite material
N	Number of fibers released from burned composite material
L	Average length of released single fibers
$\bar{d}$	Average fiber diameter of unburned carbon fiber material equal to 6.88×10^{-3} mm (6.88 μm)
ρ	Carbon fiber mass density equal to 1.73×10^{-3} gm/mm^3
SWL	Safe working load; maximum permissible design load

DEFINITIONS

Deposition (fluence)	Total number of fibers or clumps deposited on (or transported through) a specified area for a given duration; generally expressed as fibers per square meter
Concentration	Total number of fibers in given volume; generally expressed as fibers per cubic meter
Exposure	Deposition divided by deposition (or transport) velocity; or concentration multiplied by time; generally expressed as fiber sec per cubic meter
Factor of Safety	Ultimate breaking strength divided by safe working load (or design load)
Jacob's Ladder	Vertical cable or rope net supporting arrays of instrumentation

CONVERSIONS

1 ft	0.305 m
1 in	2.54 mm
1 lb	453.59 gm

ABBREVIATIONS

AFGL	Air Force Geophysics Laboratory, Hanscom AFB, MA
cm	centimetre
DPG	Dugway Proving Ground, UT
E	east
fps	feet per second
ft	feet
g	gram
in	inch
kg	kilogram
km	kilometre
lb	pound
LCD	liquid crystal diode
LED	light emitting diode
m	metre
MDT	Mountain Daylight Time
mm	millimetre
mps	metres per second
MST	Mountain Standard Time
NSWC	Naval Surface Weapon Center, Dahlgren, VA
NWC	Naval Weapon Center, China Lake, CA
s	seconds
T/M	telemetering
W	west
µm	micrometre

3. JACOB'S LADDER AND INSTRUMENTATION

This section describes the details of the design, development, and operation of the Jacob's Ladder and the two airborne LED instruments. Also described are the characteristics and use of the vugraph and bridal veil fiber collectors, and background information on the two ground-based LED instruments that were fielded in the three tests.

JACOB'S LADDER

DESCRIPTION

One of the objectives of the Dugway test series was to determine the characteristics of the carbon fibers released into the plume of the JP fuel fire when carbon/graphite composite material was burned in the fire. In previous field tests of this kind, instrumentation was used that sampled or collected such fire-released carbon fibers at ground level, several feet above ground level, and in one series of tests - to an altitude of approximately 30 metres. However, none of the collection techniques used provided data which sampled the carbon fibers in the total extent of the fire plume. Since the plumes from such fires rapidly reach altitudes measured in hundreds of metres, a means was required for a structure that could support instrumentation at these high altitudes in the path of the fire plume.

To meet this objective a large, balloon-lofted, rope net was constructed and deployed crosswind more than a hundred metres downwind from the test fires. This net, referred to as the "Jacob's Ladder"*, was used to loft and support both passive carbon fiber collection instruments as well as several types of active, electronic, carbon fiber sensors.

---

*

Jacob's Ladder
A ship's ladder of rope or chain with wooden or iron rungs, used for climbing from the deck to the rigging, or a European (and related American) perennial herb of the phlox family which bears bright blue or white flowers and has a stalk whose twin leaves branch horizontally at regular intervals along the stem like the rungs of a ladder. In the biblical story, Jacob, son of Isaac, dreamt of a ladder stretching from earth to heaven and filled with angels coming and going. At the top the Lord Himself sat in great glory, blessing Jacob and his descendants, who were to be in numbers "like the dust of the earth" (Genesis 28). (ref. 2)

So that the instrumentation supported on the Jacob's Ladder would intercept the full extent of the plume, the net was designed to extend to a height of 305m (1000 ft) and a crosswind width of 305 m (1000 ft). It was supported by two helium-filled balloons supplied and operated by Air Force personnel from the Air Force Geophysics Laboratory (AFGL), Hanscom AFB, Massachusetts, and the Holloman AFB, New Mexico. The net, the net tethers and the mooring lines were fabricated from Kevlar cable. In the design, the bottom of the net was anchored to deadmen located approximately 152 m (500 ft) downwind from the center of the test fire. But this dimension was revised during field installation to approximately 117 m (385 ft) to improve certain net operational conditions. A drawing of the Jacob's Ladder in the erected position is given in Figure 3.1. A measure of its size can be seen by comparison with the scaled rendering of the Empire State Building.

The 305 m by 305 m (flight dimensions) net was constructed of 21 vertical and 21 horizontal Kevlar cables of 3.3 mm (0.13-in) dia. The vertical net cables were spaced approximately 15.2 m (50-ft) apart and the horizontal cables approximately 16.8 m (55-ft) apart. When in an erected, flight condition, this spacing afforded a projected crosswind grid spacing of approximately 15.2 m by 15.2 m (50-ft by 50-ft). The vertical and horizontal cables were fastened together securely at each intersection point. The bottom of each vertical net cable was secured to a deadman while the top of each vertical was fastened to a main catenary support cable fabricated from 9.5 mm (3/8-in) dia Kevlar cable. This main catenary cable supported the weight of the net and the instrumentation suspended from the net, and it reacted the wind loads on the net.

Each end of the main catenary extends and attaches to a juncture plate. Also attached to each juncture plate is a balloon tether, through which the lift from the balloon is transmitted; a side catenary tether, which is fixed in length and attached to a deadman at its other end; a forward tether which reacts the wind loads, and is attached to a winch; an aft tether also attached to a winch, which is used to raise and lower the net; and a fixed-length, vertical, mooring line that reacts the excess balloon lift through a deadman. The side catenary and forward tethers were fabricated from 6.4 mm (1/4-in) dia Kevlar cable and the aft and balloon tethers and mooring lines were fabricated from 9.5 mm (3/8-in) dia Kevlar cable. Fastened on either side of the net were two, light 3.3 mm (0.13-in) dia side stabilization tethers to stabilize the net if oscillatory modes were induced in the net by winds. For the most part, these side stabilization tethers proved superfluous and were generally maintained in a completely slack condition. Figure 3.2 presents elevation views of the erected Jacob's Ladder system, and Figures 3.3 and 3.4 give details of the test site layout and deadman locations.

The ladder is lowered from an erected position by slackening the forward tethers and winching in the aft tethers. During this operation, the plane formed by the net, the mooring lines, and the side tethers rotates downward toward the aft winches around a ground line passing through the side catenary tether deadmen and the mooring line deadmen. This operation - slackening the forward tethers and winching in the aft tethers - is continued until the net is stretched back and is resting on a rope table and the mooring lines, and side and forward tethers are resting on the ground. The net rope table is an array of 6.4 mm (1/4-in) dia tensioned, Dacron ropes strung atop a field of 2.1 m (7-ft) high

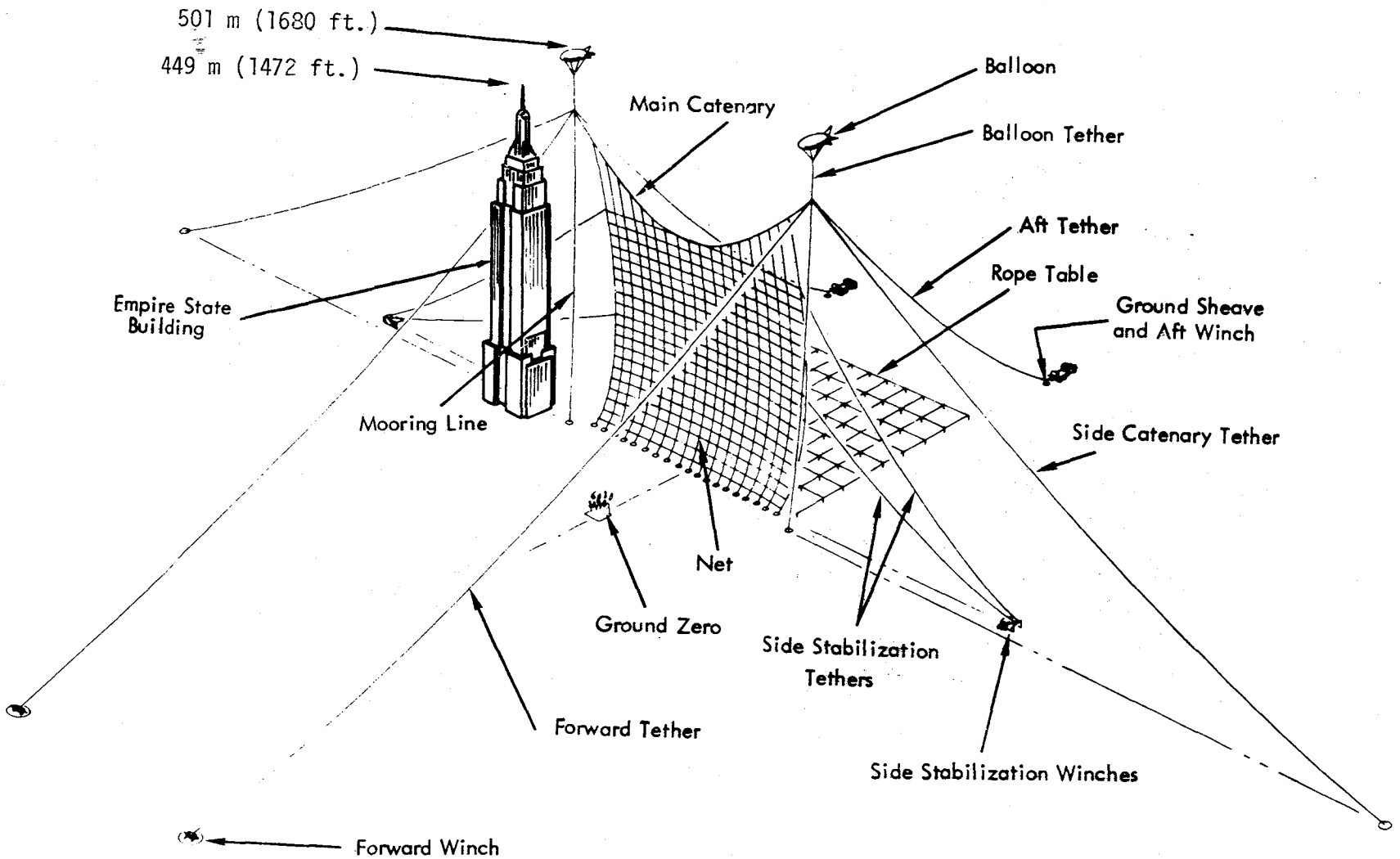

Figure 3.1 Jacob's Ladder in Erected Position
Initial Design Configuration

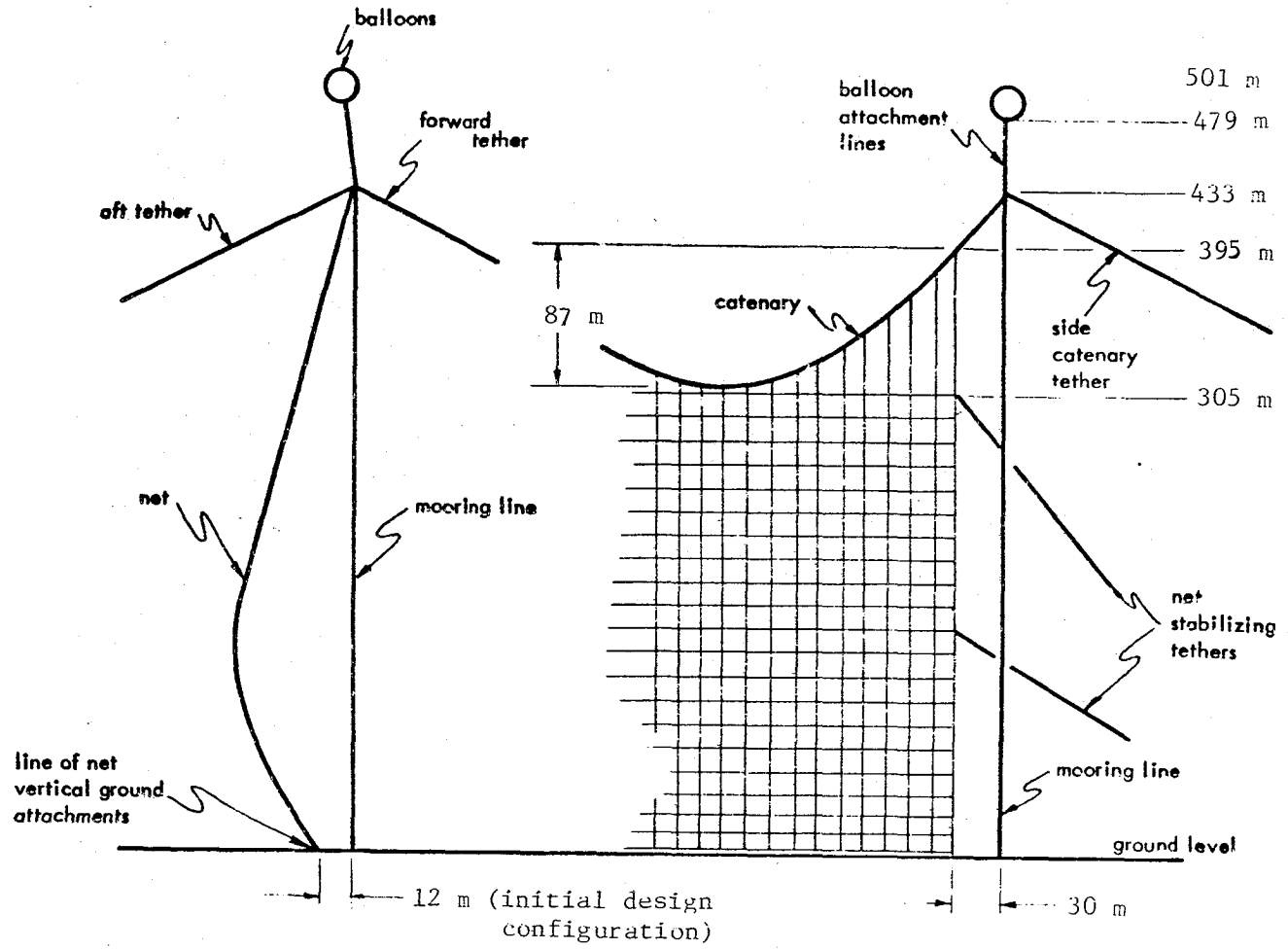

Figure 3.2 Jacob's Ladder System - Elevation Views

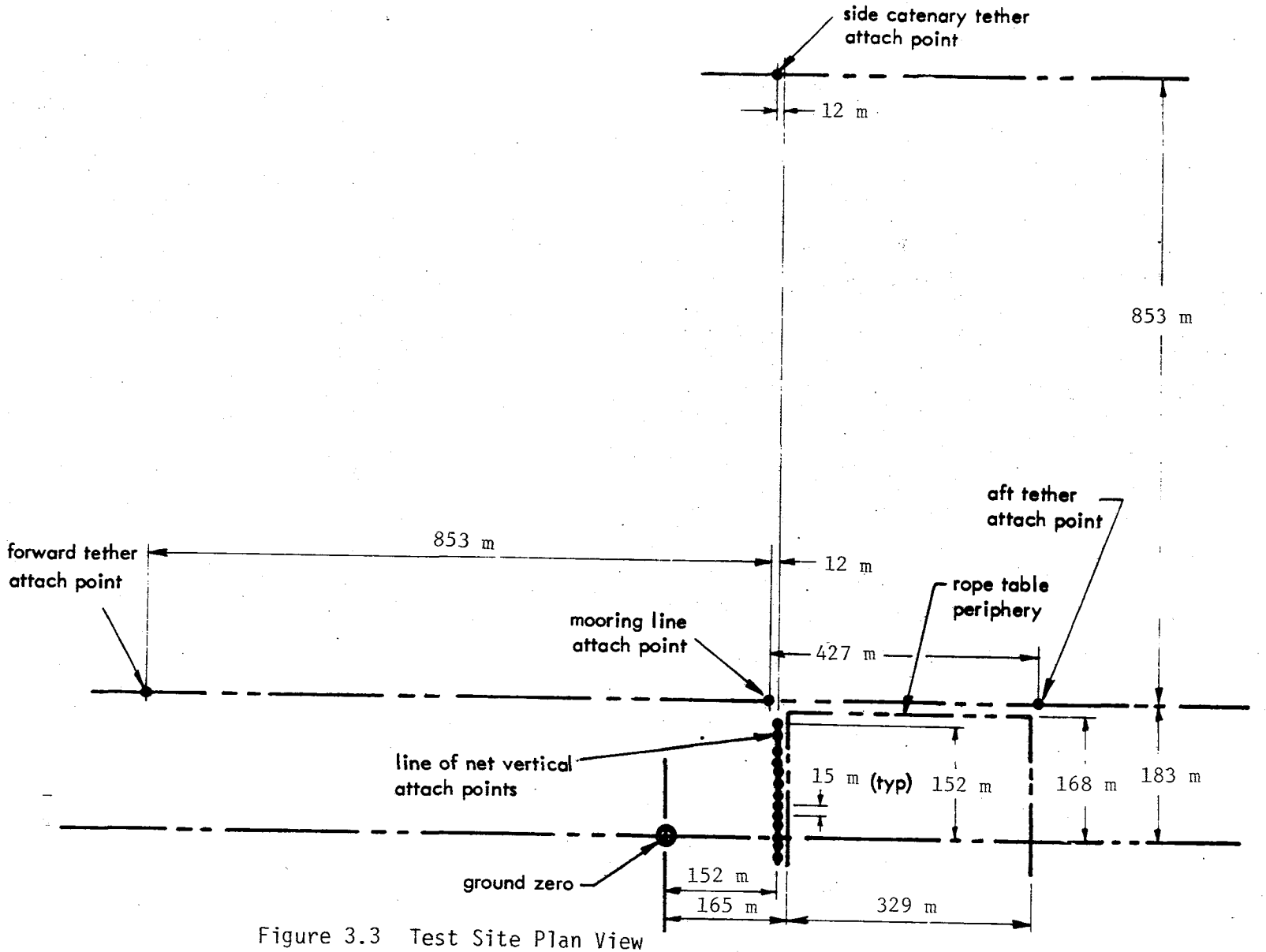

Figure 3.3 Test Site Plan View
Initial Design Configuration

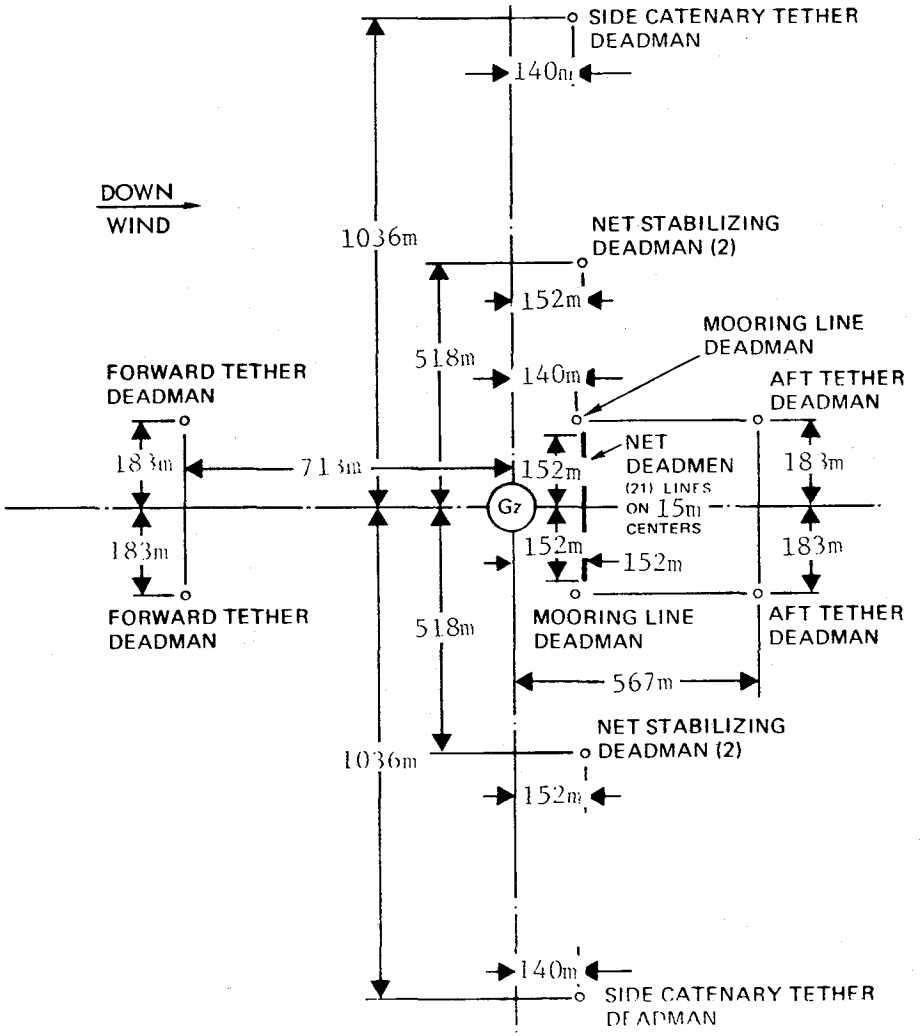

Figure 3.4 Deadman Locations
Initial Design Configuration

fence posts. In the lowered net position, the rope table supports and maintains the net vertical and horizontal cables and the attached instrumentation off the ground. Figure 3.5 shows the ladder in a nearly complete and completely lowered position with the net supported on the rope table.

As designed, the rope table consisted of an orthogonal array of tensioned Dacron ropes spaced approximately 41 m (135 ft) apart and supported atop 2.1-m (7-ft) fence posts at each intersection point. However, during the field installation, additional Dacron rope was strung diagonally, at 45-degrees, atop all fence posts to obtain additional net support.

The two balloons used to suspend the Jacob's Ladder system were aerodynamically shaped, 12.2 m (40 ft) in diameter and 30.5 m (100 ft) long. These balloons flew at an altitude of approximately 495 m (1625 ft) when the system was erected. Each balloon provided a net lift of approximately 670 kg (1475 lb) under zero wind conditions. The approximate weight of the net, all tethers and mooring lines, all attach fittings, and suspended instrumentation was 365 kg (1200 lb).

The primary instrumentation suspended from the net were 441 vugraph fiber collectors (described later in this section) which were attached at each intersection of the vertical and horizontal net cables. The net also supported two airborne LED instruments (described later), ten NIOSH millipore filter sampling systems, eight charged grid fiber sensors and associated power and signal wiring, a number of lightweight Dugway Proving Ground mesh samplers and approximately 30 directional cardboard Peterson samplers.

The system was first checked out successfully by lofting it with the 305-m by 305-m net detached from the main catenary. Later, five full-up ladder system flights were made, three flights for the three completed tests and two flights for two test trials that were eventually postponed because of unfavorable meteorological conditions. The Jacob's Ladder system operated successfully in all respects on each of these five flights, flying in a fully erected condition approximately six to seven hours in each of the flights.

Figure 3.6 is a photograph taken from ground level, upwind of the erected Jacob's Ladder. Approximately one-half of the net is shown including the balloon on the eastern side of the net. Below the balloon (to the left of the balloon in the photograph) is the juncture plate at which point all tethers, the mooring line, and the main catenary come together. These cables can be faintly seen in the photograph. The vugraph collectors can be clearly seen attached to each net cable intersection point. Also seen in the lower left area of the photograph is an airborne LED instrument suspended from one of the net horizontal cables.

Figure 3.7 is a photograph taken from a helicopter at the start of the third test. Due to the exceptional size of the ladder system and the relatively small diameter cables involved, it was difficult to obtain photo coverage that clearly showed the entire system. The only portions of the ladder system resolved in this photograph were the balloons and the deadmen locations for the ground attach points. Using these reference points, an artist's rendering of the Jacob's Ladder was overlayed on the photograph. By referring back to Figures 3.1 through 3.4, a further indication of the distances involved can be obtained.

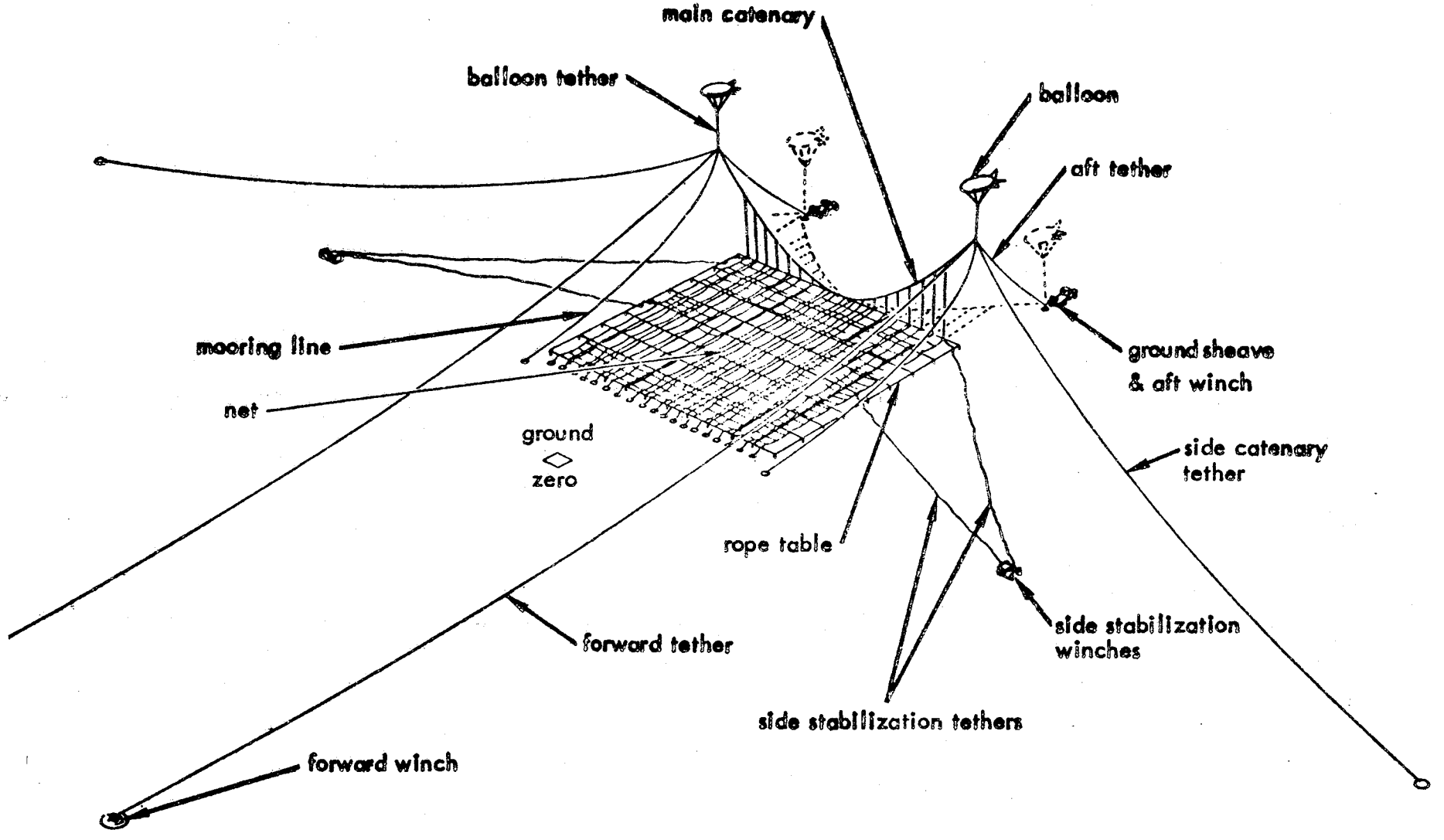

Figure 3.5 Jacob's Ladder in Lowered Position

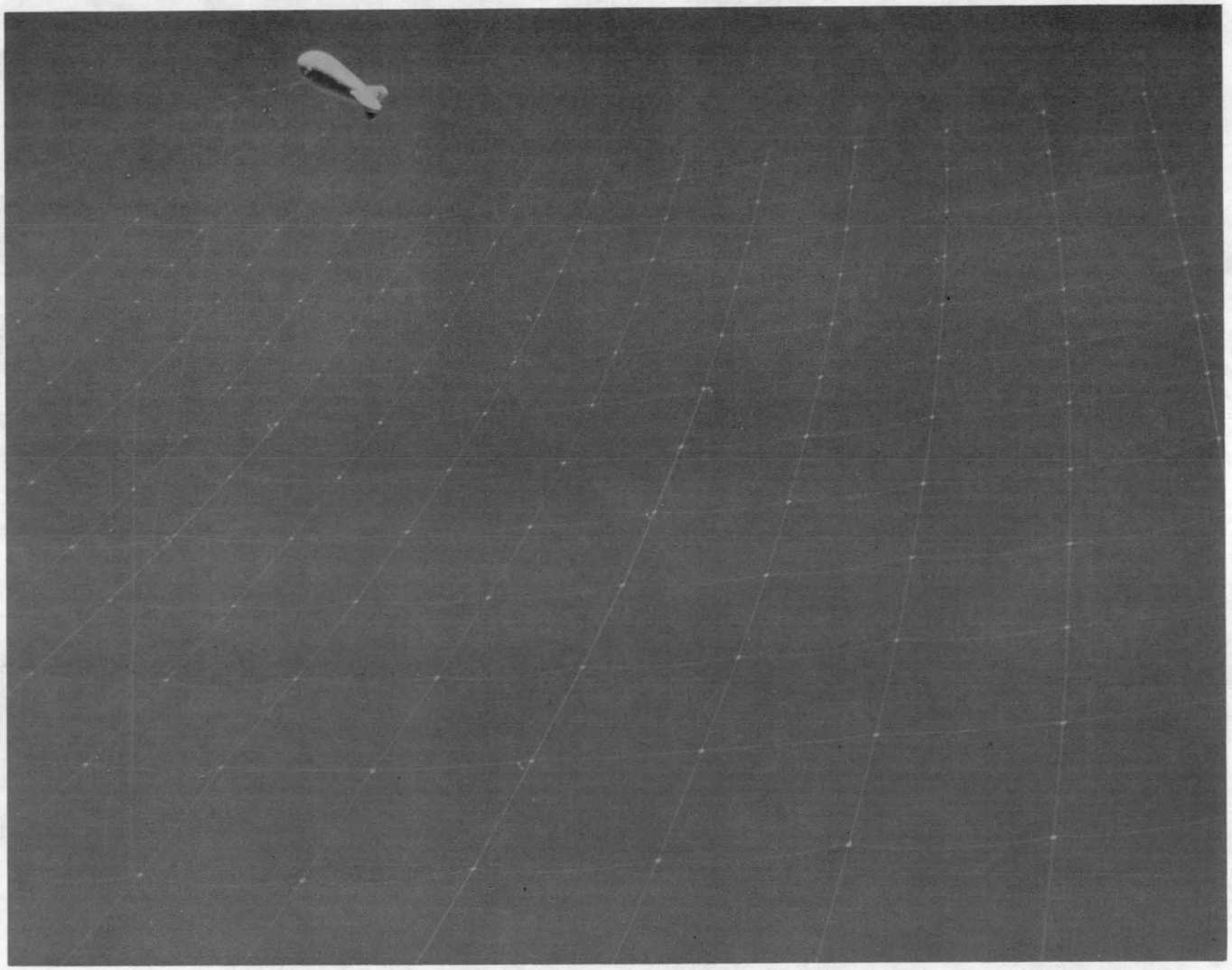

Figure 3.6 Photograph of Jacob's Ladder System

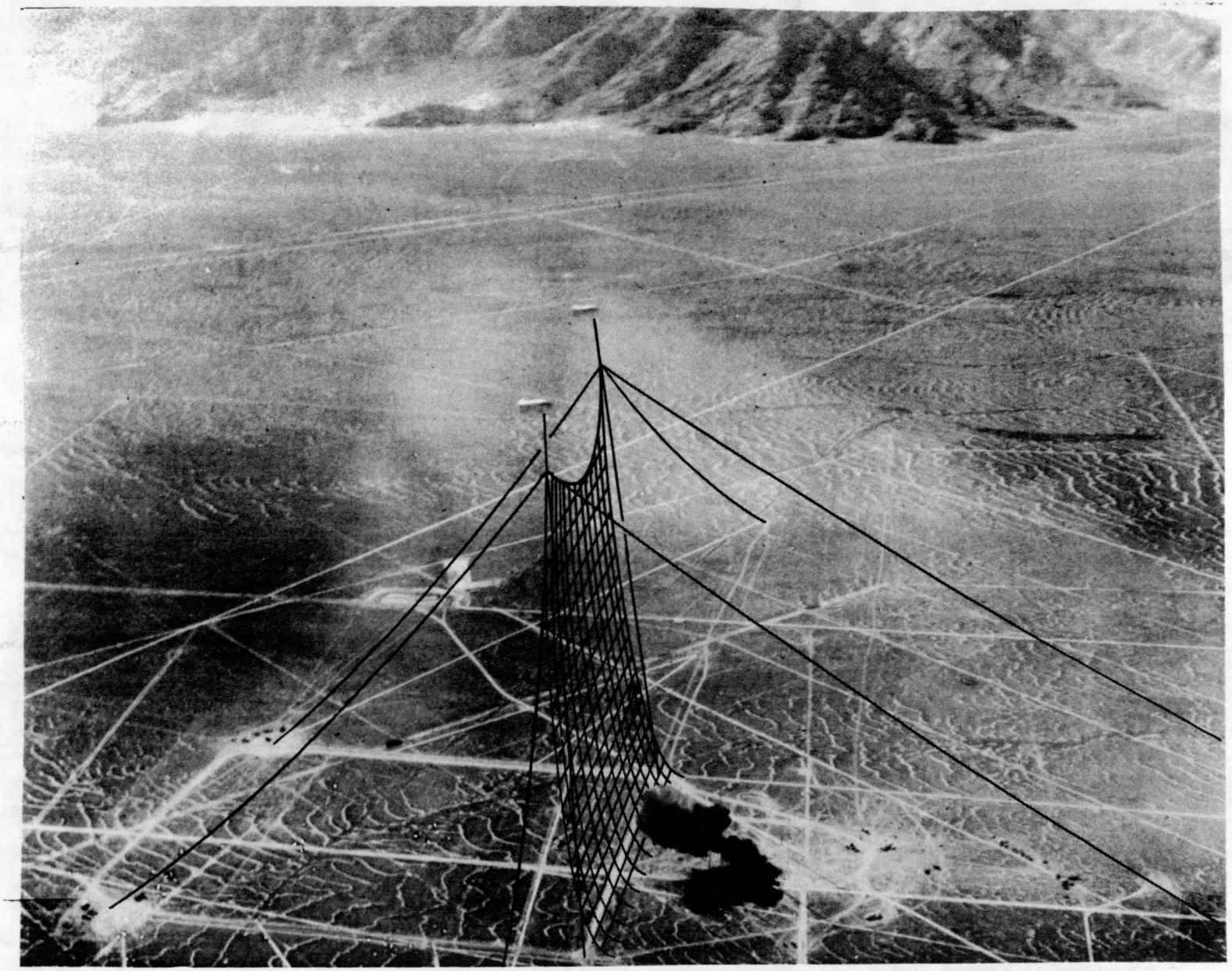

Figure 3.7 Aerial Photograph of Test Site (Test D-3)

DESIGN

Background -- The primary constraints imposed on the design of the Jacobs' Ladder system were several.

(1) The net dimensions were to be 1000 ft high and 1000 ft wide*. These dimensions were selected as a function of the maximum expected plume altitude at the downwind net distance and the wind direction limits for which a test could be conducted.

(2) The system was to be supported by two specified balloons, each having a net (available) lift of 1475 lb.

(3) The system was to operate satisfactorily in the test configuration for wind velocities from 0 to 22.5 mph. Furthermore, the system was to be capable of safely withstanding and capable of being safely lowered under these wind velocities from any direction, including gusts to 25 mph.

(4) The system was to be designed to support and suspend instrumentation weighing approximately one hundred pounds.

(5) The design of the system would permit the safe retrieval of both balloons under all operational conditions in the event any one cable, tether, line, or fitting broke.

(6) The maximum load or stress in any cable or system fitting or part was not to exceed one-fifth of its rated ultimate breaking strength for any combination of operational conditions (factor of safety equal to five).

(7) Also, all deadmen were sized with a design factor of safety equal to five.

In the early process of designing the ladder system, various configurations were explored in which the basic net cordage or cable materials were varied. Materials such as steel, nylon, Dacron, fiber glass, polypropylene and Kevlar cable or rope were investigated. Regardless of the physical configuration of the system, none of these materials except Kevlar permitted a design that could meet all of the constraints. The basic problem was one of material strength-to-weight ratio. To meet the required strength of the individual cables for all the materials except Kevlar, the required cable sizes led to a total system weight considerably greater than the available lift from the balloons. Therefore, unless Kevlar was

---

* In this section of the Jacob's Ladder design as well as in Appendixes A, B, and C, all units are given in U. S. Customary Units rather than SI units. The reason for this is that all design drawings, field layouts, load analyses, and fabrication and operational plans were developed in U.S. Customary Units. This system of units avoided confusion and errors during material procurement and field installation, checkout, and operation since all balloon, cable, hardware, and manufacturer's specifications and available tools such as measuring tapes, hand tools, load cells, and dynamometers used U.S. Customary units exclusively.

selected as the cable material, one or more of the constraints would have to be relaxed. Namely, more or larger balloons would be required, the net size reduced, the permissible wind conditions relaxed, or the factor of safety reduced. Since none of these constraint alternatives was acceptable or prudent, Kevlar was selected as the only material to be considered within the realm of conventional materials.

The remarkable strength-to-weight property of Kevlar cable ultimately permitted a balanced ladder system design in which a factor of safety of approximately ten was achieved for all cable elements for all operational conditions. In addition, the total system weight allowed a balloon lift margin (excess balloon lift) about equal to the lift of one balloon, i.e., approximately 1500 lb.

Details of the components and parts of the Jacob's Ladder system are given as part of Appendix B, Fabrication and Assembly Procedures for Jacob's Ladder. Appendix C, Operational Procedures for Jacob's Ladder, details the step-by-step operations for erecting and lowering the system.

Design Analysis -- The design analysis performed for the Jacob's Ladder system focused on three system conditions.

(1) Static calculations for head-on (test configuration) wind loads of 0, 6, 9, 12, 15 and 22.5 mph; where 22.5 mph is the maximum wind velocity the ladder was to be flown under the operational parameters specified.

(2) A failure mode analysis for a failure of any cable. Simple models were developed for each postulated cable break, and information concerning the net behavior and loads in the surviving cables was obtained.

(3) A first-order static calculation for a side-on wind condition in the event of a 90-degree change in wind direction.

In the static analysis of the ladder for head-on wind conditions, it was assumed that

- the wind loads on the net are carried totally and equally by the vertical members of the net,
- the vertical members and supporting main catenary can be modeled as catenaries, and
- the wind loads on the net are constant with height.

The analysis was performed by first calculating the wind loads on the net and lumping the loads equally on each of the vertical members. The vertical members were then analyzed as full catenaries, assuming that the top and bottom of the vertical members are in the same vertical plane. The resulting loads at the top of the vertical member along with the net dead load were then applied as a uniform load to the supporting main catenary. The main catenary was then analyzed for the reactions at its end. The loads in the forward and side catenary tethers were then calculated to maintain equilibrium.

The results of these static load calculations indicated the cable forces were approximately 50% of the safe working loads specified for the cables, thus providing an actual factor-of-safety of about ten. The results of these calculations are given in tabular format in Appendix A, Summary of Jacob's Ladder Static Loads, for incremental head-on wind velocities from 0 to 22.5 mph. These calculations also show that the lift margin (excess balloon lift) remains relatively constant through the entire wind velocity regime at a value about equal to the lift of one balloon. This lift margin, which is equal to the sum of the ground reactions of the two mooring lines, is relatively constant because of the increase in balloon lift from aerodynamic effects for increasing wind velocities.

During the field operations, a load dynamometer was installed in each of the mooring lines at the deadmen connections. The recorded measurements taken for varying wind velocities gave ground reaction forces at these points equal to approximately 85% to 90% of the calculated values. Unfortunately, the urgency of the test operation activities prevented load measurements being taken for cable elements other than the mooring lines.

The objective of the failure mode analysis was to attain a ladder design that would permit the safe retrieval of the balloons under all operational conditions in the event any one cable, tether, line, or fitting should fail. The system elements that were analyzed for individual failure were the horizontal and vertical net cables, the mooring line, the main catenary, the aft tether, the balloon tether, the forward tether, and the side catenary tether. Also, the condition in which a single balloon loses some or all of its lift was analyzed.

In some cases, the effects of a single cable element failure could be investigated adequately by a simple qualitative analysis. In other cases, a qualitative and static load analysis was required. In the case of a failure in either the forward or side catenary tether, a dynamic system model was developed to determine the time-history of the system displacement and cable element loads from the time the break occurs until the system achieves equilibrium.

The results of these analyses were evaluated for two conditions. One, that the loads did not exceed the safe working loads (SWL) for the main load-carrying cables, i.e., all cables excluding the net horizontal and vertical cables. And two, that after the system reaches an equilibrium position, the balloons could be lowered and retrieved safely.

The failure mode analyses revealed that no one failure mode induced loads in the remaining cable elements greater than the safe working load. However, minor modifications, such as the provision of cable pigtails, were added to the system to permit lowering and retrieval of the balloons after the failure. In those cases where the operations involved to lower the system and retrieve the balloons were different than the normal operational procedures, these special lowering procedures were developed and described in the operational plan (Appendix C).

Since each of the 21 horizontal net cables carries no primary loads but merely transfers internal wind loads to adjacent vertical net cables, a failure of one of the horizontal cables would have little or no effect on the system operation.

To achieve equilibrium after the failure, the net configuration in the locality of the failure would be slightly irregular; but all test operations could conceivably continue.

A failure of one of the net vertical cables would cause the load in that cable to be transferred to adjacent vertical cables through the horizontal net cables. The loads in the adjacent net verticals would increase but would remain below their safe working loads. As for a horizontal net cable failure, the net configuration would be slightly irregular locally but all test operations could continue.

A failure of one of the mooring lines would cause the loads in some of the cable members to increase. A worst case analysis indicated that for this failure mode, the loads in all cable elements would be at least 23% less than their safe working load. However, although the system configuration would be essentially unperturbed, it was deemed prudent that a failure of this redundant, but critical, cable element should cause the operations to be aborted and the system lowered.

Two failure modes were investigated for a break in the main catenary: a failure outboard of the net (between an outside net vertical cable and a juncture plate), and a failure inboard of the net (between the outside net vertical cables). A failure of the main catenary outboard of the net would cause the portion of the net system located opposite or furthest from the break to collapse and hang from the balloon. Much of the net deadweight and wind loads would be dumped, since part of the net would rest on the ground. Since a lift margin for all operating conditions is approximately equal to the lift of one balloon, this opposite balloon could easily pick up the added net loads, thereby reducing the tension in the mooring line, with perhaps some increase in the side catenary and forward tether loads. However, a worst case increase in these loads would still be within the safe working load for these cables. The condition that would exist at the side where the catenary outboard failure occurs would be the removal of essentially all deadweight and wind loads at the catenary connection to the juncture plate. This condition would increase the mooring line load on that side equal to the lift of the balloon while the side catenary and forward tethers would go slack. Both balloons would be lowered and retrieved independently.

If the main catenary failed inboard of the net, secondary damage to the net could be a more serious consequence. For a main catenary failure of this nature, the net horizontal and vertical cables would reorient themselves in an attempt to carry the catenary load by "bridging" the point of failure. For this to be possible, relatively large loads would have to be transmitted through the net horizontal and vertical cable intersection points probably causing the ties at these intersection points to slip or break. Also, the loads in the upper horizontal cables and the upper sections of the vertical cables could increase to approximately 50% of their ultimate breaking strength, thus subjecting them to possible failure. These secondary effects would occur progressively downward and outward from the point of the catenary failure with the net progressively lowering to the ground unloading its dead weight and the wind loads. Eventually, an equilibrium condition would be met where the net loads are compatible with

the strengths of the intersection ties and the net horizontal and vertical cables. Regardless of the extent of these secondary net failures, however, the position of the juncture plates essentially would not change, the loads in the side catenary and forward tethers would decrease, and the loads in the mooring lines could increase to a possible maximum value equal to the balloon lift. Both balloons could be lowered and retrieved.

When the Jacob's Ladder system is operated in head-on winds, in a fully erected position, the aft tether carries no load. Its primary purpose is for erecting and lowering the ladder system. Therefore, a failure of the aft tether would not induce any loads in the other cable elements other than those undergone during normal operations; but the balloon that is attached to the failed aft tether could not be lowered with the aft winch. If this failure mode occurs, a set of alternative procedures was developed to lower the balloon. To implement these procedures, it was necessary to install a pigtail connection to each mooring line at its ground termination end. The step-by-step, alternative procedures for lowering the balloons in the event of this mode of failure is given in Appendix C.

It was recognized early-on in the design of the Jacob's Ladder system that if a failure of a balloon tether (the cable connecting the balloon to the juncture plate) occurred, the balloon would float off into space. To prevent this from happening, two balloon tethers were installed for each balloon. This redundancy added little weight to the system but reduced the probability of losing a balloon to practically zero.

As mentioned previously, the failure modes for all the system cables except the forward and side catenary tethers could be analyzed adequately by qualitative analyses, static load calculations, or a combination of both. However, the analysis of failures of either the forward or side catenary tethers required the development of a dynamic model to determine the time-history of the system displacement and cable loads.

The model used for the postulated forward or side catenary tether failures consisted of a large displacement, inverted, double pendulum with the rotations of each pendulum as the degrees-of-freedom (see Figure 3.8). Extension of the cables was neglected because of the stiffness of the Kevlar cable (3.6% strain at ultimate or 0.77% at the safe working load). Since both tethers were anchored at large distances from the net (2800 ft), it was assumed that in the event of a failure, the surviving orthogonal tether would not play an important role in carrying the unreacted loads due to the shallow angles. Therefore, the bar of the bottom pendulum was considered to be the mooring line, while the bar of the top pendulum was the balloon tether. The mass of the bottom pendulum was taken to be one-half the mass of the net, while the top pendulum mass was considered to be the mass of the balloon and balloon tether.

In the analysis of the forward tether failure, the forcing functions for the bottom mass were assumed to be the vector sum of the vertical components of the surviving cable tensions, one-half the dead weight of the net, and the horizontal component of the forward tether. This horizontal component varied with the relative wind velocity on the net in the form, $C_d(v_{wind} - v_{x,net})^2$. The loads on

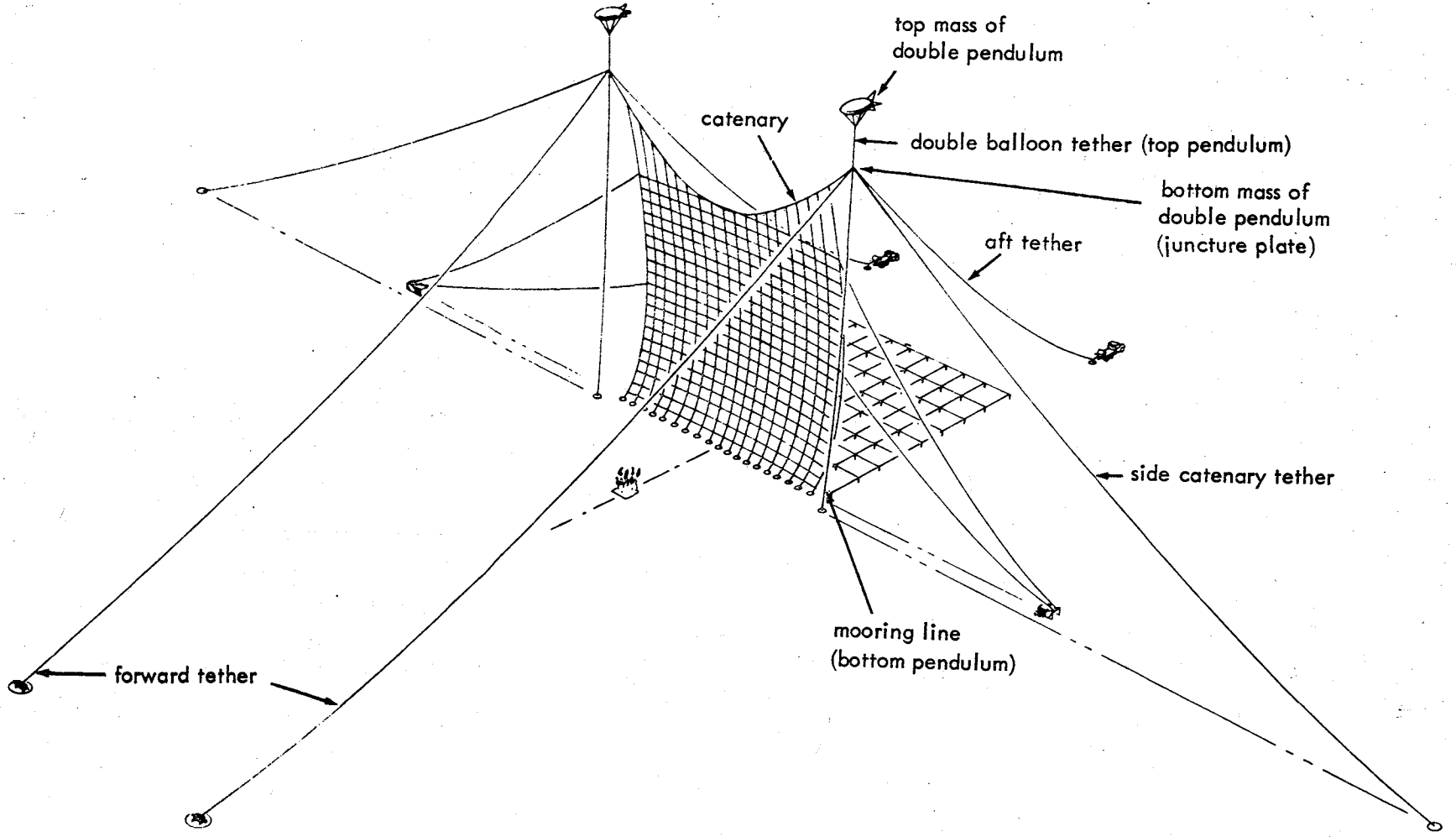

Figure 3.8 Jacob's Ladder Dynamic Model Configuration

the top pendulum mass were the lift of the balloon, the lift due to drag on the balloon, the weight of the balloon and its tether, and the vertical drag on the balloon. The lift and drag on the balloon caused by the wind were based on curves obtained from the Air Force Geophysics Laboratory (AFGL). It was assumed that the balloon would orient itself in the direction of the horizontal velocity of the net, since it was attached to its tether by a swivel. The vertical drag on the balloons caused by its loss of altitude as a result of the failure was based on the drag of an infinite cylinder using the dimensions of the balloon.

The results of the analysis performed for a failure in the forward tether at a wind velocity of 22.5 mph showed the net-tether juncture (juncture plate) moving downwind at a peak velocity of 25 ft/s (17 mph) and dragging the balloon with it in the first 6.0 sec following the failure. It is during this time that the balloon tether load peaks at a value of 2050 lb, where the safe working load is 2 x 2200 lb, or 4400 lb. After this time, the balloon and net move essentially together for the next 120 sec, at which time the net assumes an equilibrium position with the top of the net about 1240 ft downwind from its base. It is at this equilibrium position that the balloon mooring line load is maximum at 1625 lb (safe working load is 2200 lb).

For the analysis of the side catenary tether failure, the loads on the bottom pendulum mass were assumed to vary with the span of the net. This was done by analyzing the net for various spans and calculating the resulting forces. The forces were then plotted against span, and a straight-line fit was made. The loads applied to the balloons (top pendulum) were the total lift of the balloon and a drag owing to its inward motion. Again, this drag due to lateral motion was based on the drag of an infinite cylinder.

The results of the analysis for a failure in the side catenary tether at a wind velocity of 22.5 mph showed that the net-tether juncture (juncture plate) moves inward at a peak velocity of 30 ft/s dragging the balloon with it for the first 4.0 sec. It is during this time that the balloon tether realizes its maximum load of 2228 lb. Since the loads in the catenary supporting the net are a function of the span, the net-tether juncture then slows its inward movement with small oscillations because the drag of the balloon is pulling outward in opposition to the catenary loads. Finally at approximately 100 sec, the net assumes an equilibrium position 290 ft inward from its original position. This results in a reduction of the span of the net from 1000 ft to 710 ft. It is at the equilibrium position that the mooring line load peaks at 1000 lb, still within the safe working load.

In summary, failures of either the forward or side catenary tethers would cause the ladder system to undergo relatively large displacements until equilibrium positions are achieved. However, the peak loads induced in the surviving cables during the net excursions remain below the safe working loads of the cables. After the net stabilizes in its equilibrium positions, the balloons could be lowered and retrieved safely using the normal operational procedures with minor revisions. These revisions to the normal operational procedures are described in Appendix C.

The final failure mode to be analyzed was that of a balloon losing some or all its lift. The onset of this type of failure would be recognized early-on by a noticeable and probably progressive reduction of load in the associated mooring line, i.e., a reduction of lift margin on the affected side of the system. This effect would be shown by the load dynamometer that is installed in series with the mooring line and monitored during the test operations. Until this lift margin is reduced to zero, the system configuration would be unperturbed and the balloons would be lowered and retrieved.

If the loss of balloon lift was sufficient to lose all lift margin, i.e., the load in the mooring line becomes zero, then the affected balloon would descend in place and the system loads would be picked up progressively by the intact balloon. This condition would be similar in effect to that of a main catenary cable failure outboard of the net. The intact balloon (and the affected balloon if it has not descended to the ground) would be lowered and retrieved.

The third in the series of load analyses performed for the Jacob's Ladder system after the static, head-on-wind calculations and the failure mode analyses, was the side-on wind static analysis. In this side-on-wind analysis, the condition for the head-on-wind analysis was modified by placing all the wind load at the upwind juncture plate and calculating the appropriate side catenary tether forces to maintain equilibrium.

The results of the calculation for this side-on-wind condition for a wind velocity of 22.5 mph showed the upwind side catenary tether to have a load of 1780 lb which exceeds the safe working load (1200 lb) for that cable by 580 lb or 48%. This results in a factor-of-safety of approximately 3.4. Since this analysis was based on conservative assumptions and worst case conditions, this margin of safety was deemed acceptable.

Fabrication and Assembly -- To the greatest extent possible, various elements of the ladder system were prefabricated before being shipped to Dugway Proving Ground to minimize assembly and installation operations in the field. Nevertheless, the exceptional size of the entire ladder system and the extreme working conditions of a desert locale for a field project such as this, made the on-site assembly and installation task difficult and arduous. However, with the excellent cooperation and assistance of NASA, Dugway, and AFGL personnel, the system was successfully assembled, installed, and checked out prior to the first test of the series.

Prior to the field activities, a procedures document was published and approved, which gave the step-by-step details for assembling and installing the system. This document is presented in Appendix B. This document also lists the bill of materials for all elements of the ladder system.

As would be expected in a project such as this, a number of system design revisions were decided and implemented in the field. The major revision worthy of note was to relocate the 21 vertical-line deadmen of the net approximately 35 m (115 ft) upwind, thus placing the bottom or anchor points of the net 117 m (385 ft) downwind of the center of the test fire instead of 152 m (500 ft). This change was made to improve certain operational conditions. (This change is not reflected in the figures and appendixes of this report.) To accommodate this

revision, another row of rope table fence posts was emplaced approximately 30 m (100 ft) upwind of the "as designed" rope table and the tensioned Dacron rope table cables extended to these posts. In addition, as a safety precaution, a length of Kevlar cable was field-spliced to each of the net vertical cables approximately 23 m (75 ft) up from its ground connection to the deadman. Each of the free ends of these spliced-in cables was fastened to one of the 21 original deadmen located at the 152 m (500 ft) downwind station. The purpose of these additional lines was to act as snubbers, restraining the net from billowing toward the center of the test site, and avoiding the possibility of becoming entangled with the guy wires from the 60 m (198 ft) towers erected near the fire site should a 180-degree wind reversal occur.

Operational Procedures -- The document that outlines the step-by-step procedures for the Jacob's Ladder field operations is presented in Appendix C. These procedures include the safety and communication requirements, personnel responsibilities, and normal and emergency operational procedures that were followed during the field test program.

INSTRUMENTATION

VUGRAPH FIBER COLLECTORS

Fibers lofted by the fire and carried by the wind were collected on vugraph samplers attached to each of the vertical and horizontal cable intersection points on the Jacob's Ladder net. The method of attachment is described in Appendix C and an attached collector is shown in Figure 3.9. Each collector consisted of a swatch of bridal veil netting stretched across and fastened to the surface of a vugraph frame. The mesh opening of the netting is nominally 1 mm. The collection area of each vugraph is 0.046 m^2. Prior to a test and the installation of the collectors on the ladder, the netting is made sticky by spraying the up-wind surface with Rhoplex, a nondrying, commercially available adhesive. This adhesive has the unique property of remaining sticky for several days under all the encountered ambient conditions of wind, temperature, water, and solar radiation. At the time the vugraph is attached to the ladder, an identifying label is affixed to the vugraph frame corresponding to its location on the net and test number.

After each test, the vugraph collectors are removed from the net; and both sides of the bridal veil are covered with a clear acetate sheet before they are stored.

AIRBORNE LED SENSORS

Description -- The following section describes the two airborne LED fiber-detectors that were used in the Dugway Proving Ground test series of October and November 1979.

Each detector system consists of an infrared light emitter operating at 0.91μm wavelength, a collimating system, an optical filter, and a light detector, and associated signal processing electronics. The system functions by sensing the momentary reduction in light intensity caused when a carbon fiber crosses the path of the vertical, collimated light beam, which is 15 mm in diameter by 17.6 cm in length. The detector circuits produce a nearly full-scale signal when

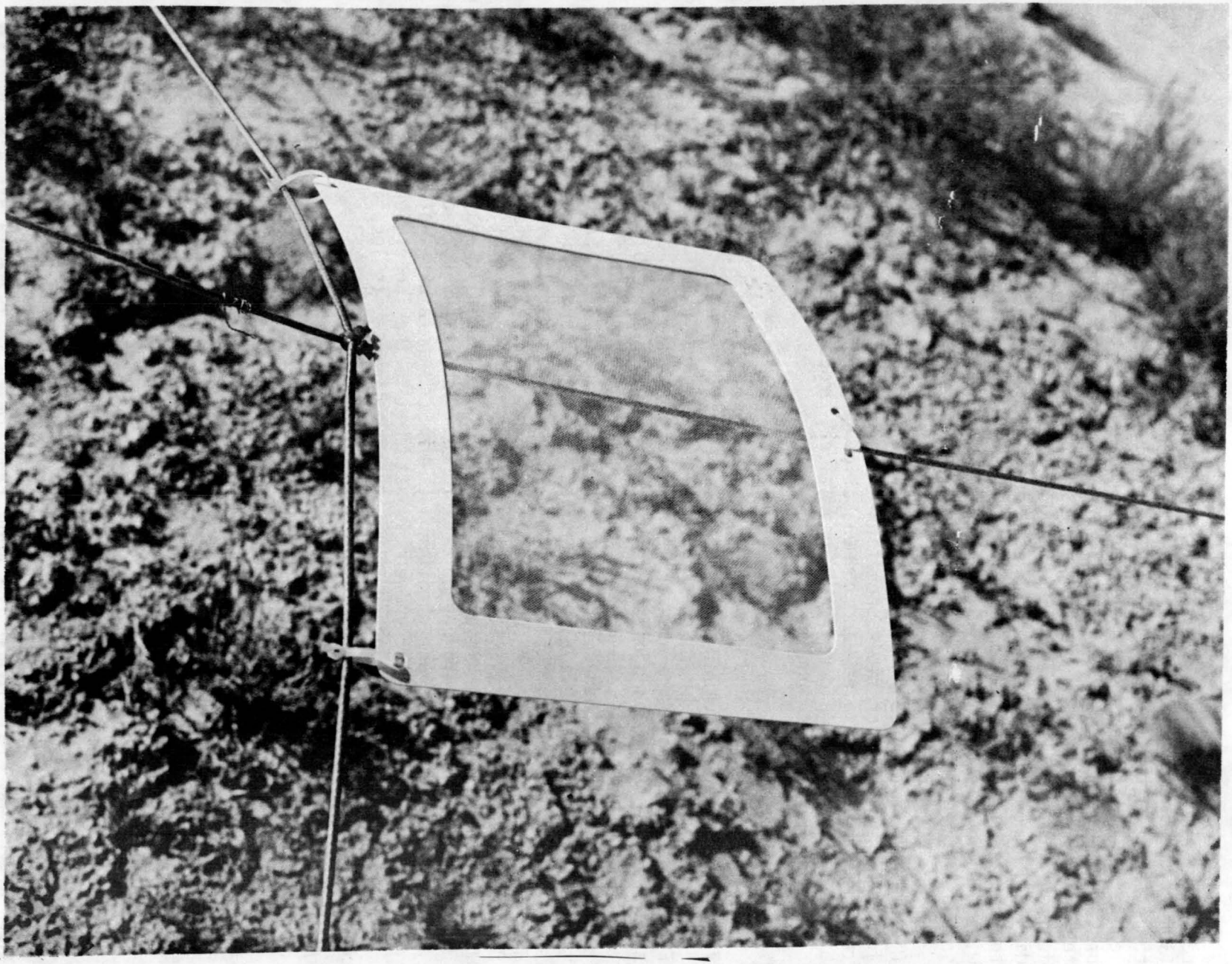

Figure 3.9 Installed Vugraph Photograph

the beam is shadowed by a 6 μm-dia x 15 mm-long fiber oriented perpendicular to the beam axis. The dynamic range is better than 10:1 in the absence of extraneous outside noise sources. The pulses obtained by fiber passage are recorded on a built-in cassette tape recorder that can use 45- or 60-minute tapes. Timing pulses every 10 s are also recorded on the recorder tape.

Two digital integral counters with LCD display are incorporated in the detector system. The signal levels above which each counter counts can be set internally. For the Dugway tests, they were set at 1.5-mm and 7-mm-length equivalents for 6 μm-dia fiber passages, (for the checkout test at NSWC, Dahlgren, these levels were set at 1.5 mm and 15-mm length equivalents).

Completely self-contained, the system uses separate batteries for the light emitter, the recorder, and the electronic circuits. To conserve battery power and tape footage, it incorporates a telemetering (T/M) receiver and battery connected to a servo-controlled switch that can turn the instrument and recorder ON or OFF.

The T/M receiver is remotely controlled with a small, portable, telemetering transmitter operated at the appropriate times from the ground. Operation of the T/M link is reliable at ranges up to at least a half kilometre.

The system shown in Figure 3.10 was designed for suspension on the Jacob's Ladder for the Dugway tests. The total system weight is 2.5 kg. The system is attached to the horizontal ladder cables by a 0.46-metre-long aluminum tube insulated with a piece of soft rubber tubing. This support tube is fastened to the detector housing by a double set of vibration isolators. Coupling between the lower box containing the LED transmitter, batteries, and T/M receiver, and the upper boxes containing the light detector and electronics circuits is made as rigid as possible with a truss structure made of thin aluminum tubes.

Design Guidelines -- The primary guidelines for the instrument design were dictated by the need to field an active carbon fiber detector system capable of meeting the environment and program requirements described in Table 3-1. These guidelines led to the identification of several problem areas; (1) a greatly increased vibration when the wind passed through a low-inertia instrument structure and net and net rope vibrations were coupled into the detector system, (2) a more uncertain and varying infrared light background, (3) weight limitations, and (4) requirement for completely remote operation of the units during the tests.

Table 3-1 LED Detector Environment Requirements

Temperature	Desert - summer or winter
Background Light	Sunup to sundown
Altitude	10-200 metres above ground level
Wind	1 to 5 metres/sec
Soot	Light to heavy
Weight	less than 3 kg
Program Requirements	
Fiber Fluence/Deposition	10^1 to 10^3 fibers/m^2
Operation Time	30 to 60 minutes
Data Acquisition Readout	immediate and permanent

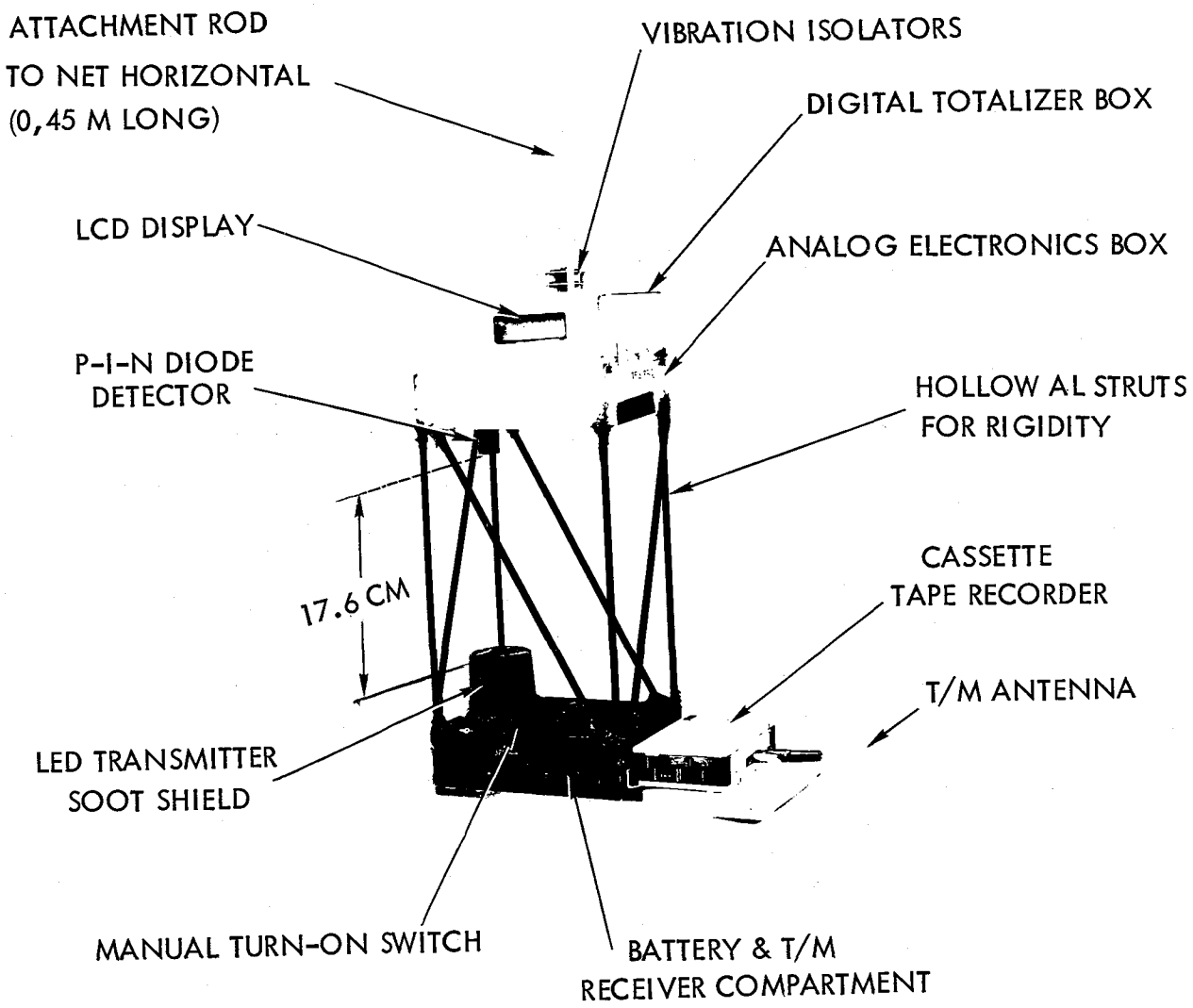

Figure 3.10. Airborne LED Fiber Detector

A light obscuration LED detector instrument used successfully by TRW under approximately these conditions at a previous test series, at Naval Weapons Center, China Lake, California, was used as a point of departure for designing the new system. The main differences were that the previous system was ground-operated, with manual turn-on; it was hard wired to main power and chart recorders; and could be manually adjusted for ambient light conditions before a test.

System Design -- A new LED, TI-T1ES35, was chosen for the transmitter. This emitter operates at a peak wavelength of 0.9100 μm with a bandwidth of 0.03 μm and was selected because of its previously demonstrated uniformity. The transmitter is followed by a three-element collimating lens, to preserve beam cross-sectional uniformity and produce a parallel beam of 15-mm-dia. The beam path length was chosen at 20 cm. At the receiver end of the system, the beam is passed through a collecting lens and through a notch filter centered at a wavelength of 0.905 μm with a 0.012-μm band pass. The notch filter removes extraneous externally produced light from the ground, clouds, or the sun. The converging beam is focused on a small aperture to remove all light generated or scattered from outside the parallel beam, and impinges on the p-i-n diode detector chip.

The transmitter, LED, and collimating lens are rigidly mounted to a bridge-like, wooden base. The base is attached to the lower compartment box at the edges, which would be zero node points for any box resonances. A thin rubber diaphragm closes off the lower box where the LED collimator protrudes without adding to the attachment loading.

To minimize the contamination from fallout of soot or carbon fibers on the LED lens, a short section of collimator was added with openings on the side to produce a positive pressure region at most wind velocities. This shortened the sensitive length of the beam to its final value of 17.6 cm between the end of this section and the end of the detector collimator.

The p-i-n silicon diode detector is similarly mounted in the lower box of the upper compartment. The instrument system is painted with flat black paint in those areas which might be seen by the detector or might reflect light into the collimator. Other areas are left unpainted, or painted white, to reflect heat during the late summer testing in the desert.

The expected test duration of 20 minutes plus checkout calibration, and short holds required a tape recording time of greater than 30 minutes. A recorder capable of recording for 45 or 60 minutes was selected.

Assuming the winds to be between 1 and 5 m/s, and the beam size to be 15 mm in diameter, the length of the pulse produced in the circuits by a fiber passage might vary from about 3 to 20 ms. The minimum bandwidth to handle these pulses without distortion is approximately 2.1 kHz. For single pulses, the frequency response extends down to DC. Since no small tape recorder has a response down to d.c., some AM or FM carrier modulation frequency was required. The 2-KHz bandwidth would dictate a center frequency of at least 4 or 5 kHz. The recorder selected for the instrument was the Craig Model 2625 mini-recorder, which uses a standard cassette. Its frequency response is flat, from 200 to 7000

Hz, and falls off rapidly outside these limits. Additionally, this recorder weighs only 0.5 kg, a strong factor in its selection. It was necessary to disable the automatic level control incorporated in the recorder electronics to provide true pulse levels. A fixed gain was then chosen to give good recorder characteristics.

A block diagram of the electronic circuits developed for the instrument is shown in Figure 3.11. The analog circuits for amplifying and filtering the p-i-n diode detector signals and for conditioning them to drive the tape recorder and two digital totalizer circuits are contained in the lower box of the upper compartment. The upper box of the same compartment is dedicated to the digital circuits needed to drive the two LCD totalizer displays.

A time-mark generator, also located in the lower box of the compartment, is derived from a 16.384-kHz crystal oscillator by countdown circuits to produce a pulse every 10 seconds on the tape recorder input. The 4.096-kHz carrier modulation frequency is also derived from the oscillator.

The preamplifier following the detector was a low noise operational amplifier connected as a transimpedance amplifier. The gain of the feedback network was approximately 20 dB more for AC signals than for DC signals. Since all circuits following the preamplifier were AC-coupled, the AC output of the preamplifier was amplified by 20 dB then split into two signal paths: one, the analog signal which was recorded by the on-board tape recorder, the other, the digital display of particle counts.

In the analog path, the signal was added to timing pulses having a 10-s repetition rate and then passed through a low-pass filter (500 Hz) and applied to a doubly balanced modulator. The signals going to the on-board digital displays were routed through a 500-Hz low-pass filter having a 14-dB gain. A voltage discriminator produced an output pulse, which was registered as a count on the 4-digit display for signals produced by 6 μm x 7-mm fibers. These signals were also amplified by an additional 14-dB and applied to a second voltage discriminator, which registered a count for passing 6 μm x 1.5-mm fibers and all larger particles. These counts were displayed on a 6-digit counter.

The battery complement powering the unit is given in Table 3-2. The power circuits interconnecting the several boxes are given in Figure 3.12.

TURN-ON Circuit Design -- Each of the airborne LED systems is remotely turned on with a commercial model airplane T/M receiver transmitter system. The T/M receiver is mounted in the lower compartment of the LED system and is turned on by the manual switch on the LED system. The digital circuits are also turned on by this switch. Drawing very little current, these circuits can be left on for several hours without draining the 12.5-V mercury battery.

Activating the T/M transmitter controls will activate remote switches in the LED units if the manual switches are in the ON position. When the remote switch is activated, the following functions occur:

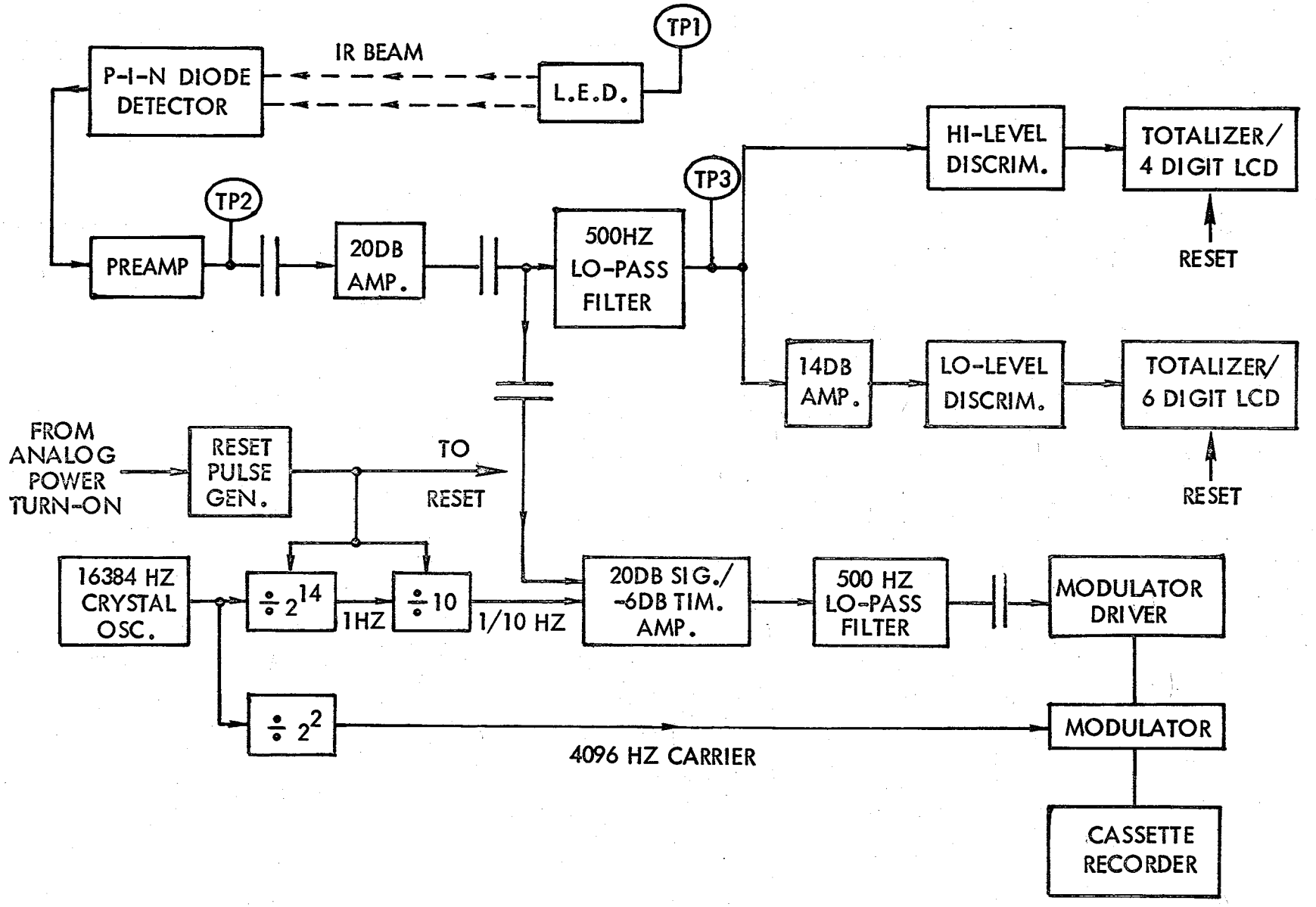

Figure 3.11. Airborne LED Detector Electronic Circuits Block Diagram

Table 3-2. Airborne LED Detector System - Battery Complement

Function	Voltage (V)	Number, Type+	Turn-on	Location
Analog Electronics	+12.5	E 289-Hg	T/M Sig.	L.C.
Analog Electronics	-12.5	E 289-Hg	T/M Sig.	L.C.
Digital Electronics	+12.5	E 289-Hg*	Manual Sw.	L.C.
LED Emitter	2.6	2-Pc E12N-Hg	T/M Sig.	L.C.
T/M Receiver	6.0	4-Pc AA alkaline	Manual Sw.	L.C.
Tape Recorder	5.0	Craig 8108 Ni-Cd pack.	T/M Sig.	Recorder
T/M Transmitter	10.5	7-Pc. AA alkaline	T/MT Sw.	T/MT

* Common with analog atteries

\+ Mercury cell types are Everready

L.C. lower compartment

T/MT T/M transmitter

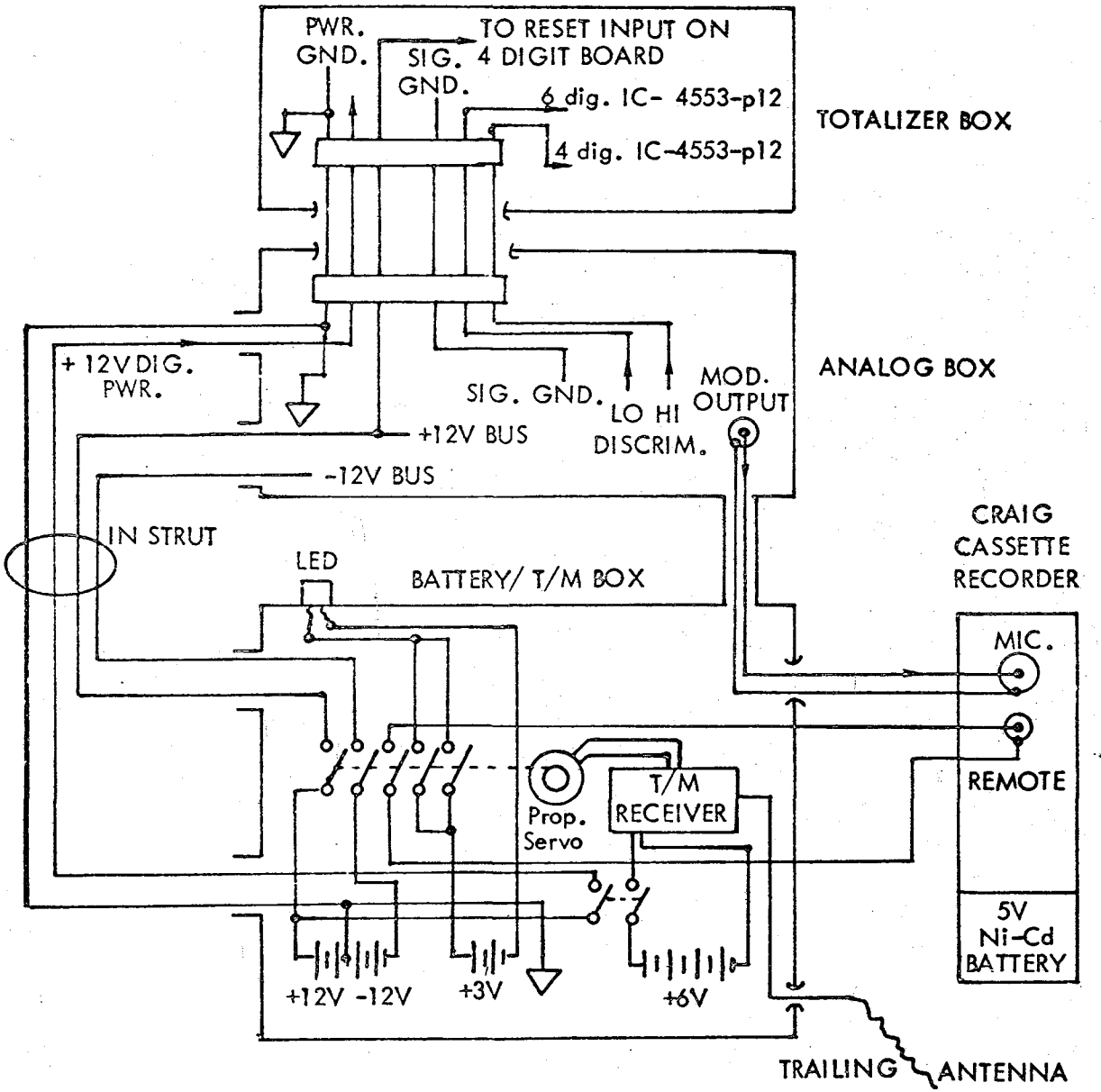

Figure 3.12. Airborne LED Fiber Detector System Interconnection Diagram

(1) The LED is turned on, producing the infrared light beam.

(2) The analog circuits are turned on.

(3) The crystal oscillator, countdown circuit, and clock pulsing circuits are activated.

(4) A reset pulse is sent simultanously from the analog circuits to the digital circuits and the clock countdown circuit about four seconds after turn-on. (This allows starting transients to die down before counting begins).

(5) The tape recorder electronics and tape drive are turned on.

Turning off the remote switch with the T/M transmitter stops the tape recorder and turns off all LED circuits except the digital display circuits. The display count will be retained until the manual switch is returned to the OFF position.

The basic structure is made up of three aluminum boxes. The upper two boxes are tied together with two aluminum plates through gaskets of polyethylene foam. The top plate of the uppermost box is bolted to two vibration isolators in series which are, in turn, screwed to a 0.19-cm diameter (3/16-in) hollow aluminum rod 0.46 m long. This tube is riveted to a short copper clasp, allowing the rod and detector system below it to swing freely about the rivet pivot in a vertical plane that also contains the net horizontal rope to which the copper clasp is attached. To help isolate the unit from the net vibrations, the net cable is covered with a short piece of split soft rubber tubing at the point of attachment. The long rod and the vertical orientation of the system, with the major weight in the bottom compartment, serve to decouple the detector from the low frequency net vibrations, allowing it to act as a unit.

The bottom compartment is separated from the top compartment by a rigid truss structure of aluminum struts. Each strut attachment uses flexible gasketing and epoxied bolts and nuts to preclude any buzzing vibrations caused by metal-to-metal contact. The attachment points are further covered with a quantity of RTV silicone rubber compound.

Each compartment is carefully filled with foam material to damp out possible box resonances. The tape recorder is positioned on an extended bottom compartment closure plate. Foam material is used between the plate and recorder to isolate the boxes from recorder motor vibrations, and the recorder is fastened to the plate with cloth tape.

Checkout and Calibration -- Prior to each field test in which the airborne LED units were used, the units were calibrated in accordance with the procedure outlined in Table 3-3.

Table 3-3. LED Detector Checkout and Calibration Procedure

TASK	PROCEDURE	REMARKS
Emitter Current Adjustment	• Adjust LED current to 100 mA	Measurement made at TP1
Optical Alignment	• Collimate IR beam with emitter optics for constant diameter beam • Adjust direction of IR beam to intercept the center of the detector • Adjust the focus of the detector optics	Requires an IR viewer to see beam
Discriminator Adjustments	• Set up large particle to small particle detection ratio • Adjust pre-amp gain for large particle detection threshold level	Requires fiber or wire 6 μm dia and >15 mm long
Tape Recorder Signal Input	• Adjust carrier signal level for minimum level • Set output level to 10 V peak-to-peak for fiber detection	Requires fiber or wire 6 μm dia and >15 mm long

GROUND-BASED LED SENSORS

Description -- A light obscuration instrument had been previously developed by TRW for use at a number of test sites under Air Force sponsorship (Figure 3.13). In particular, twenty of these LED gage systems were deployed on the ground for the 1978 burn-and-explode test series at NWC in China Lake (ref. 3). As mentioned before, this design was used as a point of departure for the development of the airborne detector system. For the Dugway large-scale burn tests in October and November 1979, two of these units were deployed on the ground.

The principle of detection is the same as described in the section on the airborne system, however, the LED beam is oriented horizontally whereas the beam for the airborne units is oriented vertically. The sensitive fiber detection area perpendicular to the beam is $3.2 \times 10^{-3} m^2$ bounded by the average beam diameter of 12 mm and the length from collimator to collimator of 26.7 cm.

LED INSTRUMENT CHECKOUT

Both the ground-based and airborne LED systems were checked out in an on-going test program in the large shock tube facility at NSWC, Dahlgren, Virginia (ref. 4). This facility had been partially converted for the test series to allow relatively large amounts of carbon composite material to burn over a 1.2 x 1.2-m JP-1 pool fire inside the shock tube. At one end of the shock tube, exhaust fans were operated to provide an air flow field in the tube. Approximately 200 m downstream of the fire, experimental instrumentation and electronic equipment were set up to measure the fiber passage and, in the case of the electronic equipment, the vulnerability to the fire-generated fibers.

TRW instruments were set up for three of these tests. For the first test, No. 52, airborne unit A-1 and ground-based unit G-10 were used together with a borrowed amplifier and tape recording unit. Difficulties were experienced with the burn and the test was aborted.

Test No. 53 -- For the second test, No. 53, the airborne detector A-2 and the ground-based detector G-10 were fielded. Vugraph bridal veil collectors, coated with Rhoplex adhesive, were mounted vertically in close proximity to the two detector systems (Figure 3.14). The floor positions of each detector at the test section are shown in Table 3-4. To provide backup coverage and test monitoring, the output of unit G-10, the input to the cassette tape recorder of unit A-2, and the output of the unit A-2 detector preamplifier were fed out of the shock tube to recording facilities in an adjacent trailer.

Since large amounts of soot were expected from the burn over a long period of time, it was anticipated that the lens systems might become coated during the test by this soot, hence a digital voltmeter was connected to the preamplifier output and the signal level monitored during the test. Loss of voltage would be attributable to (a) loss in battery voltage and (b) coating of the lens system. In either case, the pulse height for a given fiber length passing through the beam should be directly proportional to the DC level recorded (assuming the coating to be distributed over the lenses).

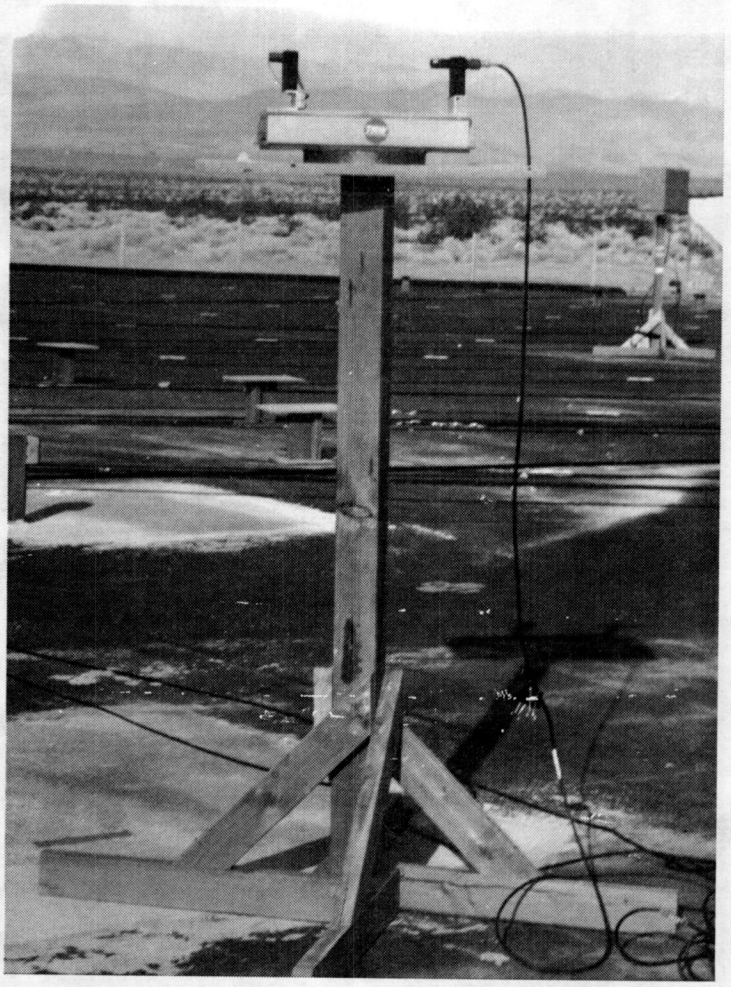

Figure 3.13. LED Gages Used at NWC Field Tests

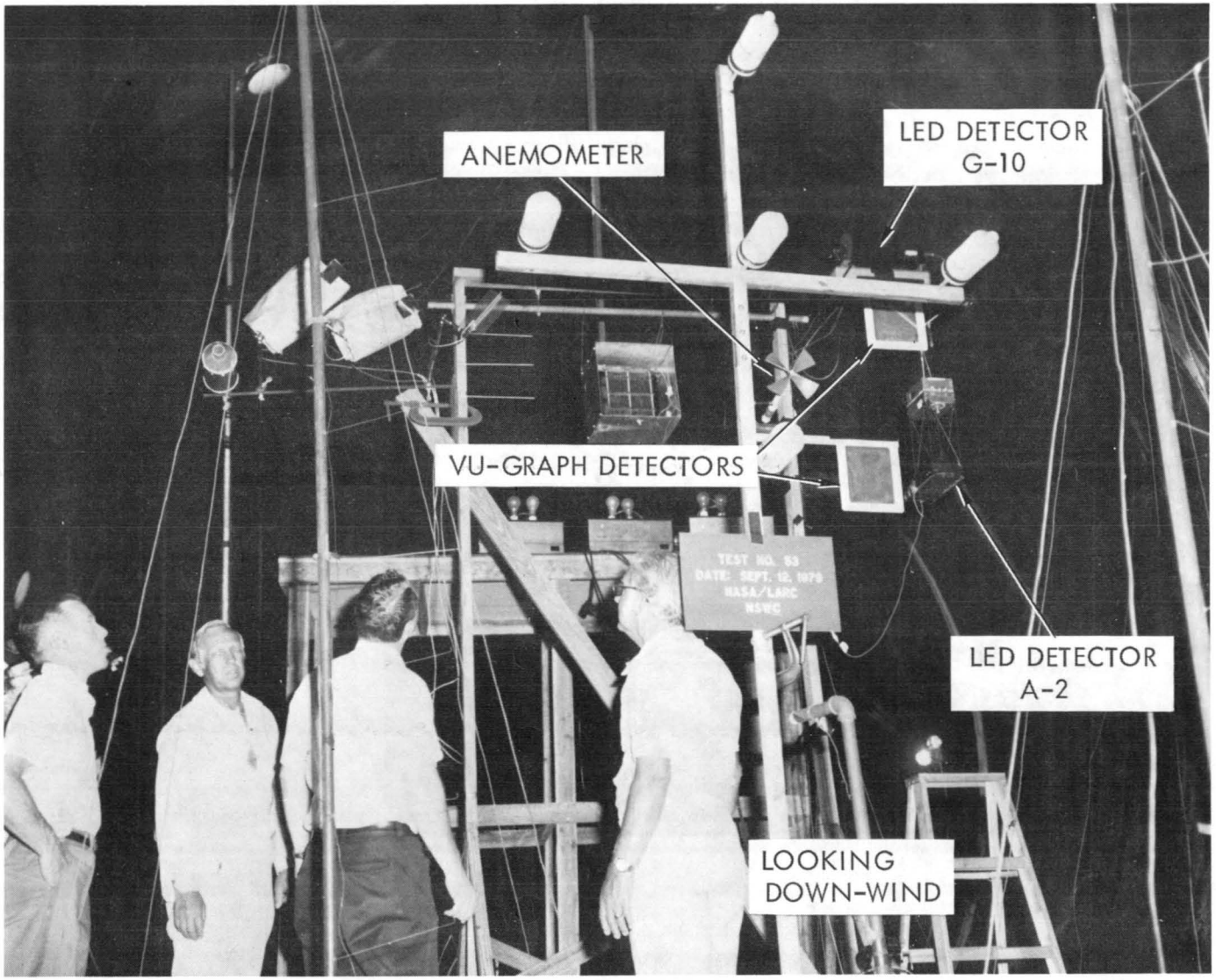

Figure 3.14. Confined Burn Test No. 53 TRW Detector Placement

Table 3-4. Detector Positioning in Test Section

Test	Unit	Vertical Position Above Floor (m)	Distance from Chamber Centerline (m)
53	A-2	2.5	1.2 South
	A-2 vugraph	2.3	0.9 South
	G-10	3.15	1.0 South
	G-10 vugraph	2.9	1.04 South
	Anemometer	2.6	0.6 South
54	A-1	2.4	0.15 North
	Vugraph above A-1	2.9	0.15 North
	A-2	2.45	1.1 South
	Vugraph above A-2	2.9	1.1 South
	G-10	3.15	0.65 South
	Anemometer	Variable	~0.3 South

Material and soot were first detected at the G-10 location, 2 min 28 s into the burn. Fiber counts were received at the A-2 location at 3 min 3 s into the burn, followed by soot at 3 min 43 s into the burn. For some minutes after this, the soot was heavy enough to saturate the outputs from both detectors. Not until twenty minutes into the burn could individual counts, from fibers, be distinguished with certainty. At 134 min, the A-2 preamp output was measured at 0.400 V, which can be compared with a measurement of 0.69 V before the test was started. Such a drop can be attributed entirely to a drop in LED current input from the expected loss in battery voltage; hence, it did not appear that soot was coating the lens systems. This was confirmed after the test by careful cleaning of the lens surfaces with an alcohol-soaked cotton swab.

Figure 3.15 presents the results taken from the oscillograph recording for both active detectors. The minimum length sensitivities given for each detector primarily are due to background noise limitations and are accurate to about ±1 mm length.

Integration of the G-10 data over the length of the experiment gives a fluence/deposition through the detector of 1.4×10^6 fibers/m^2, assuming that the fiber flux remains constant from the onset of soot to the first data point at 20 min. (Assumption of a constant rise from zero flux at onset to the value at 20 min reduces the value reported by less than 5%).

Integration of A-2 data over the length of the experiment gives 1.0×10^6 fibers/m^2 if the flux is assumed level from soot onset to 20 minutes. If the data point at 3 1/2 min is included with a smooth falloff to the 20-min value, the integration gives a fluence of 1.1×10^6 fibers/m^2.

A small area of the vugraph detector positioned under G-10 was analyzed with a 100 power microscope with the primary aim of determining fiber lengths and diameters passing through the active detectors. The raw data are tabulated in Table 3-5 in terms of the length and diameter measurements for each fiber encountered. Using these data and the area measured, a length spectrum was determined and is presented in Figure 3.16. Since the mesh opening in the vugraph is approximately 0.9 mm, interpretation of fiber counts below this length must eventually include calibration of the "slippage" or percentage of particles passing through the mesh. These slippage values for the very short lengths displayed were not factored into the graph. As noted in the figure, integration of fiber lengths greater than 1 mm gives a fluence/deposition of 1.3×10^6 fibers/m^2. At the estimated threshold of 2 mm length for G-10, this drops to 4×10^5 fibers/m^2 showing agreement with the active G-10 data within a factor of 2 or 3.

Digital outputs on A-2 were 4-digit - 5250 counts, and 6-digit - 11852 counts, representing, for 6-μm-dia fibers, those counts above 1.5 mm and 15 mm lengths, respectively. These counts were meaningless because of the long amount of time the detector operated in heavy soot.

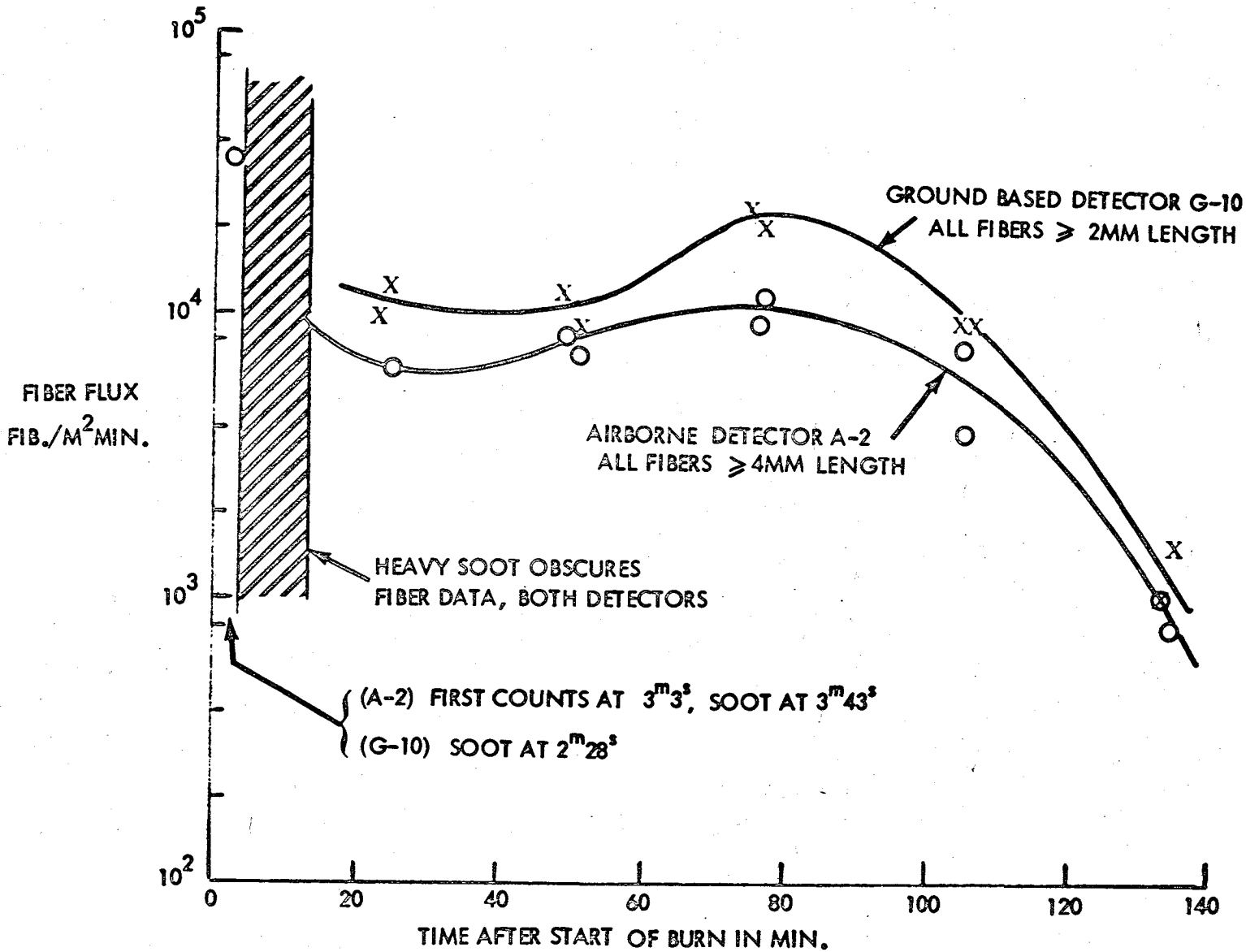

Figure 3.15. Composite Burn Test No. 53 - TRW LED Detectors Fiber Flux Data

Table 3-5 Burn Test No. 53 - Vugraph Fiber Deposition

Lgth (0.1 mm)	Dia (μm)	Lgth (0.1 mm)	Dia (μm)	Lgth (0.1 mm)	Dia (μm)	Lgth (0.1 mm)	Dia (μm)
>40	5	6	4	3	4	0.9	(6 + debris)
40	6	6	3	3	1 to 4	0.8	7
35	6	6	(<1-4-2)	3	2	.8	6
30	6	6	(<1-4-2)	3	2	.8	6
>25	(<1 to 4)	6	2.5	3	(<1-2-<1)	.8	6
20	4	6	2.5	3	1	.8	5
20	4	6	1	3	<1	.8	5
20	(1 to 3)	6	<1	2.5	<1 to 3	.8	4
20	2.5	>5	5	2.5	1.5	.8	4
18	2	>5	4	2.5	1	.8	2
16	6	>5	4	2	6	.8	1
14	6	5	6	2	6	.8	1
14	5	5	6	2	5	.8	1
14	3	5	5	2	5	.8	1
13	5	5	5	2	5	.8	1
12	5	5	4	2	5	.8	1
12	5	5	4	2	3	.8	1
12	5	5	4	2	2	.8	1
12	4	5	<1 to 3	2	2	.8	<1
12	4	5	1.5	2	2	0.7	1
12	1 to 3	5	1.5	2	<1 to 1.5	.7	1
12	2	5	1	2	1	.7	<1
11	4.5	5	1	2	1	0.6	<1
>10	(2 to 4)	4+	6	2	1	.6	<1
10	5	>4	6	2	1	.6	<1
10	5	>4	5	2	1	.6	<1
10	5	>4	4	1.5	5	.6	<1
10	4	>4	2	1.5	4	0.5	6
10	4	4	6	1.5	<1	.5	5
10	4	4	5	1.5	<1	.5	5
10	4	4	5	1.2	<1	.5	3
10	4	4	5	1	6	.5	3
10	(2 to 4)	4	5	1	6	.5	2
10	1.5	4	5	1	6	.5	2
10	1	4	5	1	6	.5	1
9	6	4	5	1	5	.5	1
9	6	4	4	1	5	.5	<1
9	4	4	4	1	5	.5	<1
8	6	4	4	1	5	0.4	5
8	6	4	3	1	5	.4	1
8	6	4	3	1	1 to 5	.4	1
8	6	4	1 to 3	1	4	.4	<1
8	5	4	2	1	4	.4	<1
8	5	4	2	1	4	0.3	6
8	4	4	1	1	3	.3	<1
8	1 to 4	4	1	1	3	.3	<1
8	1 to 3	4	1	1	3	.3	<1
8	<1	4	<1	1	3	0.2	1.5
>7	5	4	<1	1	3		
7	7	3	6	1	2		
7	4	3	6	1	1.5		
7	2	3	6	1	1		
>6	6	3	5	1	1		
>6	4	3	5	1	1		
>6	4	3	5	1	1		
6	6	3	5	1	1		
6	5	3	1 to 5	1	1		
6	5	3	4	1	1		

Notes: Vugraph area counted - 24.6 mm^2
Vugraph mesh opening nominally 0.9 mm

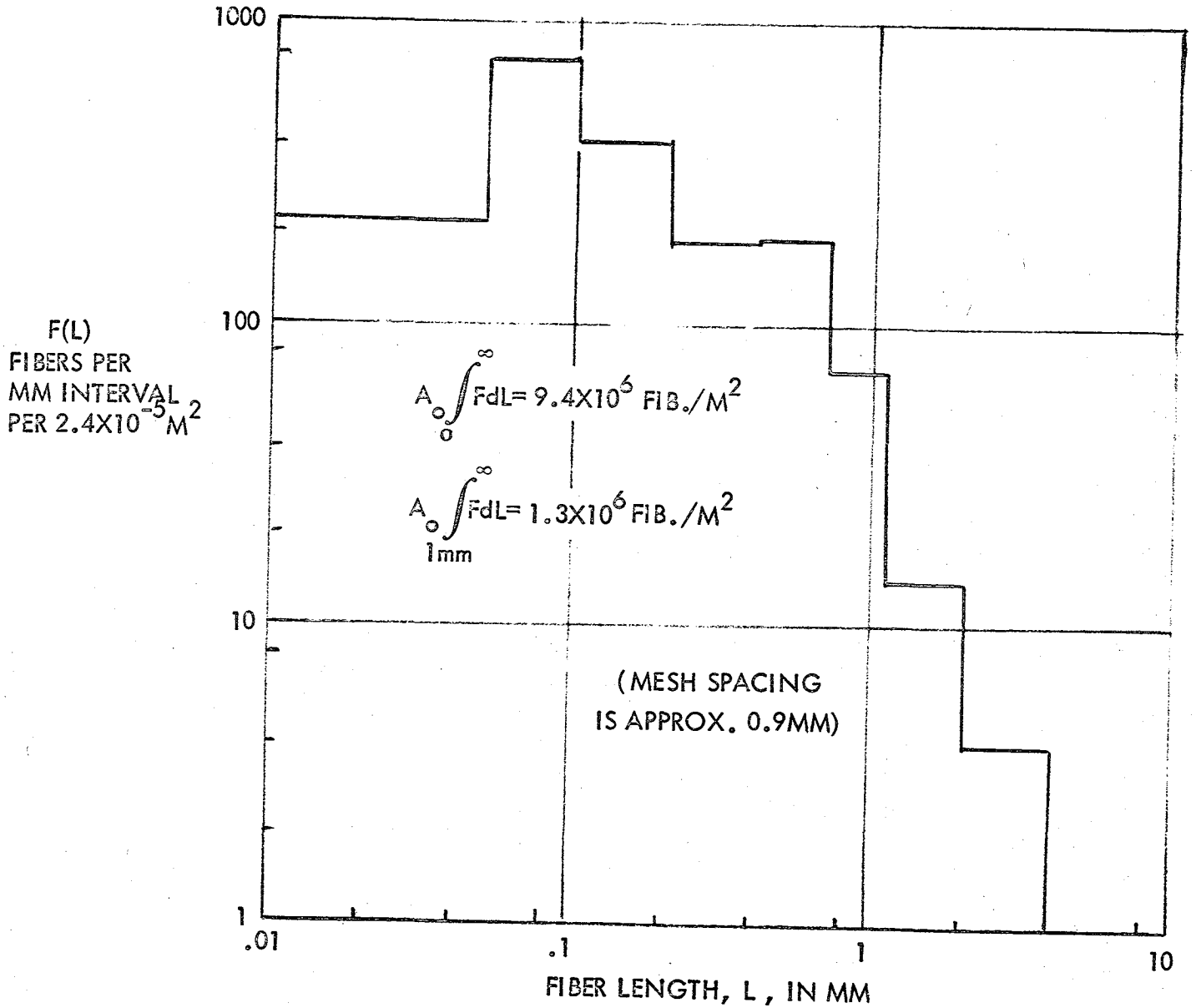

Figure 3.16. Composite Burn Test No. 53 - TRW Vugraph Fiber Length Study

Although the backup parallel output line to the trailer recorders worked well, the built-in tape recorder on unit A-2 did not operate. It was discovered later that the recorder pause button was inadvertantly depressed, preventing the unit from recording.

Test No. 54 -- In this test, designed as a baseline test for detector systems and vulnerability tests, a large quantity of fiber glass epoxy composite was burned. Detection systems and equipment sensitive only to conductive fibers should not detect the glass fibers. However, the LED systems cannot distinguish between glass or carbon fibers, and therefore, the test could serve as a further checkout of the systems with some attempt made to remove the sensitivity to the soot environment. For this test, the ground-based detector G-10 was again fielded together with both airborne units A-1 and A-2 and two vugraph collectors. Placement coordinates of the systems are given in Table 3-4.

For the small obscuration ratios required for detecting single fibers (typically 1×10^{-4}), the fiber obscuration ratio will remain unchanged as the detector length is reduced (although the detection efficiency will be reduced) while the soot obscuration ratio at a given density will be reduced linearly. Hence, over a limited range of soot densities up to the point where the DC preamplifier saturates, a shortened detector length will see fiber passage at a correspondingly higher density of soot. For this test, detector system A-1 was modified by adding a blackened cardboard tube attached to the p-i-n diode detector end of the unit. By this means, the sensitive LED beam length was reduced from 17.6 to 4.8 cm, a reduction factor of 3.7.

The setup for the No. 54 test was similar to the previous tests. As before, calibrations were made on each unit and recorded on tape recorders and an optical recorder. The output voltage from each airborne detector was monitored as before. Some loss in preamplifier output was noted for each airborne detector. The loss in each case was gradual, and after a two-hour shutdown the output recovered almost to original levels. Since the heavy soot was noted only during the first 20 to 30 minutes, loss caused by soot accumulation should have produced abrupt reductions in output levels without recovery; hence, the loss in signal was not due to soot accumulating on the lenses but to loss in battery voltage. For best performance over long operating periods, future designs could include a current regulator in the LED supply lines.

Digital integral counts for the two detectors were obtained, but because of the heavy soot and consequent saturation of outputs, do not have any meaning. Future tests operating in the heavy soot environment, even if briefly, will unfortunately not have digital outputs as useful quick-look data.

As before, the detector recordings were analyzed for each detector system (Figure 3.17). No data could be obtained before 15 min into the burn, and then only on the modified detector A-1. Qualitatively, it appears that the ability to discriminate against a soot background is indeed an inverse function of the sensitive length of the detector.

The flux values obtained for detector A-1 and the average of G-10 and A-2 were integrated over the experiment time, giving a total fluence/deposition of 7×10^5 and 2.3×10^5 fibers/m^2, respectively.

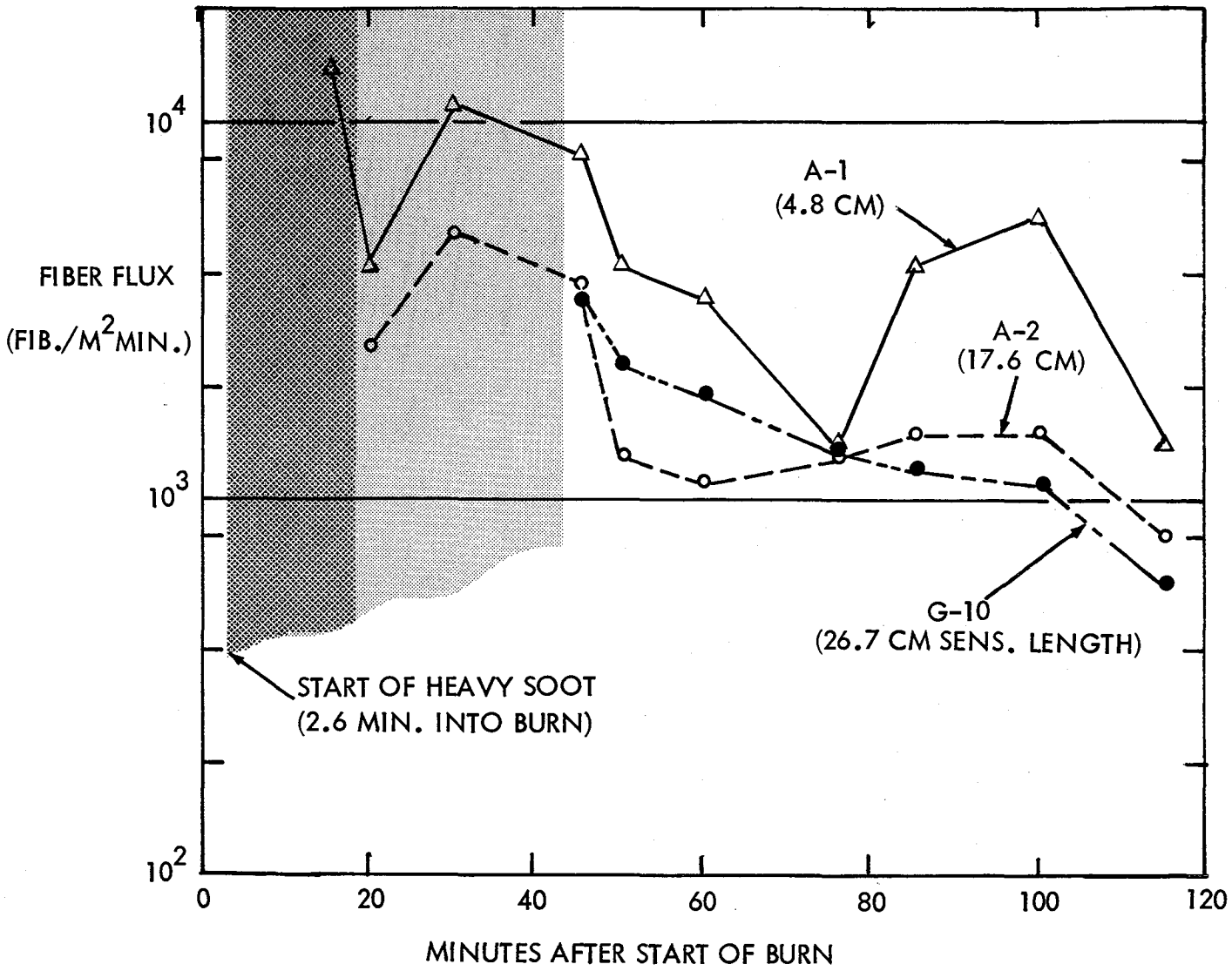

Figure 3.17. Test No. 54 - TRW LED Detector Outputs

An analysis of the vugraph data near the A-1 detector gives the fiber glass length distribution shown in Figure 3.18. All fibers observed had a diameter of approximately 10μm. This diameter applied to the pulse-height thresholds for the active detectors and the calibrations of these detectors with a 6μm fiber translate to a glass fiber length threshold for the three detectors of 2 ± 1 mm for A-1, 1 ± 0.5 mm for A-2, and 0.8 ± 0.4 mm for G-10. As in the previous vugraph count data, these results have not been corrected for "slippage" through the 0.9 mm mesh opening for the fiber in the short length regime. Integration of all fiber lengths observed over 0.8 mm in length gives a fluence/deposition of 4×10^4 fibers/m^2. This value is about a factor of ten less than that obtained by the active detectors. This discrepancy may be attributable to the significant number of large soot agglomerates observed on the vugraph records, many of which have a cross-sectional area at least as large as fibers (this phenomenon was not seen in the previous test which burned carbon composite).

The following conclusions may be drawn from the testing:

(1) In their present configuration, the units cannot distinguish fiber passage in the presence of "large" amounts of soot.

(2) Soot deposition on critical lens surfaces is not significant, even over periods up to one hour.

(3) Some gain in discrimination sensitivity against a soot background can be achieved by reducing the path length of the light beam, but only at the expense of reduced detection sensitivity.

(4) The digital "quick-look" fiber counters operate effectively if the detectors are not in the soot stream. Since they are integral counters, any time spent in a high soot environment during the detector activation time will seriously compromise or negate the usefulness of the display counts in interpreting data.

(5) Ground-based and newly developed airborne LED detector outputs appear to track well.

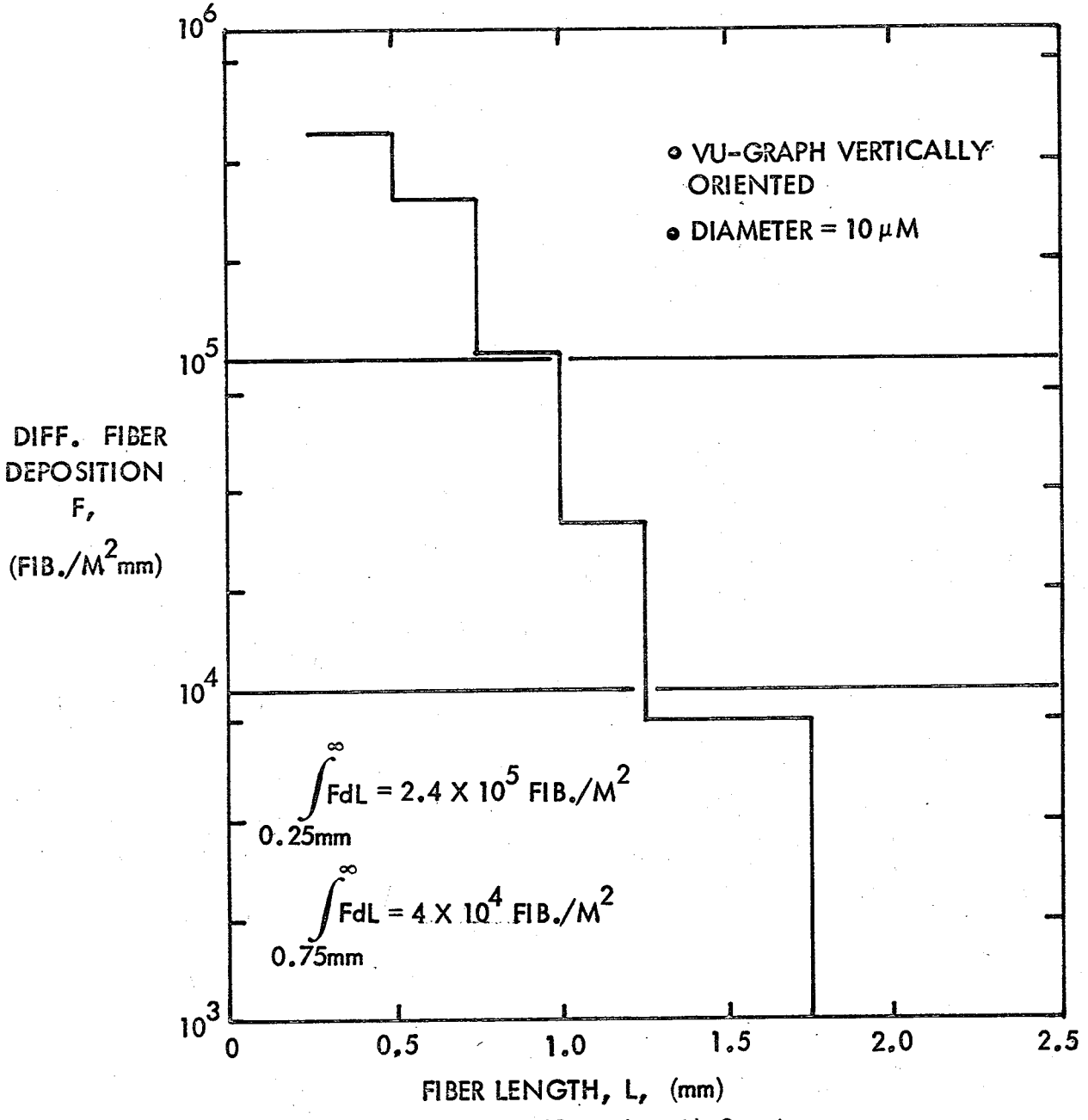

Figure 3.18. Test No. 54 - Fiber Glass Length Spectrum

4. DUGWAY FIELD TESTS

The first part of this section of the report presents a summary of the test conditions under which the three field tests (D-1, D-2, and D-3) were conducted at Dugway Proving Ground during the month of October and November 1979 (ref. 1). A more complete description of the overall test plans and procedures is presented in an Army test operations document (ref. 5) published prior to the conduct of the tests. This referenced document presents the overall test objectives, site layout and descriptions of all test operations, plans, procedures and fielded instrumentation, including test elements and instrumentation not the subject of this TRW report but fielded by other contractors and government agencies.

The second part of this section describes the layout and operational conditions of the Jacob's Ladder, vugraph collectors, and airborne and ground LED fiber detectors as they were fielded for each of the three tests. Due to variations inherent in the erection of the Jacob's Ladder and in the locations of the LED instruments from test to test, slight but significant differences in operational conditions existed for each test.

TEST CONDITIONS

The first burn test, designated D-1, was conducted on 26 October 1979 at 3:03 pm (MDT). Approximately 46 kg of carbon fiber composite material was exposed over a 10.7 m dia JP-4 fuel fire. Some of the items burned are shown in Figure 4.1. The average wind speed and direction at the time of the test was 6.4 m/s and 40° to the west (to the right, looking downwind) of the test site centerline. The total burn time was approximately 19 minutes.

The second test, designated D-2, was conducted on 31 October 1979 at 9:41 am (MST). The same amount of carbon fiber composite material, approximately 45 kg, was burned as in test D-1. Figure 4.2 is a photograph of some of the items in place to be burned. The average wind speed was 5.8 m/s while the average wind direction was 31° to the east (to the left looking downwind) of the test site centerline. The total burn time was approximately 20 minutes.

The third test, designated D-3, was conducted on 9 November 1979 at 12:31 pm (MST). The items burned consisted of a set of right and left F-16 horizontal stabilizers and the exterior surfaces of an F-16 vertical stabilizer. These parts were positioned over the 10.7 m dia pool fire as shown in Figure 4.3. The horizontal stabilizers were constructed of an inner core of aluminum honeycomb with exterior surfaces of carbon fiber composite of varying thickness. These horizontal stabilizer parts were recovered from an actual F-16 aircraft crash in which they were partially damaged as can be seen in the photographs. The vertical stabilizer parts were only the exterior carbon composite surfaces of an F-16 vertical stabilizer. The approximate mass of the carbon fiber composite was 70 kg.

The average wind speed for this third test was 5.3 m/s, somewhat lower than the first two tests. The average wind direction was 6° to the west of the test site centerline. The total burn time for test D-3 was approximately 23 minutes.

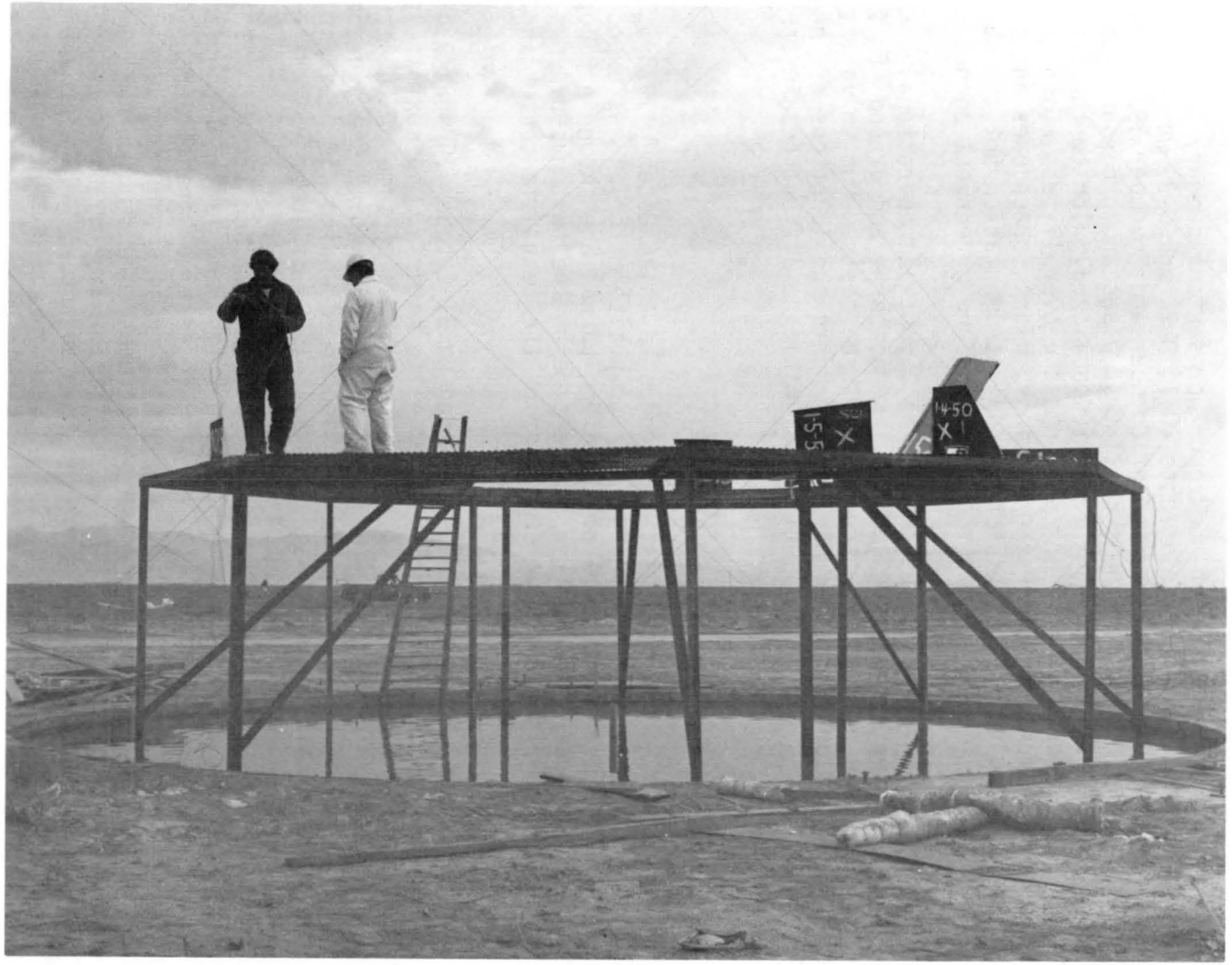

Figure 4.1. Burn Site Photograph for Test D-1

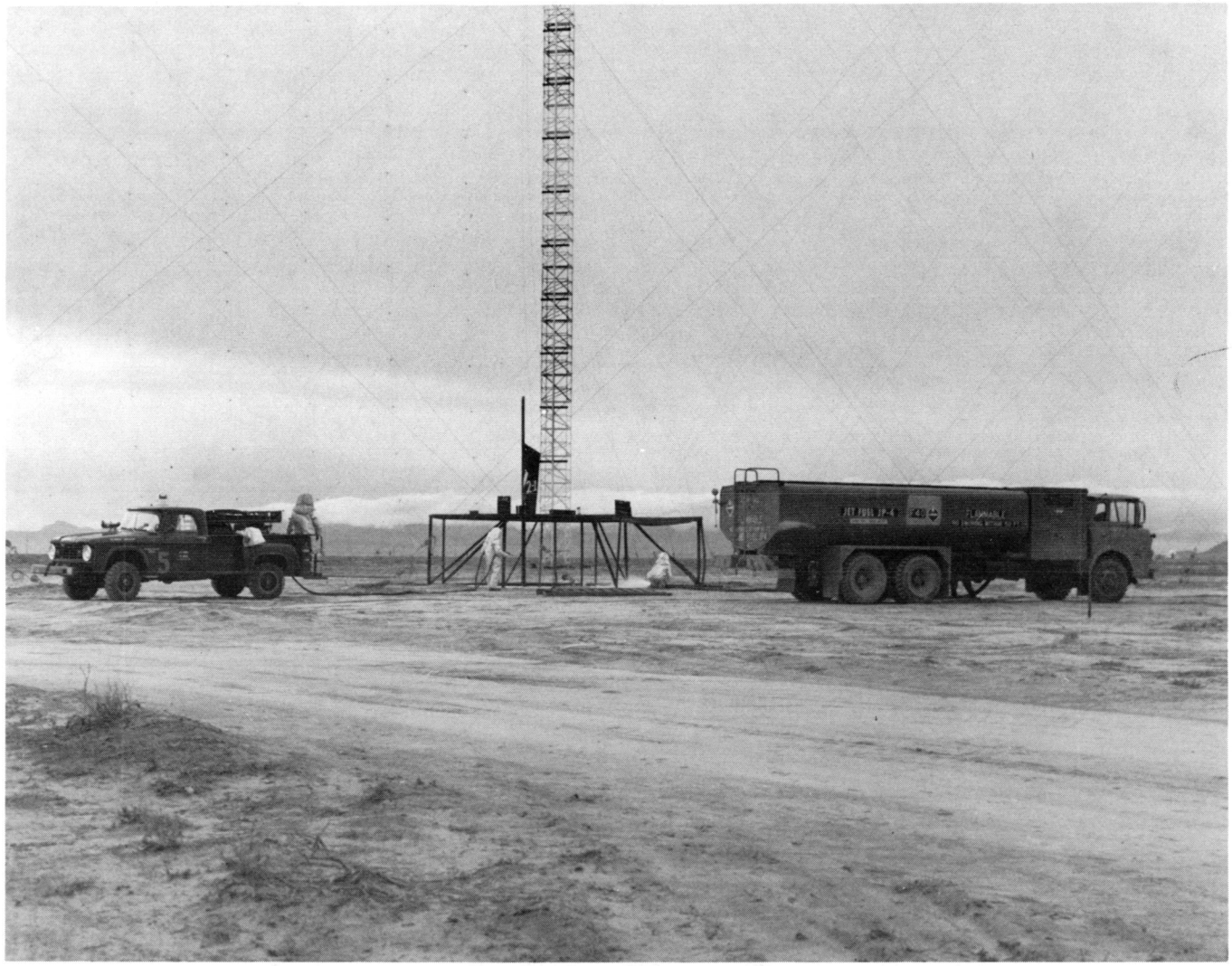

Figure 4.2. Burn Site Photograph for Test D-2

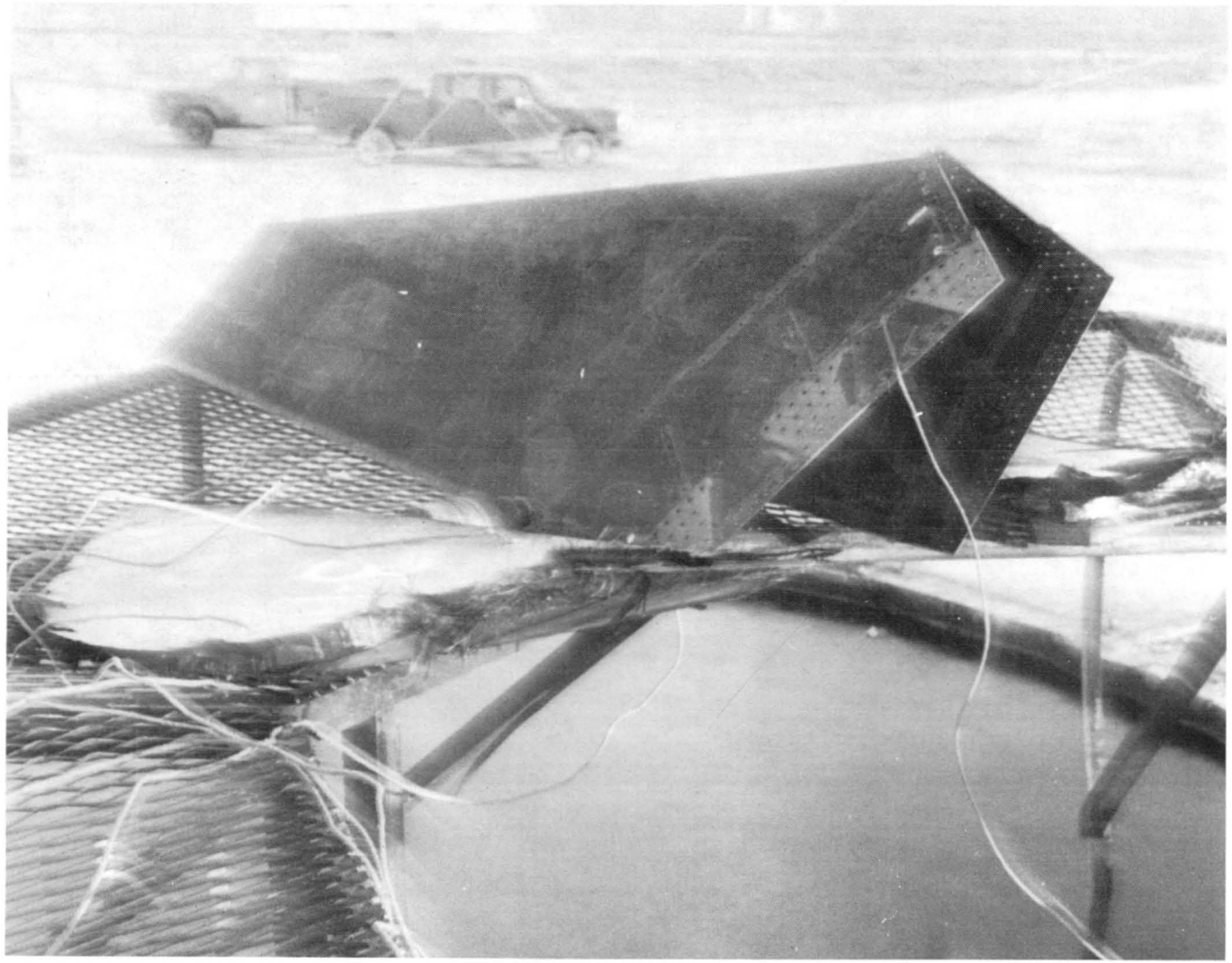

Figure 4.3. Burn Site Photograph for Test D-3

Of particular significance in this test was the observation that approximately seven minutes into the burn period, the structure supporting the composite burn samples partially collapsed due to thermal weakening of the structure. This collapse lowered the burn samples from an initial height of about eight feet over the fire to a height of 2 to 3 ft, placing the stabilizers in a less intense region of the flame.

A summary of the test conditions for the three tests is given in Table 4-1. All three tests were conducted under a neutral stability meteorological condition.

INSTRUMENTATION LAYOUT

JACOB'S LADDER

The Jacob's Ladder was installed with its base located 117.3 metres downwind from the center of the fire pool used for the three tests. The base of the net extended crosswind 152 metres on either side of the test site centerline. Vertically, the net nominally extended to an altitude of 304 metres. Other details of the Jacob's Ladder installation are included in Section 2 and Appendixes B and C.

The Jacob's Ladder profile for each test is shown in Figure 4.4, and photographs of a part of the net and the test site were shown previously in Figures 3.6 and 3.7. Indicated in Figure 4.4, are the estimated vertical net intersection (vugraph collector) locations for each test. These estimates for tests D-1 and D-3 were determined from observations of the mooring line geometry made during the test. Test D-2 setup was assumed to be similar to test D-3 as no observations were made. The angle α, was used to correct the fiber count data for net geometry as described in Section 5.

VUGRAPH FIBER COLLECTORS

Vugraph collectors were attached to the Jacob's Ladder net on the day preceding the scheduled test date. The installation procedure used is described in Appendix C, and a photograph of an installed vugraph was previously shown in Figure 3.1. Prior to installation, the vugraphs were sprayed with Rhoplex to provide a sticky surface on the vugraph bridal veil mesh.

Following the test and lowering of the Jacob's Ladder, the vugraphs were removed, covered with acetate sheets, and boxed. To prevent contamination of vugraphs by personnel prior to their being covered by acetate sheets, the vugraphs furthest downwind on the Jacob's Ladder were collected first.

Table 4-1. Test Condition Summary

Test	Date	Time	Pool Fire Diam (m)	Approx. Burn Duration (min)	Average Wind		Burn Sample Weight (kg)	
					Speed (m/s)	Direction (degrees)	Carbon Composite	Carbon Fiber .
D-1	10/26/79	3:03 pm	10.67	19	6.4	40 to west	46.2	32.3
D-2	10/31/79	9:41 am	10.67	20	5.8	31 to east	45.48	31.8
D-3	11/9/79	12:31 pm	10.67	23	5.3	6 to west	70.77	49.5

VUGRAPH VERTICAL LOCATION SCHEDULE

VERTICAL NET INTERSECTION DESIGNATION	TEST D-1		TEST D-2 AND D-3	
	ALTITUDE (m)	α * DEGREES	ALTITUDE (m)	α * DEGREES
H-5	216	9	222	3
H-6	200	10	206	4
H-7	184	11	190	6
H-8	168	13	174	7
H-9	153	25	158	8
H-10	138	26	142	10
H-11	122	27	126	11
H12	106	30	110	12
H-13	91	32	94	14
H-14	76	34	79	15
H-15	62	37	64	16
H-16	49	41	49	27
H-17	36	45	35	34
H-18	24	50	23	43
H-19	13	54	11	55
H-20	5	62	3	70

* VUGRAPH PLANE WITH RESPECT TO VERTICAL

TEST	θ (DEG)	A (m)
D-1	~ 70	280
D-2	~ 80	290
D-3	~ 80	290

NET PROFILE

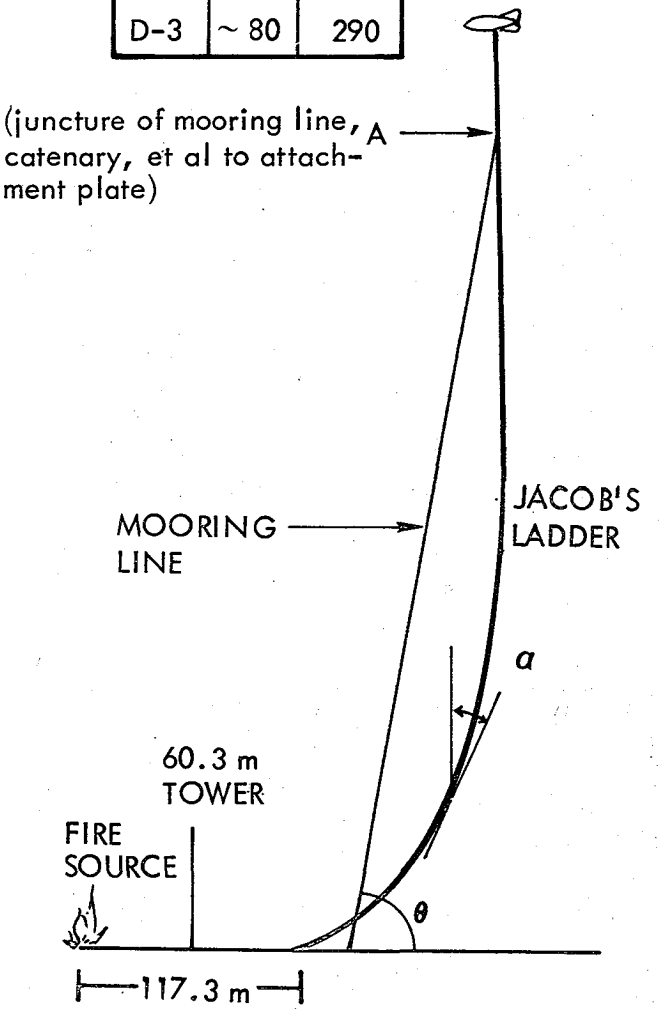

Figure 4.4. Crosswind Vertical Profile of Net

Vugraphs were labeled as they were installed on the net in accordance with their position on the Jacob's Ladder net. The coordinate system used an H-( ) number and a V-( ) number to represent the net horizontal line and vertical line intersection where the vugraph was located. The ladder horizontals were numbered H-1 through H-20, starting at the top horizontal, with the ladder erected. The ladder verticals were numbered V-1 through V-21, starting with the vertical to the east (left looking downrange) of the test site centerline. As discussed above, the vertical position (altitude) of each vugraph varied slightly among the three tests due to the differing ladder profiles for each test.

LED FIBER DETECTORS

Four of the LED detector systems were fielded for each of the three tests at the Dugway Proving Ground. The two airborne units designated A-1 and A-2 were attached to, and lofted by, the Jacob's Ladder. Placement of these units was dictated initially by the desire to obtain a vertical fiber flux profile near the test site centerline. Hence, for tests D-1 and D-2, both were attached to horizontal net cables within two metres of the net centerline vertical cable, V-11. Detector A-1 was attached to the H-17 net horizontal cable (35 m altitude), and A-2 was attached to horizontal H-11 (about 121 m altitude).

The two ground-based units, designated G-10 and G-15, were mounted about 1.2 metres above ground level for all three tests. The positioning of these ground-based units is shown in Figure 4.5, which also defines their relationship to the fire origin and several other instrument systems fielded by Dugway Proving Ground (DPG). This positioning was used for all of the three tests. For tests D-1 and D-2, the vertical projection to the ground of the position of detector A-1 falls almost on top of detector G-10.

The wind directions for tests D-1 and D-2 were such that airborne detectors intercepted only the extreme edges of the fiber clouds. To insure that at least one airborne detector would intercept a more central portion of the fiber cloud, the airborne detectors were repositioned for test D-3. Detector A-1 was positioned at the intersection of net cables H-10 and V-7, at an altitude of 141 m and 61 m east of the test site centerline, while detector A-2 was positioned on the same net horizontal cable (H-10) at its intersection with the net vertical V-15, 61 m west of the centerline. The recording and associated power and amplifier equipment for the ground-based LED systems was located in a small two-man tent about 180 m from the detectors. This location is shown in Figure 4.5. Use of the tent served to keep the dust, dirt, carbon fibers, and rain from the equipment inside. During the cold, windy periods, it also served to keep the equipment at a relatively even and warm temperature.

Prior to each test, all non-rechargeable batteries were replaced in each airborne unit, in the ground-based amplifiers and detectors, and in the telemetric transmitters. The rechargeable batteries for the airborne detector cassette tape recorders and the marine lead-acid batteries supplying power for the ground-based detectors were kept in a fully recharged condition between tests and were emplaced in the field the day before each test.

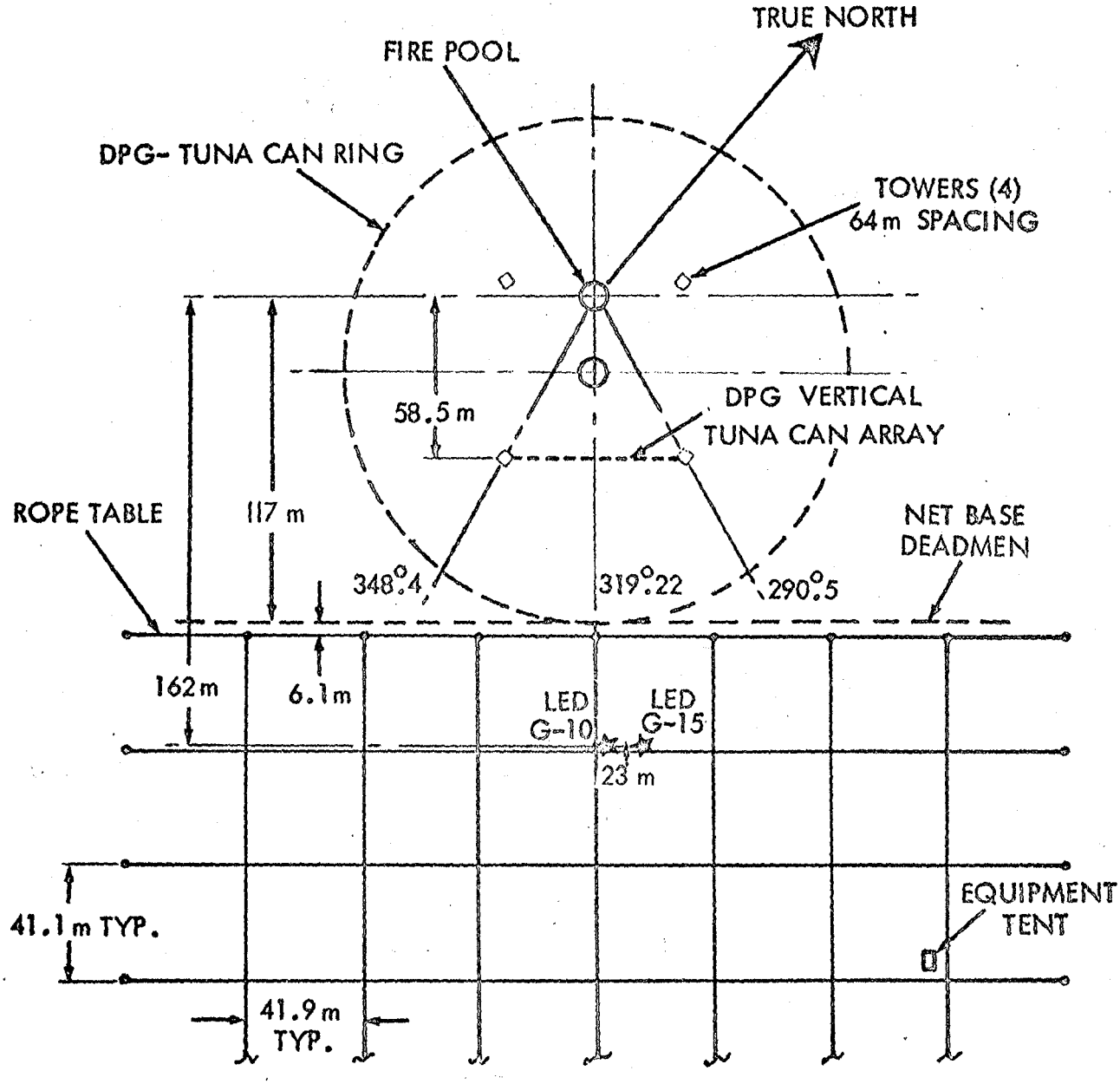

Figure 4.5. Ground Based LED Fiber Detector Locations

Prior to the three tests, a checkout flight of the Jacob's Ladder was conducted in which the airborne LED detectors were attached to the net and operated. Data returned from the detectors showed a very high noise background not present before, and suspected to be caused by net vibrations. Therefore, before the first test (D-1), the detectors were mounted on short pieces of "bungey" cord, which was "ty-wrapped" on the ends, to the net horizontal. With the full weight of the detector on the "bungey" cord, the cord assumed an included angle of about 90^{o}. However, results from test D-1 showed even higher noise levels returned, such that it would be extremely difficult to detect fibers of length much less than 8 mm. Before the last two tests in the series were conducted, experiments were made with a simulated net horizontal, and it was decided that the shortest attachment to the net would be the best. Accordingly, a one-inch split piece of soft rubber tubing was used between the one-inch copper clasp and net rope to further attenuate the higher frequencies associated with wind driven "humming." No further extensions were used beyond the clasp. Data returned from the last two tests indicated some improvement in the noise levels, but they never came down to levels seen on the ground or out of the wind.

5. DATA ANALYSIS AND RESULTS

This part of the report presents the results obtained by the analysis and evaluation of the information contained in the reduced vugraph and LED sensor data. Before displaying and discussing these results, the techniques used for reducing the raw vugraph and LED sensor field data are described. These techniques are important to a full understanding of the results since they have a direct bearing on the accuracy and completeness of the test results. Also, knowing the data reduction techniques used for each of the sets of data acquired by the many different types of instrumentation fielded in the test series will provide the basis for better quantitative comparisons of the results.

VUGRAPH COLLECTOR DATA

DATA REDUCTION TECHNIQUES

The data reduction of the vugraph fiber collectors proceeded first with a qualitative screening of each collector. Next, sets of collectors were selected from each test for fiber counting and categorization. Finally, the tabulated fiber counts were corrected for collection efficiency and orientation geometry. This process provided tabulated data that could be analyzed for fiber characterizations and distributions.

At first examination, the vugraphs indicated that the collected fibers generally were distributed unevenly over the bridal veil mesh surface. To compensate for this uneven distribution, it was decided to examine approximately 50% of each collector surface, and count the fibers. The area examined was 0.019 m^2 out of the 0.046 m^2 total vugraph mesh collection area (Figure 5.1). Approximately 50% of the total 441 vugraph collectors fielded in each test showed evidence of collected fibers. Of this number, approximately 50% were selected for the fiber-counting process for tests D-1 and D-2, and 100% for test D-3 (Table 5-1).

Table 5-1 Vugraph Collector Data Reduced for Each Test

Test	Vugraphs Counted
D-1	95
D-2	100
D-3	223

Both the number of single fibers and fiber clumps (multiple fibers) were counted. The single fibers were categorized into intervals of fiber lengths. Seven intervals were used: 0.5 to 1 mm, 1 to 2 mm, 2 to 4 mm, 4 to 6 mm, and 8 to 10 mm; and fibers greater than 10 mm. The actual length of all fibers greater than 10 mm were measured and tabulated. In counting the fiber clumps, the approximate number of fibers in each clump, and the average length of the fibers, were estimated and recorded.

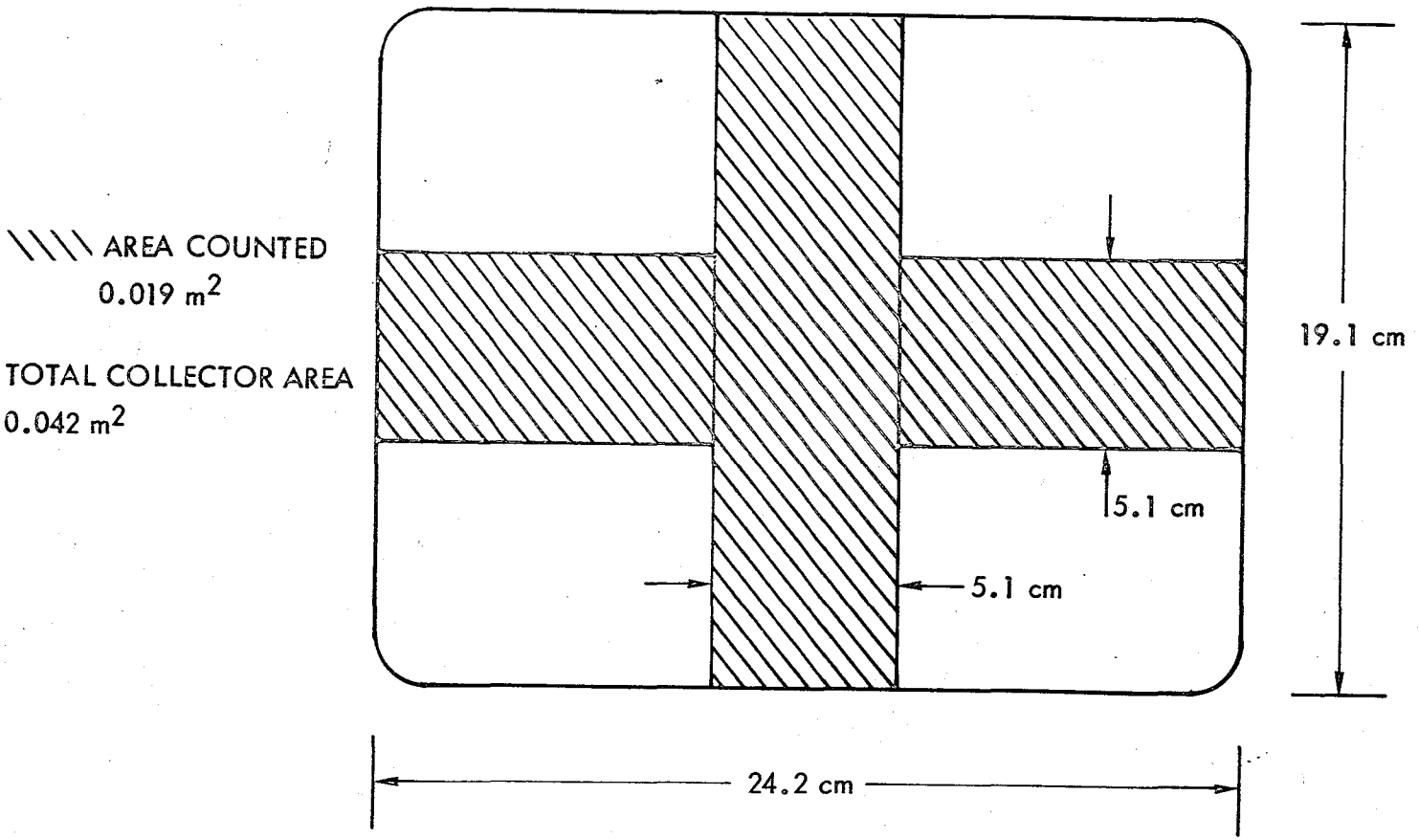

Figure 5.1. Vugraph Collector

The count data for the single fibers were then corrected for the vugraph mesh collection efficiency by applying a slippage factor (Table 5-2). The slippage factor, based on data obtained from Dr. John Trethewey of Dugway Proving Ground, is the percentage of incident fibers that pass through the bridal veil mesh (ref 6).

Table 5-2 Vugraph Collector Slippage Factors

Fiber Length (mm)	Slippage Factor (%)
0.5 - 1	32
1 - 2	16
2 - 3	9
> 3	Negligible

Both the single fiber and fiber clump data were corrected for the vugraph capture profile by applying a factor that accounts for the angle between the direction of the fiber path and the plane of the vugraph collector. This angle varied as a function of the altitude of the vugraph collectors suspended on the net because of the catenary shape of the net caused by the wind loading and weight of the net. Since the variations of wind loading and tether geometry varied with each of the three tests, the factors used for the correction were unique for each test. This net geometry, i.e., the catenary shape, was also used to determine the vertical position, or altitude, of each vugraph on the projected plane of the net. Net geometries are given in Section 4 of this report.

Finally each of the vugraph collectors was examined to determine the envelope of the soot cloud in the fire plume. The soot cloud was categorized qualitatively into "light" soot and "dense" soot regions.

RESULTS AND EVALUATION

Each of the vugraph collectors fielded on the Jacob's Ladder for the three tests in the series (D-1, D-2, and D-3) was processed using the counting techniques described in the previous paragraph. This provided a count of the fibers accumulated on each collector. These data were analyzed and evaluated systematically to obtain integrated information on the characteristics of the fiber cloud for each of the tests. The first step in this process was to apply factors to correct the fiber counts for collection efficiency and net geometry as described in the paragraph on data reduction techniques. These corrected data were then analyzed to obtain such information as the spatial distributions of the fibers; the average fiber length, and distributions by fiber lengths; the total fibers released; and the mass of fibers released from the burned composite. These results were obtained both for single fibers and fiber clumps.

Spatial Distribution in Fiber Deposition -- The spatial distribution of fibers in the projected vertical plane of the Jacob's Ladder was obtained by computing the number of single fibers per square metre (vertical deposition) for each vugraph collector suspended from the ladder. To obtain this value, the total

single-fiber count for each vugraph (corrected for slippage, net geometry, and percentage of vugraph area counted) was divided by the vugraph collection area (0.0462 m). Thus, this value is an estimate of the total number of fibers that transported through a vertical area of one square metre in the vicinity of each vugraph collector. The vertical depositions for each vugraph are given in Tables 5-3 to 5-5 for tests D-1, D-2, and D-3, respectively, as a function of altitude and crossrange distance. Although all single fibers down to 0.5 mm long were counted during the data reduction process, only fibers greater than 1 mm long were included in determining these vertical deposition values.

From these three tables, it may be seen that only for test D-3 did the Jacob's Ladder intercept the full width of the fiber cloud as it was transported downwind. For test D-1, the wind direction had an easterly component that directed the cloud to the west side of the net causing the westerly part of the cloud to pass outside the array of vugraph collectors. By assuming that the fiber cloud was approximately symmetrical about its vertical "centerline" (line of maximum deposition), the area of the fiber cloud sampled by collectors was estimated to contain 74% of the total number of fibers in the cloud. For test D-2, the wind had a westerly component and part of the cloud passed outside of the array on the east side. For this test, the cloud area sampled was estimated to contain 83% of the total number of fibers in the cloud.

For all three tests, the heaviest deposition occurred between ground level and about ten to fifteen metres altitude. The maximum deposition observed was for test D-1, at 65.2×10^3 fibers/m^2. The maximum depositions for test D-2 and D-3 were 40.3×10^3 and 42.9×10^3 fibers/m^2, respectively. In each of the tests, the fiber cloud extended to an altitude of approximately 200 to 220 m.

Figures 5.2 to 5.4 present a more or less qualitative display of the fiber deposition distribution for each of the tests. In addition, the fiber distribution displayed in these figures is overlaid with a crossrange profile of the fire plume soot density distribution showing the extent of "dense" soot and "light" soot regions. Of particular significance, as seen on these figures, is the fact that for all three tests the heaviest fiber depositions occur close to ground level where little or no soot is visible.

Figures 5.5 to 5.7 are similar displays showing the distribution of multiple fiber, or fiber clump, depositions. These depositions are given in intervals of the number of clumps per square metre in the fiber cloud. Again, the maximum depositions occur at near-ground-level altitudes where little or no soot was evident.

Figures 5.8 to 5.10 also present crossrange profiles of the fire plume soot densities for each of the three tests, as well as representative vertical and horizontal profiles of the single fiber depositions. A comparison of these profiles for the three tests shows that both the horizontal and vertical fiber deposition profiles can vary anywhere from essentially a single-peak distribution to distributions having as many as three significant peaks.

The deposition data presented previously in Tables 5-3 to 5-5 were converted to single-fiber exposure values by dividing the previous data by the average wind velocity for each test. These single-fiber exposures are given in Tables 5-6 to

Table 5-3. Single Fiber Vertical Deposition for Test D-1

ALTITUDE (METRES)	→ W CROSS RANGE (METRES) (LOOKING DOWNWIND)										
	0	15.2	30.4	45.6	60.8	76	91.2	106.4	121.6	136.8	152
200			.1				.6		.2	.2	
184	0	.1	1.4	0	2.8	.05	1.1	.2	1.8	.9	2.2
168			.6				1.8				2.1
153	0	.05	1.7	.1	1.4	1.0	5.7	2.3	7.8	6.0	5.7
138				.5					9.8		
122	0	.1	2.8	1.8	3.7	10.2	10.6	14.6	21.9	7.8	4.2
91	.7	.4	1.2	1.5	14.0	15.6	8.5	12.7	13.6	9.9	11.5
76									10.6		
62	0	0	.3	4.4	13.2	20.8	7.0	12.4	17.6	12.2	4.4
36	.05	.4	1.4	3.2	5.3	7.9	6.1	13.1	41.2	6.9	3.7
13	.1	1.9	3.5	2.5	4.2	20.7	33.7	15.9	14.2	9.0	5.0
5	.3	5.2	5.1	19.4	31.6	65.2	18.1	24.2	24.9	15.1	5.8

Notes: Vertical deposition given in 10^3 Fibers/m^2
Includes all fibers of length > 1mm

Table 5-4. Single Fiber Vertical Deposition for Test D-2

ALTITUDE (METRES)	CROSS RANGE (METRES) (LOOKING DOWNWIND) E ←										
	152	136.8	121.6	106.4	91.2	76	60.8	45.6	30.4	15.2	0
222	.7	1.5	.9	1.3	.8						
206	2.5	4.5	4.2	2.7	2.5	1.6	.9				
190	3.6	2.7	3.1	4.6	1.5	3.2	2.1	2.0	1.6	.5	.8
158	3.3	9.1	10.1	15.9	8.8	8.8	4.2	4.3	3.9	5.3	.8
126	11.8	10.0	13.5	17.9	9.5	15.4	10.5	11.0	9.3	3.7	.5
94	3.4	4.3	5.9	18.1	18.9	7.0	12.5	18.0	17.3	3.6	.9
64	15.6	16.1	13.5	17.2	2.9	13.7	12.5	22.0	11.0	2.4	1.0
35	1.7	2.0	12.0	8.8	16.5	9.1	6.3	6.8	1.4	1.4	1.1
11	.2	0	2.9	7.8	40.3	3.2	16.7	3.9	3.7	2.5	
3	0	1.3	0	1.3	15.1	10.5	15.4	14.7	15.1	4.2	

Notes: Vertical deposition given in 10^3Fibers/m^2
Includes all fibers of length >1mm

Table 5-5. Single Fiber Vertical Deposition for Test D-3

ALTITUDE (METRES)	CROSS RANGE (METRES) (LOOKING DOWNWIND) E ← → W																	
	106.4	91.2	76	60.8	45.6	30.4	15.2	0	15.2	30.4	45.6	60.8	76	91.2	106.4	121.6	136.8	152
222					.3			.1										
206					.3	1.3		8.8	.6				.1					
190				.3	.8	.4	.5	0	1.2			.05	.9	.4				
174			.7	.6	.2	.6	1.9	.9	.2	.4		.3	.1	.2				
158				.2	2.4	2.5	5.3	1.7	2.7	3.3	.3	1.2	.3	.4				
142		.05	.05	.5	1.0	.8	2.0	8.9	7.9	10.5	.7	1.1	2.4	.9	1.4	.4		
126		.4	.8	2.3	5.0	2.1	10.9	9.4	19.3	8.3	1.0	1.9	1.1	2.3	2.3	2.1		
110	.5	.9	2.0	2.9	8.4	28.3	8.0	16.5	11.6	14.2	1.0	2.9	1.9	1.0	.5	.3		.05
94	1.1	1.5	3.6	4.6	22.3	16.4	12.6	20.7	11.3	12.9	4.6	3.3	3.4	1.9	1.0	6.4	.4	.5
79		1.2	5.3	10.6	2.1	1.5	13.3	18.9	18.4	8.6	9.4	13.4	4.3	2.3	.3	.5	.2	.5
64		1.1	6.9	2.4	.4	21.8	16.0	9.9	21.4	12.6	3.4	4.9	8.5	8.1	1.6	.3	.3	
49			2.4	8.2	3.6	2.6	15.8	20.0	23.4	2.2	12.2	17.1	6.3	3.7	.3	.2		
35		.2	.5	3.3	5.5	8.1	15.3	16.0	32.8	7.8	.9	1.7	6.8	1.0	.3	.9	.2	
23		.05	1.5	2.6	3.8	6.7	14.8	14.7	15.9	6.5	4.2	17.6	8.1	4.6	2.0	1.1	.3	
11			3.7	1.2	.1	1.5	6.3	4.9	3.0	14.1	23.3	10.2	8.0	2.3	8.7	3.7	.9	
3			1.3	3.2	1.2	2.9	22.0	4.1	7.9	19.5	42.9	31.4	25.0	8.5	6.7	5.8		

Notes: Vertical deposition given in 10^3 Fibers/m^2
Includes all fibers of length > 1mm

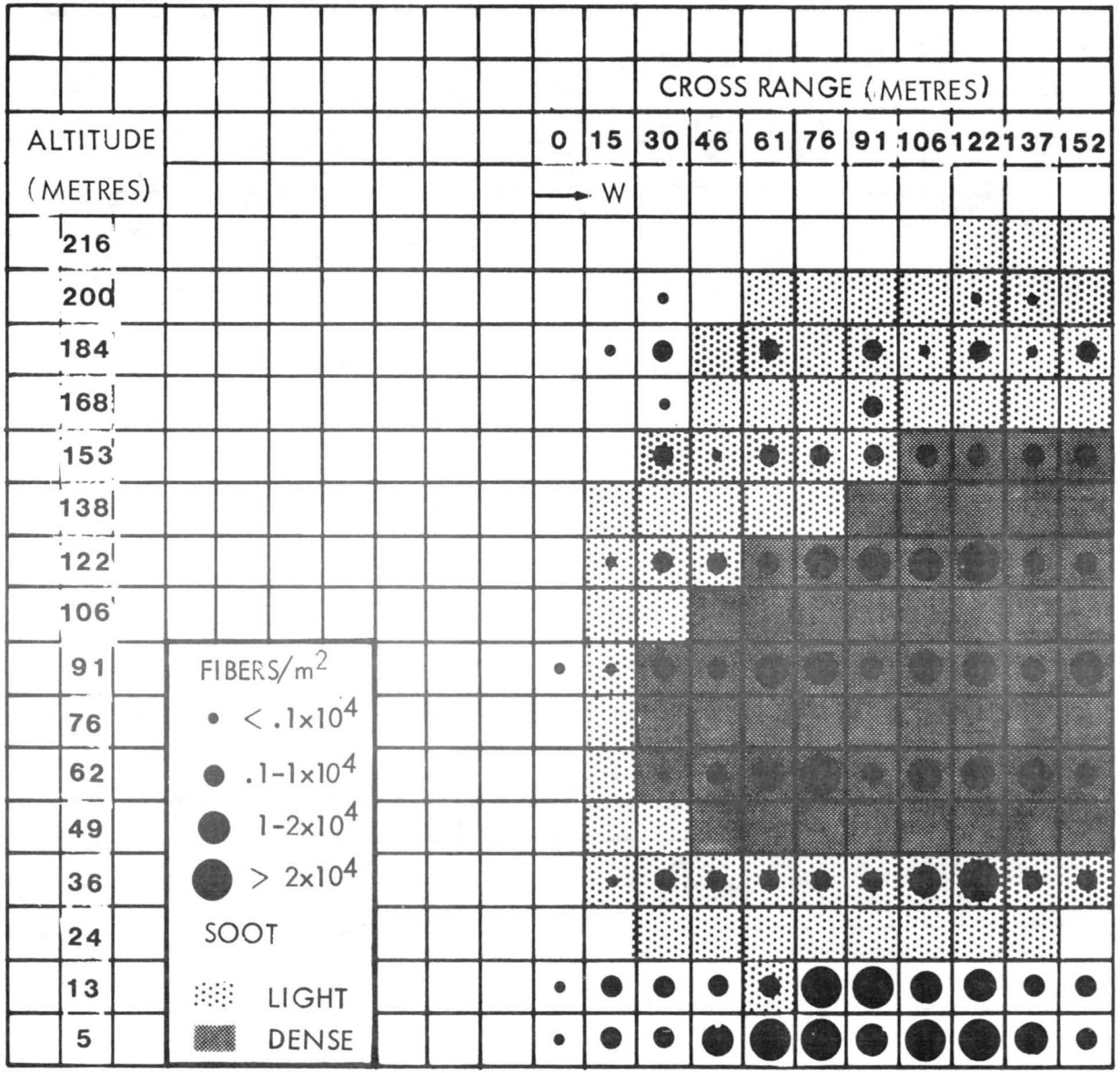

Figure 5.2. Region of Single Fiber and Soot Deposition for Test D-1

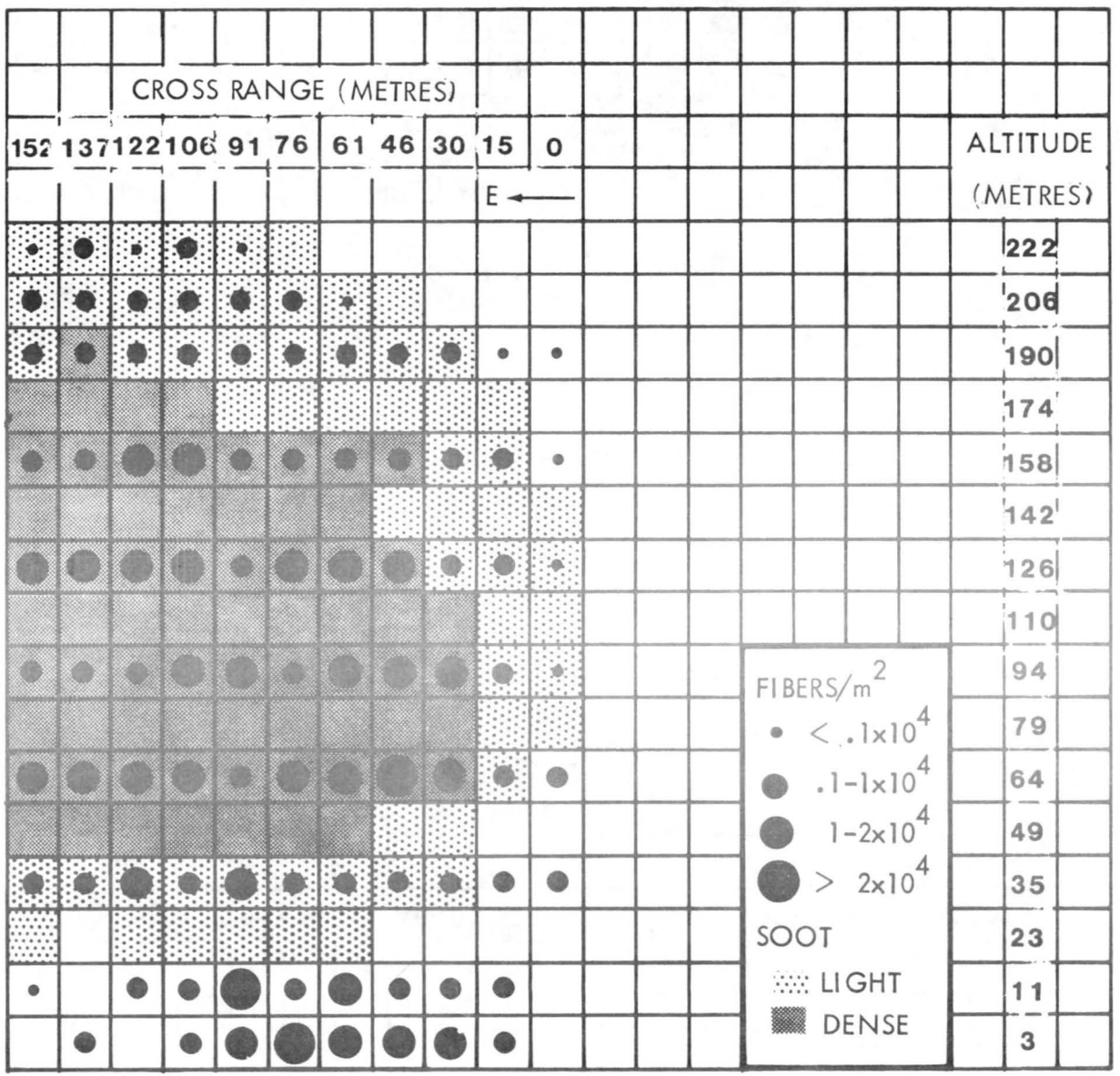

Figure 5.3. Region of Single Fiber and Soot Deposition for Test D-2

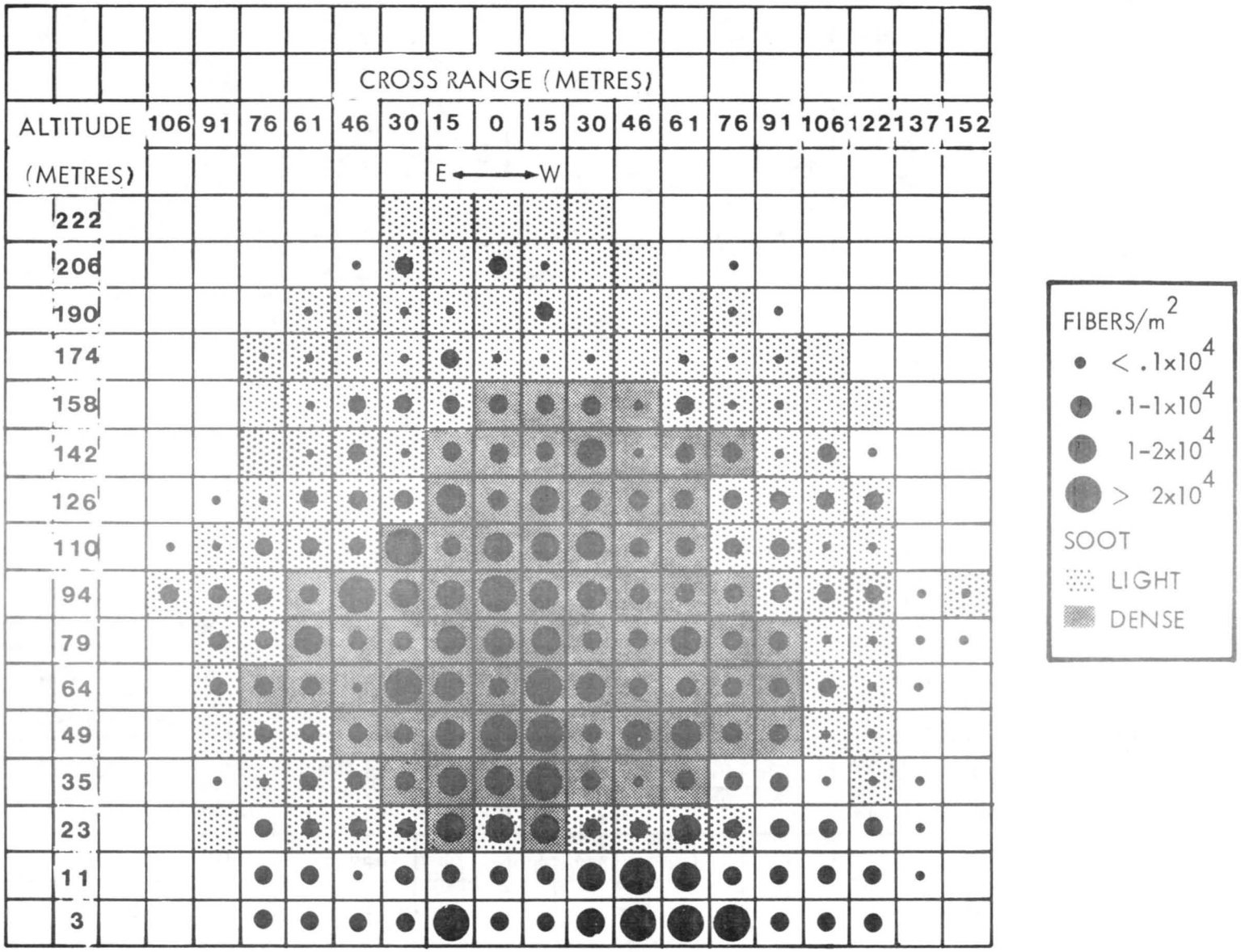

Figure 5.4. Region of Single Fiber and Soot Deposition for Test D-3

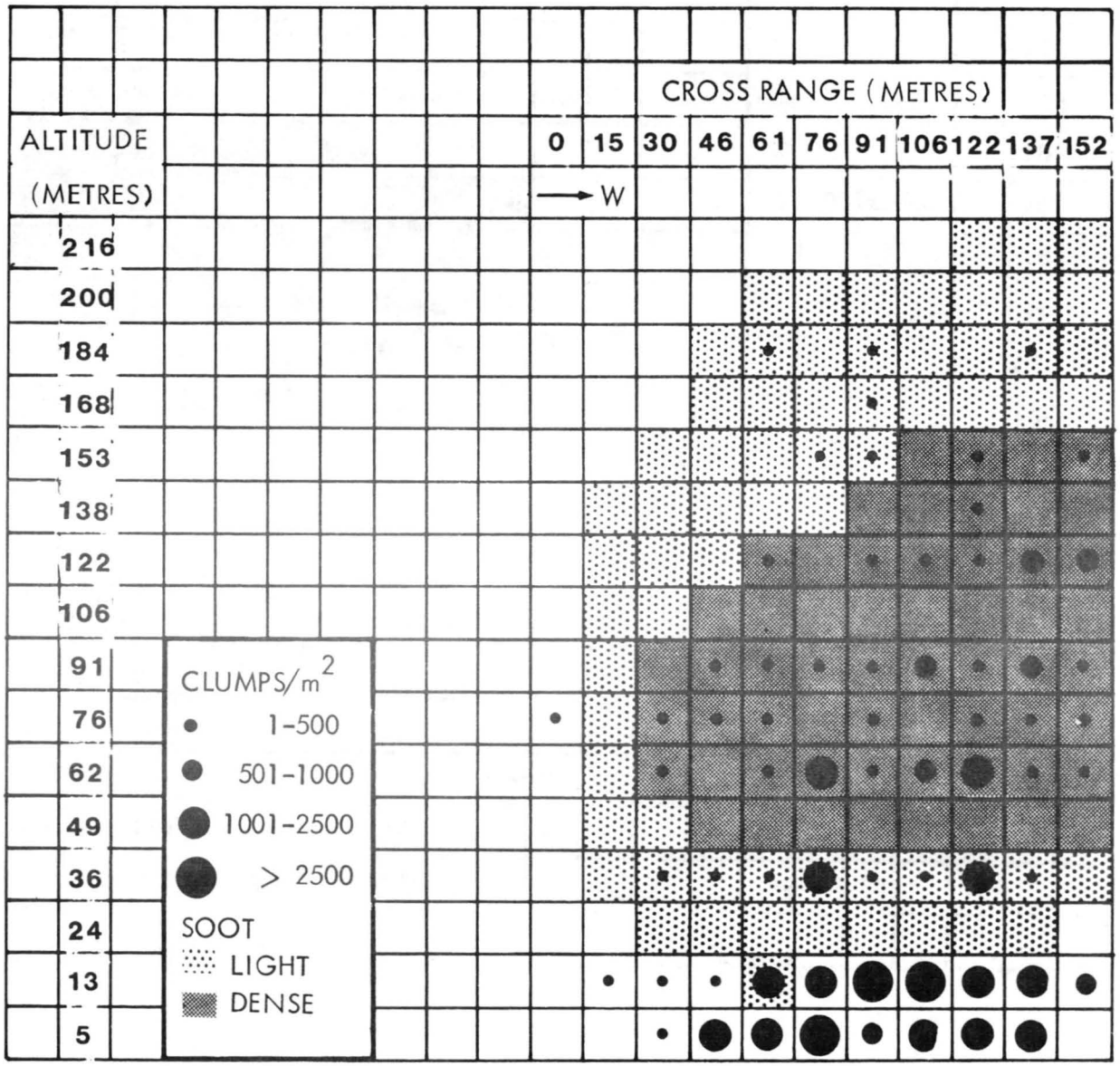

Figure 5.5. Region of Fiber Clumps and Soot Density for Test D-1

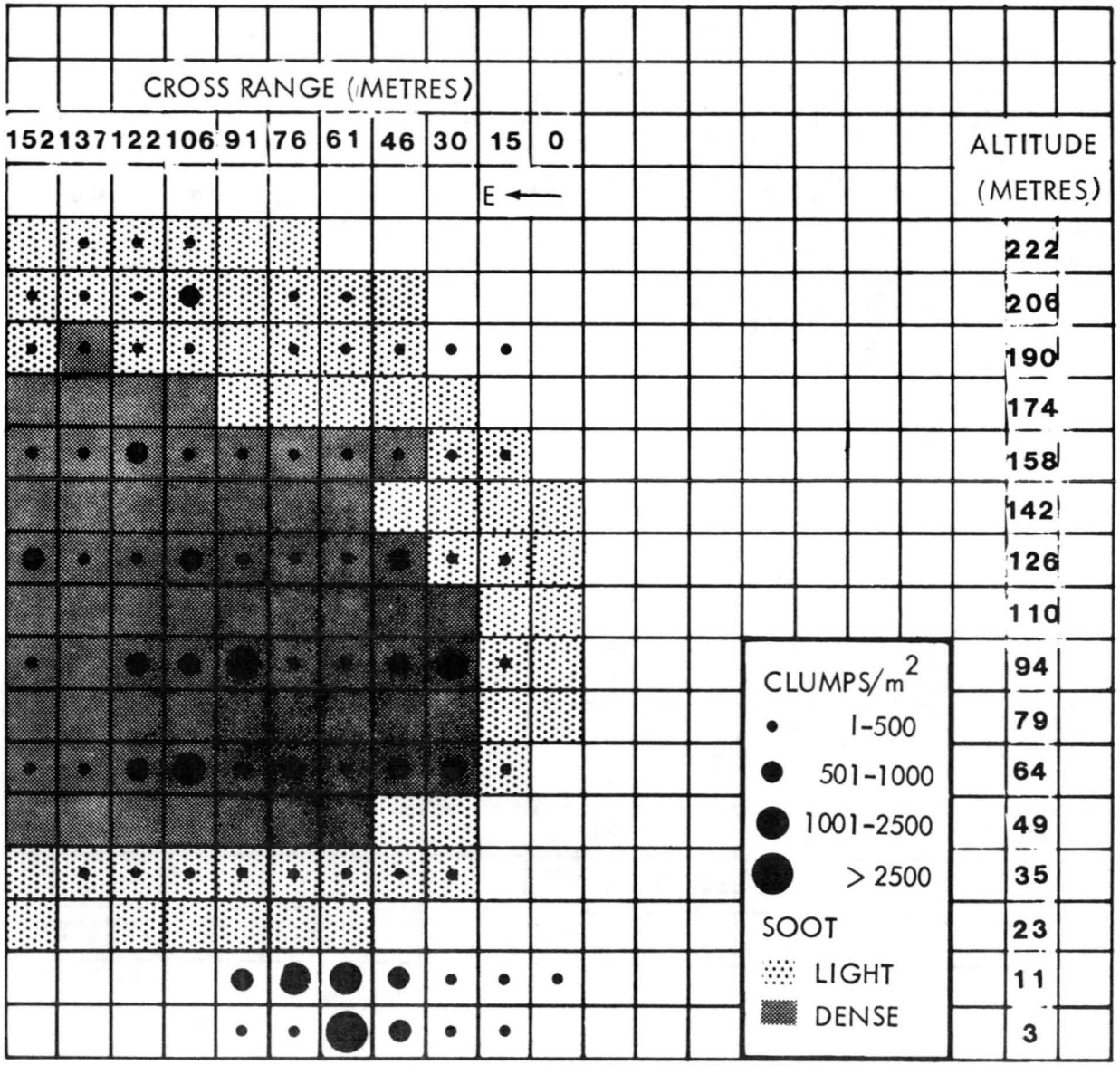

Figure 5.6. Region of Fiber Clumps and Soot Density for Test D-2

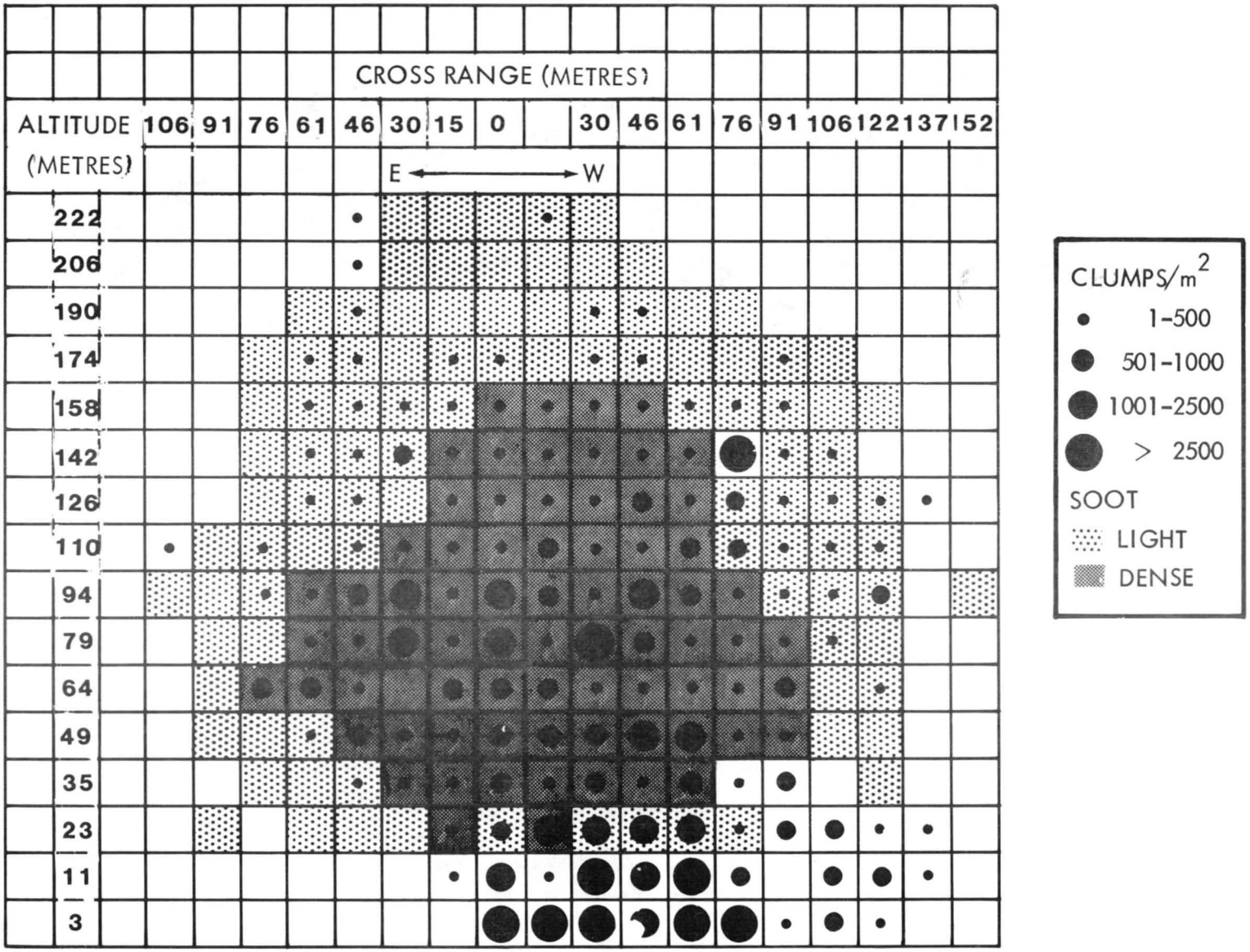

Figure 5.7. Region of Fiber Clumps and Soot Density for Test D-3

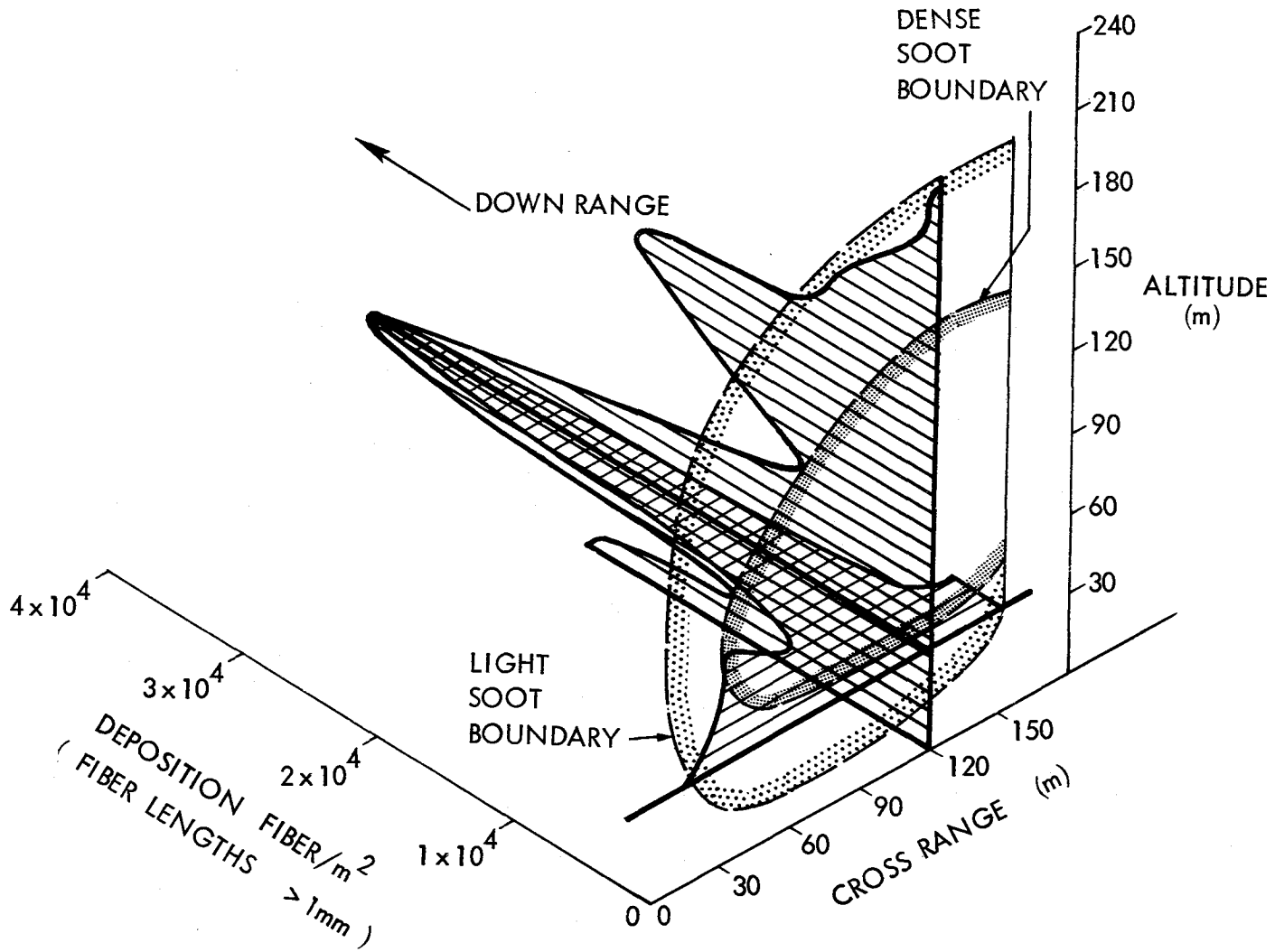

Figure 5.8. Representative Vertical and Horizontal Single Fiber Deposition Profiles for Test D-1

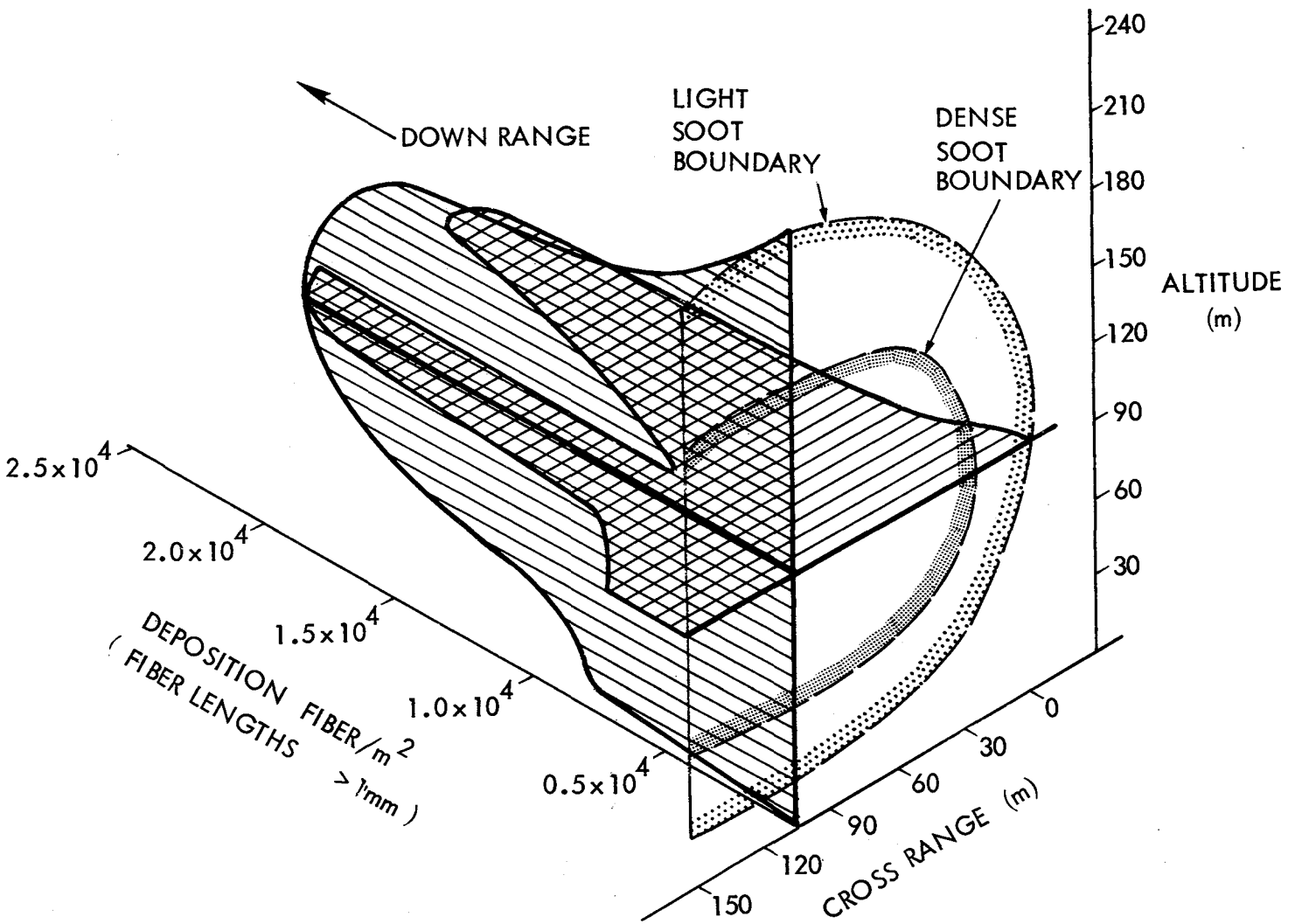

Figure 5.9. Representative Vertical and Horizontal Single Fiber Deposition Profiles for Test D-2

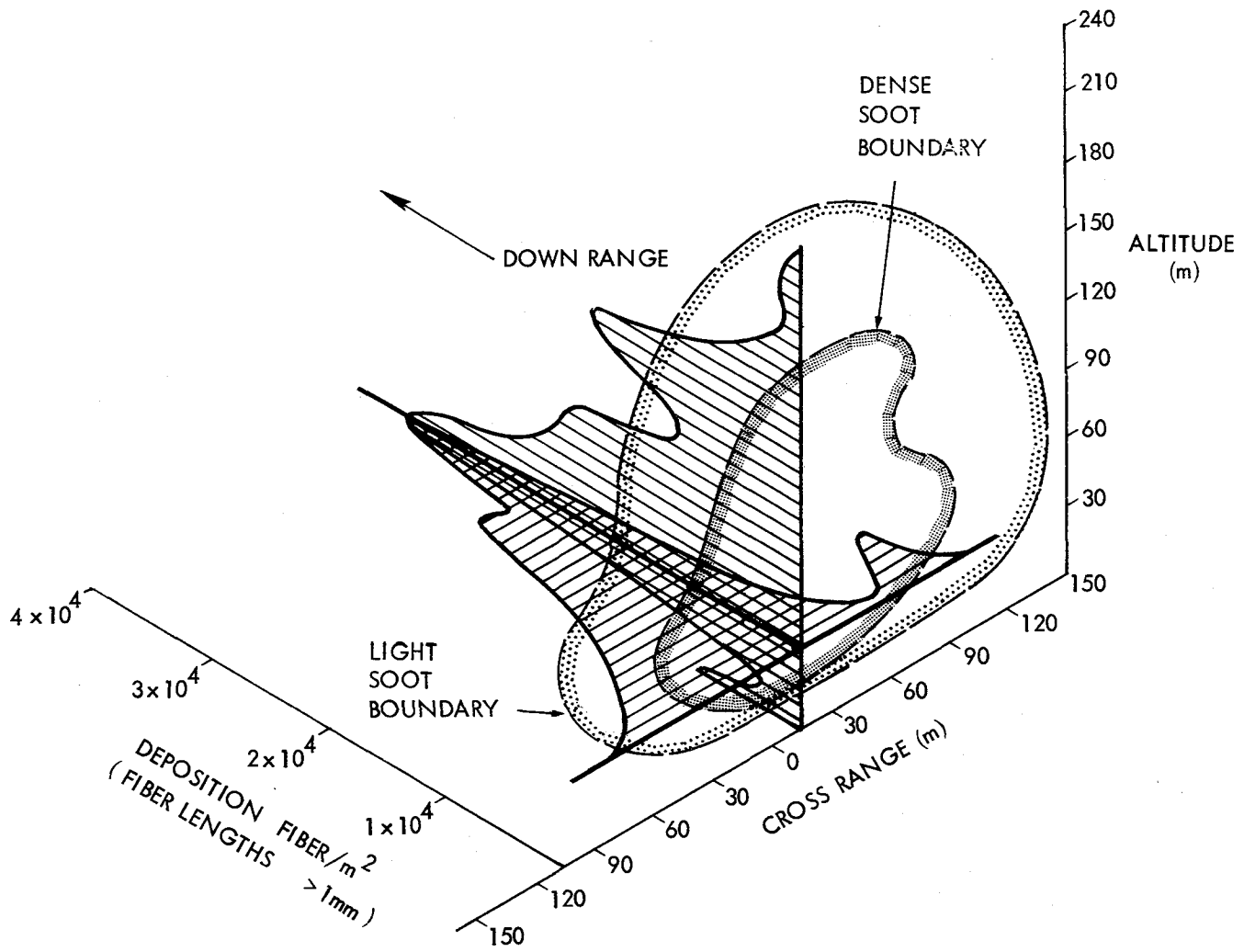

Figure 5.10. Representative Vertical and Horizontal Single Fiber Deposition Profiles for Test D-3

5-8 for the three tests. The maximum exposure values (in fiber-s/m^3) for the tests are 102 x 10^2 for D-1; 69 x 10^2 for D-2; and 81 x 10^2 for D-3; and they occur at near-ground-level altitudes.

Single-Fiber Distribution by Length -- In the data reduction, or counting, process, each single fiber counted on a vugraph collector was measured for length, and the lengths were classified by particular intervals: 0.5 to 1 mm, 1 to 2 mm, 2 to 4 mm, 4 to 6 mm, 6 to 8 mm, 8 to 10 mm, and fibers whose lengths were greater than 10 mm. For those fibers longer than 10 mm, the exact length was measured and noted. From these data, the number of single fibers in the portion of fiber cloud intercepted by the vugraph collector array was determined for each length interval. These resulting data are given in Tables 5-9 to 5-11 for the three tests.

The number of fibers in each fiber length interval is given as a function of the altitude interval between each horizontal row of vugraph collectors that were data-reduced. The vugraph collector altitudes shown can be essentially considered as the "mean" altitude for each of the altitude intervals. Also, the total number of fibers in the intercepted portion of the fiber cloud is given for each fiber length interval as well as the total number of all fiber lengths (except those < 1 mm) that occur in each altitude interval.

The maximum number of single fibers in the fiber cloud for all three tests fall in the length intervals of 1 to 2 mm, and 2 to 4 mm (approximately 40% in each interval). This percentage distribution is shown in the bottom entries of Tables 5-9 to 5-11, and graphically in Figure 5.11.

These data were used to compute the average single fiber length for each of the three tests, again excluding fibers shorter than 1 mm. These average lengths were as follows: test D-1, 3.22 mm; test D-2, 3.14 mm; and test D-3, 3.18 mm.

Figure 5.12 presents the cumulative distribution of all single fibers in the fiber cloud longer than 1 mm as a function of altitude. For all three tests, the distribution of the number of single fibers in the cloud is essentially linear to an altitude of 80 to 100 m, with approximately 50% of the fibers in the cloud contained between ground level and an altitude of 50 to 70 m. Approximately 80% of the single fibers are contained in the bottom half of the fiber cloud.

Tables 5-12 to 5-14 present the spatial distribution of the single fibers >1 mm in length in the form of number of fibers per metre of height (altitude) in each altitude interval. These values are given for each crossrange interval (15.2 meters) as well as the total for all crossrange intervals at the same altitude. These fibers per metre of altitude totals are plotted as a function of altitude on Figure 5.13 for each of the tests. These curves again show, as in Figure 5.12, that approximately an equal number of fibers are contained at all altitude levels up to approximately 100 metres except for the near-ground level where the number of fibers per metre of altitude increases by about a factor of two.

NOTE: The numbers of single fibers given in this section on single fiber length distribution are the numbers of fibers in that portion of the fiber cloud intercepted by the vugraph

Table 5-6. Single Fiber Exposure for Test D-1

ALTITUDE (METRES)	→ W CROSS RANGE (METRES)(LOOKING DOWNWIND)										
	0	15.2	30.4	45.6	60.8	76	91.2	106.4	121.6	136.8	152
200			.2				.9		.3	.3	
184	0	.2	2.2	0	4.4	.1	1.7	.3	2.8	1.4	3.4
168			.9				2.8				3.3
153	0	.1	2.7	.2	2.2	2	8.9	3.6	1.2	9.3	8.9
138				.8					15		
122	0	.2	4.4	2.8	5.8	16	17	23	34	12	6.6
91	1.1	.6	1.9	2.3	22	24	13	20	21	15	18
76									17		
62	0	0	.5	6.9	21	32	11	19	27	19	6.9
36	.1	.6	2.2	5.0	8.3	12	9.5	20	64	11	5.8
13	.2	3.0	5.5	3.9	6.6	32	53	25	22	14	7.8
5	.5	8.1	8.0	30	49	102	28	38	39	24	9.1

Notes: Exposure given in 10^2Fiber-sec/m^3
Includes all fibers of length >1mm
Average windspeed-6.4m/s

Table 5-7. Single Fiber Exposure for Test D-2

ALTITUDE (METRES)	CROSS RANGE (METRES)(LOOKING DOWNWIND) E ←										
	152	136.8	121.6	106.4	91.2	76	60.8	45.6	30.4	15.2	0
222	1.2	2.6	1.5	2.2	1.4						
206	4.3	7.8	7.2	4.6	4.3	2.7	1.6				
190	6.2	4.6	5.3	7.9	2.6	5.5	3.6	3.4	2.8	.9	1.4
158	5.7	16	17	27	15	15	7.2	7.4	6.7	9.1	1.4
126	20	17	23	31	16	26	18	19	16	6.4	.9
94	5.9	7.4	10	31	33	12	21	31	30	6.2	1.6
64	27	28	23	30	2.9	24	21	38	19	4.1	1.7
35	2.9	3.4	21	15	28	16	11	12	2.4	2.4	1.9
11	.3	0	5.0	13	69	5.5	29	6.7	6.3	6.3	
3	0	2.2	0	2.2	26	18	26	25	26	7.2	

Notes: Exposure given in 10^2Fiber-sec/m^3
Includes all fibers of length >1mm
Average windspeed-5.8m/s

Table 5-8. Single Fiber Exposure for Test D-3

ALTITUDE	CROSS RANGE (METERS) (LOOKING DOWNWIND) E ← → W																	
(METERS)	106.4	91.2	76	60.8	45.6	30.4	15.2	0	15.2	30.4	45.6	60.8	76	91.2	106.4	121.6	136.8	152
222					.6			.2										
206					.6	2.4		17	1.1				.2					
190				.6	1.5	.8	.9	0	2.3			.1	1.7	.8				
174			1.3	1.1	.4	1.1	3.6	1.7	.4	.8		.6	.2	.4				
158				.4	4.5	4.7	10	3.2	5.1	6.2	.6	2.2	.6	.8				
142		.1	.1	.9	1.9	1.5	3.8	17	15	20	1.3	2.1	4.5	1.7	2.6	.8		
126		.7	1.5	4.3	9.4	4.0	21	18	36	16	1.9	3.6	.2	4.3	4.3	40		
110	.9	1.7	3.8	5.5	16	53	15	31	22	27	1.9	5.5	3.6	1.9	.9	.6		.1
94	2.1	2.8	6.8	8.7	42	31	24	39	21	24	8.7	6.2	6.4	3.6	1.9	12	.8	.9
79		2.3	10	20	4.0	2.8	25	36	35	16	18	25	8.1	4.3	.6	.9	.4	.9
64		2.1	13	4.5	.8	41	30	19	40	24	6.4	9.2	16	15	3.0	.6	.6	
49			4.5	15	6.8	4.9	30	38	44	4.1	23	32	12	7.0	.6	.4		
35		.4	.9	6.2	10	15	29	30	60	15	1.7	3.2	13	1.9	.6	1.7	.4	
23		.1	2.8	4.9	7.2	13	28	28	30	12	7.9	33	15	8.7	3.8	2.1	.6	
11			7.0	2.3	.2	2.8	12	9.2	.6	27	44	19	15	4.3	16	7.0	1.7	
3			2.4	6.0	2.3	5.5	41	7.7	15	37	81	59	47	16	12	11		

Notes: Exposure given in 10^2 Fiber-sec/m3
Includes all fibers of length >1mm
Average windspeed-5.3m/s

Table 5-9. Single Fiber Length Distribution for Test D-1

VIEWGRAPH COLLECTOR ALTITUDE (METERS)	ALTITUDE INTERVAL (METERS)	NUMBER OF SINGLE FIBERS PER FIBER LENGTH INTERVAL							TOTAL FIBERS >1 mm	CUMULATIVE % FIBERS >1 mm AT ALTITUDE
		0.5 - 1mm	1 - 2 mm	2 - 4 mm	4 - 6 mm	6 - 8 mm	8 - 10 mm	>10 mm		
184	32	1.14×10^6	1.95×10^6	1.75×10^6	$.976 \times 10^6$	3.68×10^5	$.975 \times 10^5$	1.70×10^5	5.29×10^6	100
153	31	3.68×10^6	5.82×10^6	6.29×10^6	1.70×10^6	8.01×10^5	2.59×10^5	2.12×10^5	1.51×10^7	97.6
122	31	5.04×10^6	1.37×10^7	1.43×10^7	5.91×10^6	1.53×10^6	5.18×10^5	6.83×10^5	3.67×10^7	90.9
91	30	5.82×10^6	1.34×10^7	2.02×10^7	5.68×10^6	1.27×10^6	5.33×10^5	6.26×10^5	4.17×10^7	74.6
62	27	7.39×10^6	1.53×10^7	1.52×10^7	4.23×10^6	1.56×10^6	9.03×10^5	5.74×10^5	3.79×10^7	56.2
36	25	5.17×10^6	1.38×10^7	1.17×10^7	4.94×10^6	1.58×10^6	6.65×10^5	1.31×10^6	3.40×10^7	39.4
13	15	5.84×10^6	1.04×10^7	1.00×10^7	2.68×10^6	1.05×10^6	5.24×10^5	6.61×10^5	2.53×10^7	24.3
5	9	9.35×10^6	1.34×10^7	1.12×10^7	2.38×10^6	1.37×10^6	5.54×10^5	5.68×10^5	2.94×10^7	13.0
TOTAL		4.44×10^7	8.72×10^7	9.06×10^7	2.85×10^7	9.53×10^6	4.06×10^6	4.80×10^6	2.25×10^8	
LENGTH DISTRIBUTION %		-	38.8	40.3	12.7	4.2	1.8	2.2		

Table 5-10. Single Fiber Length Distribution for Test D-2

VIEWGRAPH COLLECTOR ALTITUDE (METERS)	ALTITUDE INTERVAL (METERS)	NUMBER OF SINGLE FIBERS PER FIBER LENGTH INTERVAL							TOTAL FIBERS >1 mm	CUMULATIVE % FIBERS >1 mm AT ALTITUDE
		0.5 - 1	1 - 2 mm	2 - 4 mm	4 - 6 mm	6 - 8 mm	8 - 10 mm	>10 mm		
222	16	2.43×10^5	5.47×10^5	5.35×10^5	9.73×10^4	4.86×10^4	1.22×10^4	3.65×10^4	1.30×10^6	100.0
206	16	1.47×10^6	2.03×10^6	1.59×10^6	6.20×10^5	2.43×10^5	6.08×10^4	1.09×10^5	4.66×10^6	99.6
190	24	1.35×10^6	3.83×10^6	3.94×10^6	8.76×10^5	5.29×10^5	3.65×10^4	2.01×10^5	9.47×10^6	98.0
158	32	8.12×10^6	1.46×10^7	1.57×10^7	3.94×10^6	1.39×10^6	5.59×10^5	4.62×10^5	3.67×10^7	94.8
126	32	1.24×10^6	1.70×10^7	2.57×10^7	6.92×10^6	4.07×10^6	7.41×10^5	7.66×10^5	5.52×10^7	82.3
94	21	9.37×10^6	2.00×10^7	2.14×10^7	5.73×10^6	2.33×10^6	1.60×10^6	8.02×10^5	5.19×10^7	63.5
64	30	1.47×10^7	2.37×10^7	2.41×10^7	6.07×10^6	2.39×10^6	9.50×10^5	1.21×10^6	5.85×10^7	45.8
35	26	7.93×10^6	1.31×10^7	9.46×10^6	2.31×10^6	1.09×10^6	3.57×10^5	2.38×10^5	2.66×10^7	25.8
11	16	1.09×10^7	1.52×10^7	8.66×10^6	1.49×10^6	1.02×10^6	3.15×10^5	4.93×10^5	2.72×10^7	16.7
3	7	3.32×10^7	7.52×10^6	9.73×10^6	1.53×10^6	2.41×10^6	2.34×10^5	2.82×10^5	2.17×10^7	7.4
TOTAL		8.85×10^7	1.17×10^8	1.21×10^8	2.96×10^7	1.55×10^7	4.86×10^6	4.59×10^6	2.93×10^8	
LENGTH DISTRIBUTION %		-	39.9	41.3	10.1	5.3	1.7	1.6		

Table 5-11. Single Fiber Length Distribution for Test D-3

VIEWGRAPH COLLECTOR ALTITUDE (METERS)	ALTITUDE INTERVAL (METERS)	NUMBER OF SINGLE FIBERS PER FIBER LENGTH INTERVAL							TOTAL FIBERS >1 mm	CUMULATIVE % FIBERS >1 mm AT ALTITUDE
		0.5 - 1 mm	1 - 2 mm	2 - 4 mm	4 - 6 mm	6 - 8 mm	8 - 10 mm	>10 mm		
222	16	7.30×10^4	4.86×10^4	3.65×10^4	1.22×10^4	1.22×10^4	0	0	1.1×10^5	100
206	16	4.13×10^5	1.11×10^6	1.09×10^6	3.52×10^5	9.73×10^4	3.65×10^4	3.65×10^4	2.72×10^5	99.9
190	16	1.95×10^5	5.72×10^5	3.77×10^5	1.09×10^5	3.65×10^4	3.65×10^4	2.43×10^4	1.16×10^6	98.8
174	16	2.80×10^5	5.35×10^5	7.30×10^5	1.09×10^5	6.08×10^4	4.86×10^4	4.86×10^4	1.53×10^6	98.4
158	16	6.44×10^5	2.04×10^6	1.76×10^6	5.47×10^5	4.62×10^5	1.09×10^5	6.08×10^4	4.98×10^6	97.8
142	16	1.53×10^6	3.95×10^6	3.96×10^6	1.36×10^6	4.13×10^5	2.19×10^5	7.30×10^4	9.97×10^6	95.8
126	16	2.43×10^6	7.71×10^6	7.50×10^6	1.61×10^6	5.84×10^5	3.65×10^5	3.04×10^5	1.82×10^7	91.8
110	16	5.28×10^6	1.08×10^7	1.01×10^7	2.42×10^6	7.05×10^5	3.04×10^5	2.07×10^5	2.46×10^7	84.4
94	15.5	5.05×10^6	1.26×10^7	1.15×10^7	3.53×10^6	1.21×10^6	7.89×10^5	7.77×10^5	3.04×10^7	74.4
79	15	4.12×10^6	9.09×10^6	9.44×10^6	3.09×10^6	1.88×10^6	8.55×10^5	1.03×10^6	2.54×10^7	62.0
64	15	5.06×10^6	1.12×10^7	1.03×10^7	3.32×10^6	1.45×10^6	9.01×10^5	2.28×10^5	2.74×10^7	51.6
49	14.5	3.71×10^6	9.36×10^6	1.15×10^7	2.67×10^6	1.17×10^6	7.71×10^5	5.95×10^5	2.61×10^7	40.4
35	13	4.83×10^6	7.57×10^6	7.52×10^6	2.66×10^6	1.29×10^6	7.61×10^5	3.26×10^5	2.01×10^7	29.5
23	12	4.43×10^6	8.41×10^6	7.77×10^6	1.68×10^6	7.47×10^5	2.28×10^5	3.01×10^5	1.91×10^7	21.3
11	10	3.69×10^6	6.38×10^6	5.33×10^6	1.38×10^6	4.94×10^5	3.04×10^5	2.28×10^5	1.41×10^7	13.5
3	7	8.45×10^6	1.09×10^7	6.29×10^6	1.47×10^6	4.20×10^5	2.02×10^5	1.28×10^5	1.94×10^7	7.8
TOTAL		5.02×10^7	1.02×10^8	9.52×10^7	2.63×10^7	1.10×10^7	5.93×10^6	4.37×10^6	2.45×10^8	
LENGTH DISTRIBUTION %		-	41.6	38.8	10.8	4.6	2.4	1.8		

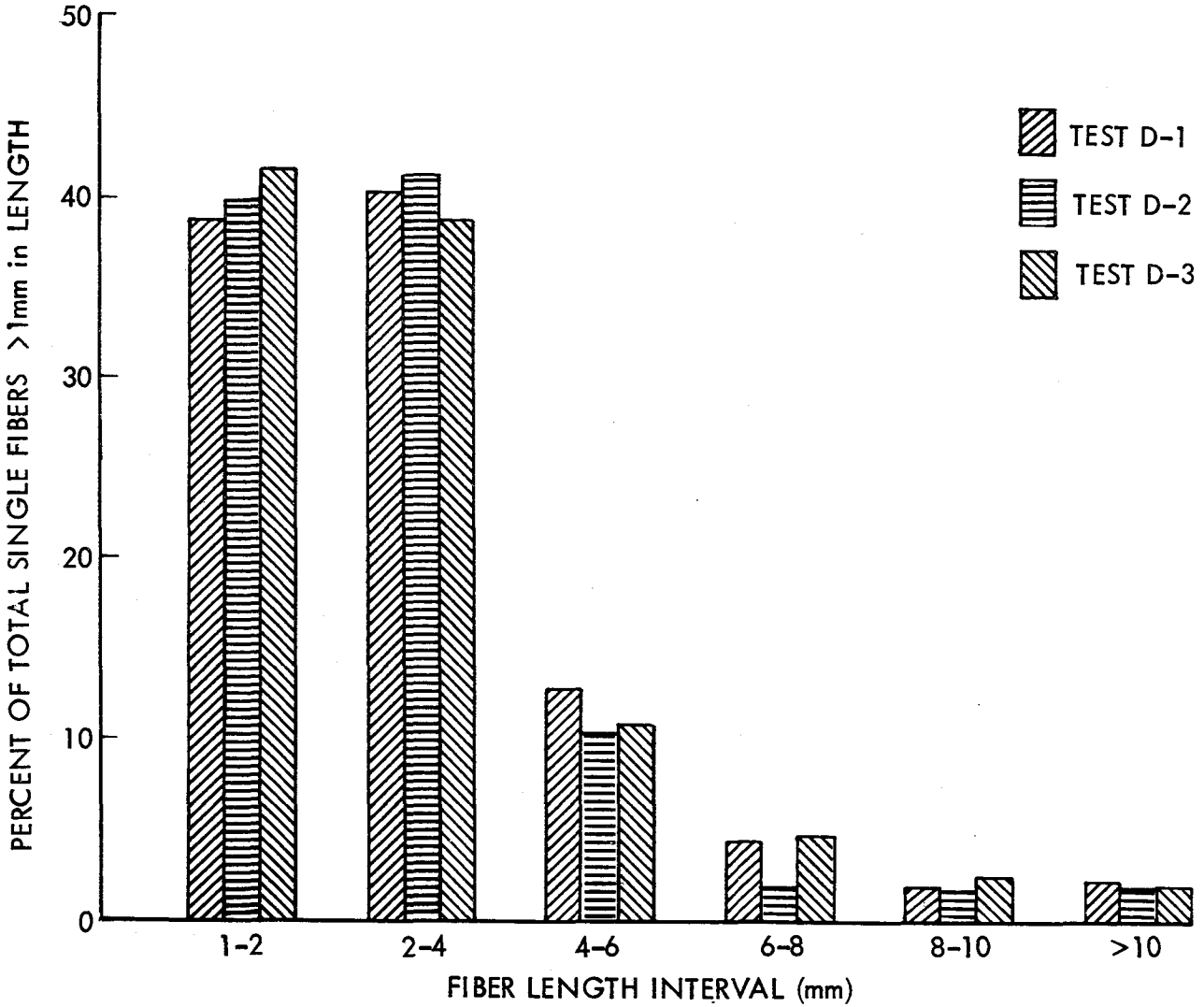

Figure 5.11. Total Single Fiber Length Distribution

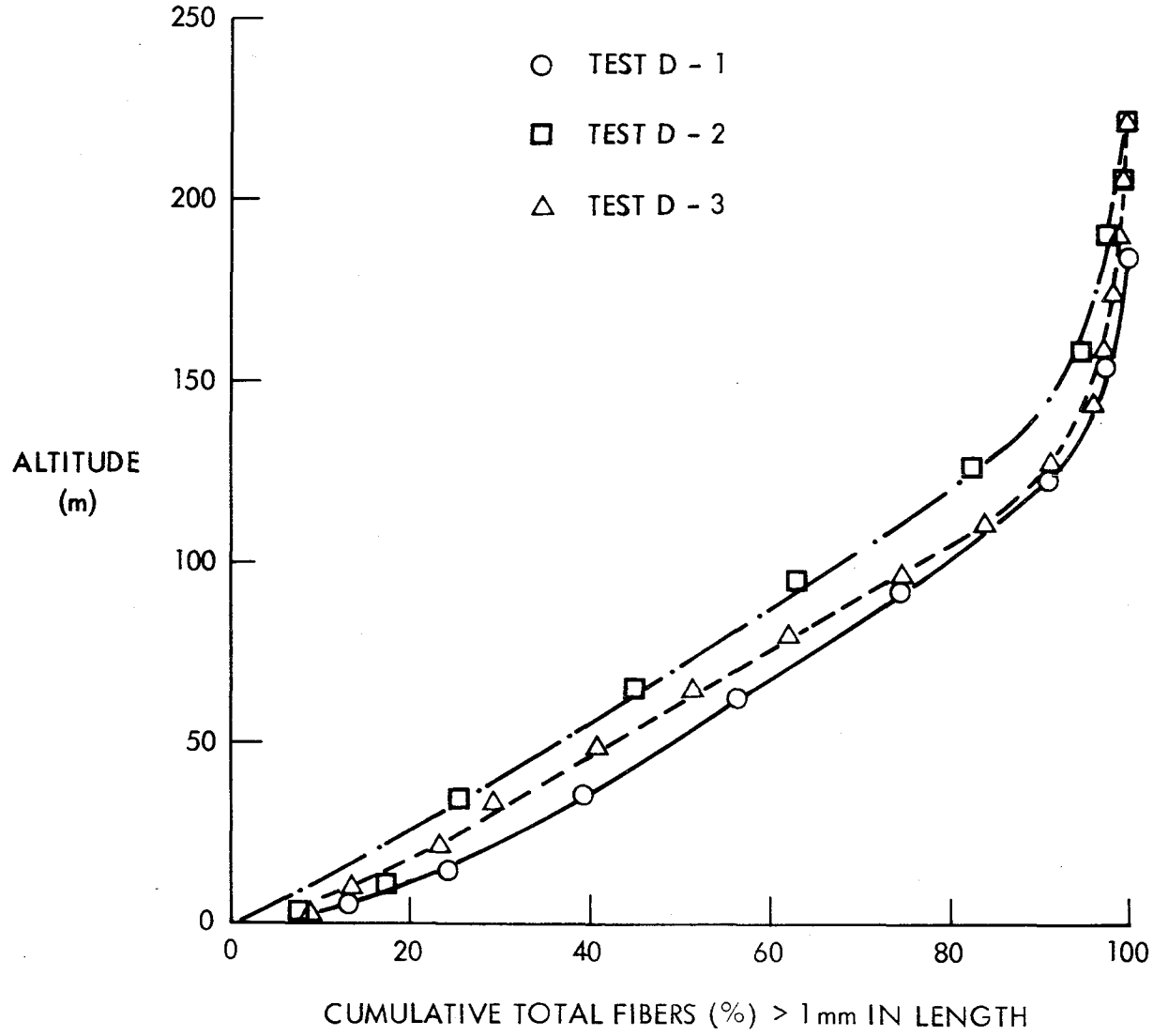

Figure 5.12. Cumulative Distribution of Single Fibers as a Function of Altitude

Table 5-12 Single Fibers per Metre of Altitude Distribution for Test D-1

VEIWGRAPH COLLECTOR ALTITUDE (METERS)	ALTITUDE INTERVAL (METERS)	CROSS RANGE (METERS) (LOOKING DOWNWIND) → W											TOTAL
		0	15.2	30.4	45.6	60.8	76	91.2	106.4	121.6	136.8	152	
184	32	0	2.33	21.75	0	43.49	0.78	17.09	3.88	27.96	13.98	34.17	165.43
153	31	0	.84	26.00	2.52	21.81	15.10	87.24	35.23	118.28	92.27	87.24	486.53
122	31	0	1.70	42.65	27.29	56.30	155.24	162.06	221.77	332.66	118.56	64.83	1183.06
91	30	10.93	7.29	19.13	23.69	216.86	241.46	131.21	196.81	210.48	153.99	178.59	1390.44
62	27	0		5.71	66.58	200.70	315.79	106.53	188.34	267.28	185.48	66.58	1402.99
36	25	1.07	6.45	21.50	48.37	80.62	120.40	92.45	199.94	626.70	105.35	56.97	1359.82
13	15	2.58	29.73	54.28	38.78	64.62	315.37	513.13	242.99	215.85	137.01	76.26	1690.60
5	9	4.86	79.40	77.78	294.92	481.28	991.73	275.48	367.85	379.19	230.11	89.12	3271.72

NOTE: VALUES GIVEN IN 10^3 FIBERS/m

INCLUDES ALL FIBERS OF LENGTH > 1mm

Table 5-13 Single Fibers per Metre of Altitude for Test D-2

VIEWGRAPH COLLECTOR ALTITUDE (METERS)	ALTITUDE INTERVAL (METERS)	CROSS RANGE (METERS) (LOOKING DOWNRANGE) E ←											TOTAL
		152	136.8	121.6	106.4	91.2	76	60.8	45.6	30.4	15.2	0	
222	16	10.64	22.80	14.44	20.52	12.92							81.32
206	16	38.76	68.40	64.60	41.80	38.76	25.08	13.68					291.08
190	24	54.72	41.80	74.12	69.92	22.80	48.64	32.68	31.60	25.08	7.60	12.92	394.88
158	32	50.92	148.20	154.28	241.68	133.78	133.78	63.84	66.12	60.04	81.32	12.92	1146.88
126	32	179.73	152.62	206.08	272.70	144.10	234.74	160.37	168.11	141.00	56.55	8.52	1724.52
94	31	51.71	65.81	90.10	275.79	287.55	107.34	190.39	275.79	264.04	54.84	13.32	1676.68
64	30	237.50	245.42	205.83	262.04	45.12	208.21	190.00	334.88	167.83	36.42	15.83	1949.08
35	26	25.64	31.13	182.22	134.60	251.81	139.18	96.14	103.47	21.06	21.06	17.40	1023.71
11	16	4.00	1.33	5.33	44.00	118.67	613.33	504.00	254.67	60.00	56.00	38.67	1700.00
3	7	0	20.12	0	20.12	230.24	471.65	1607.18	234.70	223.53	230.24	64.82	3102.60

NOTE: VALUES GIVEN IN 10^3 FIBERS/m

INCLUDES ALL FIBERS OF LENGTH > 1mm

Table 5-14 Single Fibers per Metre of Altitude Distribution for Test D-3

VIEWGRAPH COLLECTOR ALTITUDE (METERS)	ALTITUDE INTERVAL (METERS)	CROSSRANGE (METERS) (LOOKING DOWNRANGE) E ← → W																	TOTAL
		106.4	91.2	76	60.8	45.6	30.4	15.2	0	15.2	30.4	45.6	60.8	76	91.2	106.4	121.6	136.8	152	
222	16					5.32	0	0	1.52	0										6.84
206	16					5.32	19.76	0	133.76	9.88				1.52						170.24
190	16				4.56	12.92	6.84	7.6	0	19.00	0	0	.76	13.68	6.84					72.20
174	16			10.64	9.12	3.80	9.88	28.88	13.68	3.80	6.08	0	5.32	1.52	3.04					95.76
158	16		0		3.04	36.48	38.00	80.56	26.60	41.04	50.92	5.32	18.24	5.32	6.08					311.60
142	16		.77	8.49	15.43	12.34	30.09	31.63	135.80	121.14	160.49	10.80	16.97	37.04	13.89	22.38	6.17			623.43
126	16		6.97	13.17	34.86	75.92	109.24	165.79	143.32	294.39	127.05	15.49	29.44	17.82	35.64	34.86	31.76			1135.72
110	16	8.55	13.99	31.08	45.07	128.22	429.73	122.00	251.00	177.18	216.03	15.54	43.52	28.75	15.54	7.77	5.44	0	.78	1542.19
94	15.5	16.45	23.50	55.63	70.52	340.04	249.15	191.96	315.75	172.37	195.88	70.52	50.14	52. 9	29.77	14.89	97.15	7.05	8.62	1961.88
79	15	0	18.02	81.48	161.40	32.12	23.50	202.93	287.55	280.49	130.84	142.60	207.31	65.81	36.04	5.48	8.62	3.13	7.84	1695.16
64	15	0	16.62	104.50	37.21	7.12	331.71	243.04	151.21	325.38	192.38	53.04	75.21	129.83	123.50	25.33	5.54	4.75	0	1826.37
49	14.5	0	0	37.57	125.53	55.50	40.13	240.81	304.85	356.94	34.16	185.30	259.60	95.64	57.21	5.12	3.42			1801.78
35	13		3.66	8.24	51.28	84.24	123.61	232.58	243.57	499.04	119.04	14.65	26.55	103.47	15.57	5.49	13.73	3.66		1548.38
23	12		1.04	22.90	39.56	58.30	103.07	225.92	223.84	242.58	98.90	63.51	267.56	123.89	69.75	30.19	17.70	5.20		1593.31
11	10		0	56.00	18.67	1.33	22.67	96.00	74.68	46.67	214.67	354.67	156.00	122.67	44.00	133.33	56.00	13.33		1410.69
3	7			20.12	49.18	17.88	44.70	335.29	62.59	120.70	297.29	650.47	478.35	380.00	129.65	162.82	89.41			2777.80

NOTE: VALUES GIVEN IN 10^3 FIBERS/m INCLUDES ALL FIBER OF LENGTH > 1mm

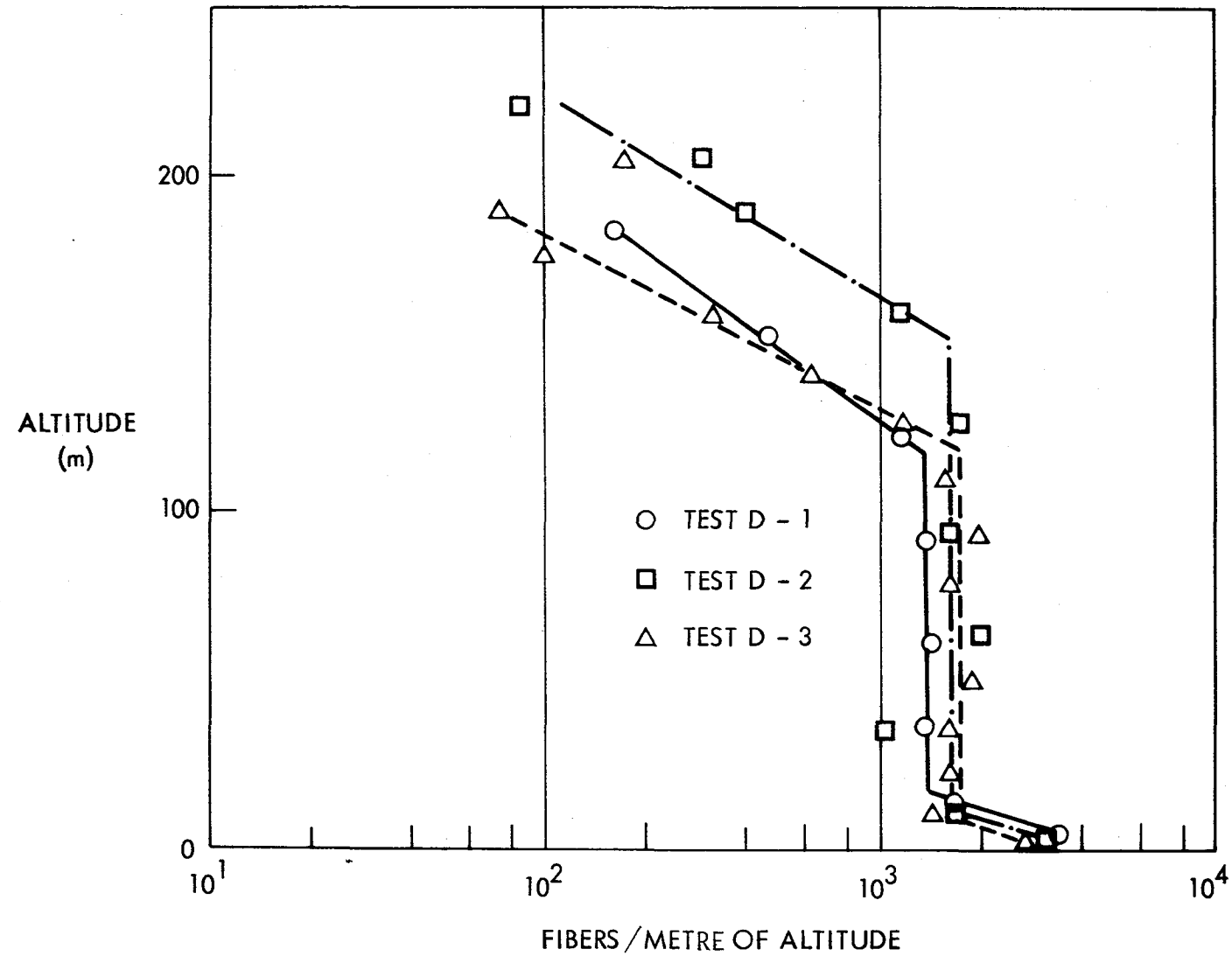

Figure 5.13 Fibers per Metre of Altitude vs Altitude

collector array. For test D-1, it is estimated that 74% of the cloud fibers were sampled; for test D-2, 83%; and for test D-3, 100%. However, for the assumption that the fiber distributions derived from the sampled data also apply to the "missed" portion of the test D-1 and D-2 fiber clouds, the results given in percentages can be considered valid for the entire fiber cloud.

Fiber Clump Distribution -- In the data reduction process, each multiple fiber or fiber clump collected on the vugraph samplers was counted. The number of fibers in each clump counted was estimated and classified by a fiber number interval. These intervals were 2 to 5, 6 to 10, 11 to 20, 21 to 50, 51 to 100, 101 to 300, and 301 to 500, and over 500 fibers per individual clump. From these data, the number of fiber clumps in the portion of fiber cloud intercepted by the vugraph collector array was determined for each fiber number interval. These resulting data are given in Tables 5-15 for D-1; 5-16 for D-2; and 5-17 for D-3. The format for the tables is similar to the format used in the three preceding tables for single-fiber length distribution.

As the data in these tables show, the highest percentage of clumps (40% to 60%) contain 2 to 5 fibers with approximately 65% to 75% of the total number of clumps containing 2 to 10 fibers. These results are graphically shown in Figure 5.14.

Figure 5.15 presents the cumulative distribution of all clumps in the fiber cloud as a function of altitude. The distributions of fiber clumps as a function of altitude, shown in this figure, do not exhibit the similarity among the three tests as did the distributions for single fibers (see Figure 5.12). For the fiber clumps, 50% are contained between ground level and a spread of altitudes from 20 to 75 m depending on the test. Also, depending on the test, approximately 65% to over 90% of the fiber clumps are contained in the bottom half of the fiber cloud.

NOTE: The numbers of fiber clumps given in this section on fiber clump distribution are the number of clumps in that portion of the fiber cloud intercepted by the vugraph collector array. For test D-1, it is estimated that 74% of the cloud clumps were sampled; for test D-2, 83%; and for test D-3, 100%. However, for the assumption that the clump distributions derived from the sampled data also apply to the "missed" portion of the test D-1 and D-2 fiber clouds, the results given in percentages can be considered valid for the entire fiber cloud.

Fiber Mass Released -- The final objective of the field test data analysis was to estimate the amount of mass released as single fibers and clumps from the burned composite materials for each of the three tests.

In performing these analyses, it was assumed that the carbon/graphite fibers in the composite material were circular in cross section and averaged 6.88 μm in diameter. This average diameter was computed by weighing a 50-ft-long tow of virgin T-300 material containing 3000 individual carbon/graphite fibers and using the assumption of circular filament cross section and a material density of 1.73 gm/cm^3 (standard handbook value). The mass released from the burned composite was then calculated by

Table 5-15. Fiber Clump Distribution for Test D-1

VIEWGRAPH COLLECTOR ALTITUDE (METERS)	ALTITUDE INTERVAL (METERS)	NO. OF FIBER CLUMPS PER FIBER NUMBER INTERVAL								TOTAL FIBER CLUMPS	CUMULATIVE % FIBER CLUMPS AT ALTITUDE
		2 - 5	6 - 10	11 - 20	21 - 50	51 - 100	101 - 300	301 - 500	>500		
184	32	7.3×10^4								7.3×10^4	100
153	31	1.8×10^5	7.7×10^4		7.8×10^4					3.4×10^5	99.9
122	31	4.5×10^5	1.3×10^5	5.3×10^4	5.3×10^4	1.3×10^5	7.9×10^4	2.6×10^4	2.6×10^4	9.5×10^5	96.8
91	30.5	8.2×10^5	2.5×10^5	1.1×10^5	1.4×10^5	5.5×10^4	1.3×10^5		5.5×10^4	1.6×10^6	88.2
62	27	9.7×10^5	3.6×10^5	7.7×10^4	1.5×10^5	1.3×10^5	1.5×10^5		2.6×10^4	1.9×10^6	73.6
36	25	5.6×10^5	1.9×10^5	8.0×10^4	2.7×10^5	8.0×10^4	8.0×10^4	5.4×10^4		1.3×10^6	56.4
13	15	2.1×10^6	4.3×10^5	1.6×10^5	1.6×10^5	5.8×10^4	3.9×10^4	1.9×10^4		3.0×10^6	44.5
5	9	1.4×10^6	2.9×10^5	1.6×10^5	4.3×10^4				1.4×10^4	1.9×10^6	17.3
TOTAL		6.5×10^6	1.7×10^6	6.4×10^5	8.9×10^5	4.5×10^5	4.8×10^5	9.9×10^4	1.2×10^4	1.1×10^7	
FIBER CLUMP DISTRIBUTION %		59.1	15.5	5.8	8.1	4.1	4.4	.9	1.1		

Table 5-16. Fiber Clump Distribution for Test D-2

VIEWGRAPH COLLECTOR ALTITUDE (METERS)	ALTITUDE INTERVAL (METERS)	NO. OF FIBER CLUMPS PER FIBER NUMBER INTERVAL								TOTAL FIBER CLUMPS	CUMULATIVE % FIBER CLUMPS AT ALTITUDE
		2 - 5	6 - 10	11 - 20	21 - 50	51 - 100	101 - 300	301 - 500	>500		
222	16	7.3×10^4			1.2×10^4					8.5×10^4	100
206	16	2.3×10^5	7.3×10^4		4.9×10^4					3.5×10^5	99.2
190	24	2.9×10^5	1.4×10^5	5.5×10^4	7.3×10^4					5.6×10^5	96.1
158	32	8.0×10^5	2.7×10^5	1.2×10^5	7.3×10^4	2.4×10^4	2.4×10^4	4.9×10^4		1.4×10^6	91.1
126	32	7.6×10^5	1.7×10^5	2.7×10^5	2.9×10^5	1.9×10^5	2.5×10^4	2.5×10^4		1.7×10^6	78.6
94	31	8.5×10^6	6.5×10^5	2.2×10^5	4.8×10^5	4.8×10^4	7.3×10^4		2.4×10^4	2.3×10^6	63.4
64	30	9.0×10^5	3.1×10^5	3.1×10^5	2.1×10^5	1.2×10^5	2.1×10^5	4.7×10^4		2.1×10^6	42.9
35	26	9.5×10^4	2.1×10^5	9.5×10^4	2.4×10^5	7.1×10^4				7.1×10^5	24.1
11	16	5.7×10^5	3.0×10^5	8.5×10^5	1.1×10^5	2.1×10^4	4.2×10^4			1.1×10^6	17.8
3	7	1.4×10^5	3.7×10^5	1.6×10^4	1.4×10^5	3.4×10^5				8.9×10^5	7.9
TOTAL		4.7×10^6	2.5×10^6	1.2×10^6	1.7×10^6	8.3×10^5	3.7×10^5	1.2×10^5	2.4×10^4	1.1×10^7	
FIBER CLUMP DISTRIBUTION %		41.1	21.8	10.5	14.8	7.2	3.2	1.0	.2		

Table 5-17. Fiber Clump Distribution for Test D-3

VIEWGRAPH COLLECTOR ALTITUDE (METERS)	ALTITUDE INTERVAL (METERS)	NO. OF FIBER CLUMPS PER FIBER NUMBER INTERVAL								TOTAL FIBER CLUMPS	CUMULATIVE % FIBER CLUMPS AT ALTITUDE
		2 - 5	6 - 10	11 - 20	21 - 50	51 - 100	101 - 300	301 - 500	>500		
222	16	3.6×10^4	1.2×10^4							4.6×10^4	100
206	16				1.2×10^4					1.2×10^4	99.7
190	16	1.2×10^4			1.2×10^4	1.2×10^4				3.6×10^4	99.6
174	16	1.4×10^5	4.8×10^4	1.2×10^4						7.4×10^4	99.5
158	16	1.6×10^5	1.1×10^5	1.2×10^4	4.9×10^4					3.3×10^5	99.0
142	16	4.5×10^5	1.8×10^5	2.4×10^4	4.9×10^4	2.4×10^4	1.2×10^4			7.4×10^5	97.2
126	16	6.9×10^5	2.1×10^5	2.5×10^4	1.7×10^5	2.5×10^4	1.2×10^4			1.1×10^6	92.9
110	16	4.2×10^5	2.7×10^5	1.1×10^5	6.2×10^4	2.5×10^4	1.2×10^4			9.0×10^5	86.7
94	15.5	1.1×10^6	4.4×10^5	1.3×10^5	2.2×10^5	4.8×10^4	1.2×10^4			1.9×10^6	81.5
79	15	1.2×10^6	3.3×10^5	9.4×10^4	1.2×10^5	5.9×10^4	2.0×10^5			2.0×10^6	70.7
64	15	5.6×10^5	1.9×10^5	8.3×10^4	4.7×10^4	5.9×10^4	3.6×10^4	2.4×10^4	1.3×10^4	1.0×10^6	59.3
49	14.5	7.5×10^5	4.9×10^5	6.2×10^4	9.9×10^4	4.9×10^4				1.4×10^6	53.6
35	13	5.8×10^5	4.6×10^5	8.3×10^4	3.0×10^5	2.4×10^5	2.4×10^4	1.2×10^4		1.5×10^6	45.6
23	12	7.0×10^5	6.9×10^5	1.0×10^5	1.5×10^5	2.5×10^4				1.7×10^6	37.1
11	10	7.7×10^5	5.8×10^5	1.2×10^5	2.4×10^5	2.7×10^4	5.3×10^4			1.8×10^6	27.4
3	7	1.2×10^6	1.0×10^6	2.6×10^5	3.9×10^5	7.8×10^4	1.6×10^4	1.6×10^4		3.0×10^6	17.1
TOTAL		8.8×10^6	5.0×10^6	1.1×10^6	1.9×10^6	4.5×10^5	3.8×10^5	5.2×10^4	1.3×10^4	1.8×10^7	
FIBER CLUMP DISTRIBUTION %		49.4	28.2	6.2	10.8	2.8	2.2	.3	.1		

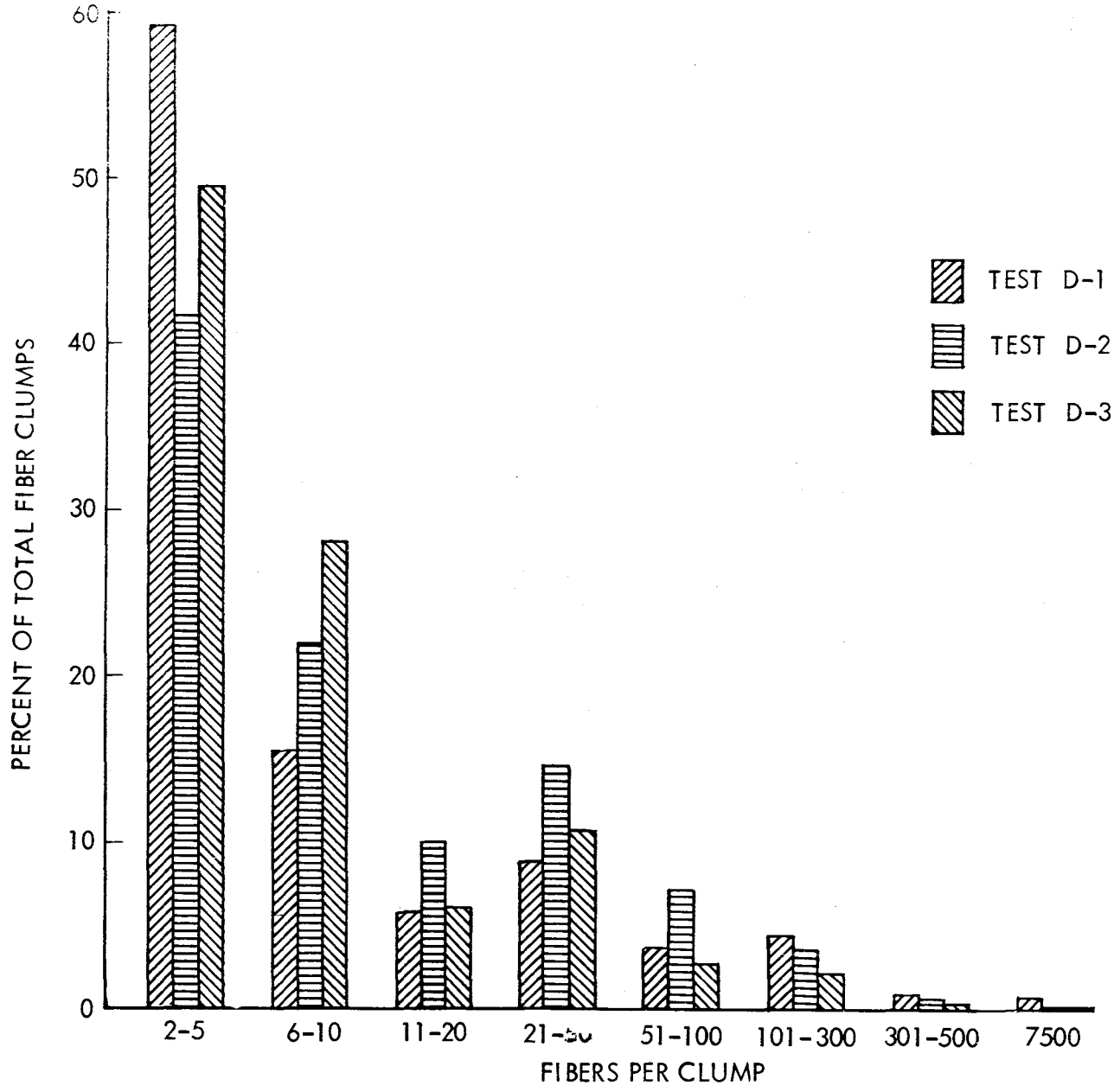

Figure 5.14. Number of Fibers per Clump Distribution

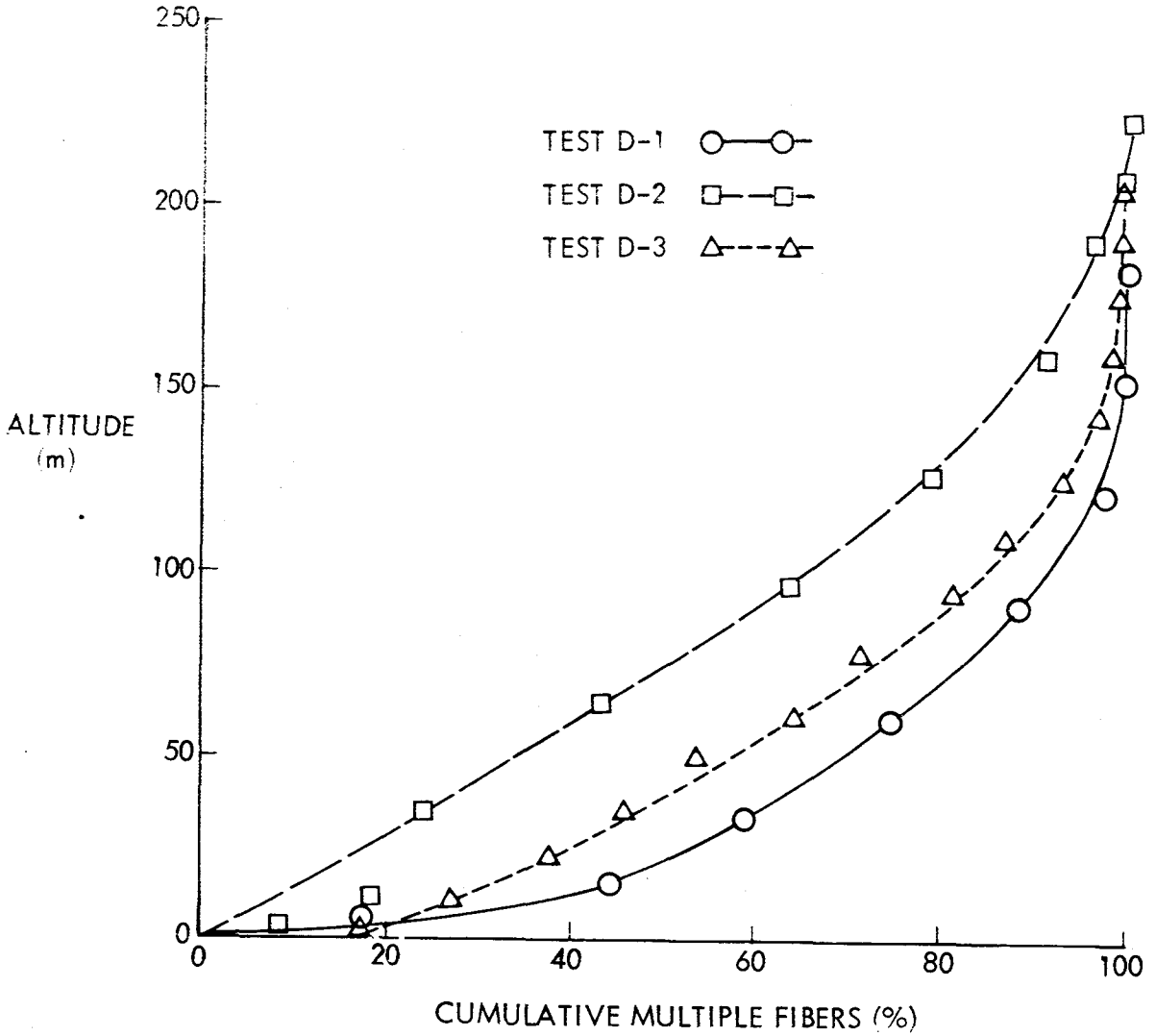

Figure 5.15. Cumulative Distribution of Fiber Clumps as a Function of Altitude

$$M = \frac{\pi}{4} \bar{d}^2 L \rho N$$

where

M is the mass released (gm)

$\bar{d}$ is 6.88×10^{-3} (mm)

L is the average fiber length (mm)

ρ is 1.73×10^{-3} gm/mm^3

N is the number of fibers

In the calculations of mass released, the values of the numbers of fibers presented in the previous sections were corrected to include an estimate of the fibers in that portion of the fiber cloud not intercepted by the vugraph collector array for tests D-1 and D-2. (For test D-3, the entire cloud was sampled.) Also, the following values were used for the initial carbon/graphite fiber mass in the unburned composite samples for each of the tests.

Table 5-18 Initial Carbon Fiber Mass in Unburned Composite Sample

Test	Carbon Fiber Mass (kg)
D-1	32.3
D-2	31.8
D-3	49.5

The mass-released calculations were performed for both single fibers and fiber clumps. The results for each of the tests are given in Tables 5-19 to 5-21 for single fibers, and Tables 5-22 to 5-24 for fiber clumps. Summaries for all three tests are given in Table 5-25 for single fibers, Table 5-26 for fiber clumps, and Figure 5.16 for both single fibers and fiber clumps. Note that the data in the summary charts for single fibers are for single fibers longer than 1 mm.

The summary Table 5-25 and Figure 5.16 show that for tests D-1 and D-2, approximately 0.2% of the initial, unburned carbon fiber mass was released as single fibers of lengths greater than 1 mm. However, for test D-3, approximately 0.1% of the initial carbon fiber mass was released for this regime of single fibers. This smaller percentage of mass release obtained for test D-3 may have been the result of the collapse of the composite sample support structure about seven minutes into the twenty-minute burn period, thus placing the composite samples into a less intense portion of the fire for the remainder of the test.

A comparison of the fiber mass released as fiber clumps with that of the mass released for single fibers shows that approximately two to three times as much mass was released as fiber clumps in all these tests as shown in Figure 5.16.

Table 5-19. Single Fiber Mass Released in Test D-1

FIBER LENGTH INTERVAL (mm)	AVERAGE FIBER LENGTH (mm)	MEASURED NO. OF SINGLE FIBERS	CLOUD FIBERS INTERCEPTED BY NET (%)	ESTIMATED SINGLE FIBERS IN FIBER CLOUD		SINGLE FIBER MASS RELEASED					
				(NO.)	%	gms	% *	gms	% *	gms	% *
0.5 - 1	0.75	4.47×10^7	74	6.04×10^7	16.5	2.91	0.009	2.96	0.009		
1 - 2	1.6	8.82×10^7	74	11.92×10^7	32.5	11.50	0.036	35.23	0.109		
2 - 4	3	9.10×10^7	74	12.30×10^7	33.6	23.73	0.073				
4 - 6	5	2.87×10^7	74	3.88×10^7	10.6	12.48	0.039			66.31	0.205
6 - 8	7	9.61×10^6	74	1.30×10^7	3.5	5.85	0.018	28.12	0.087		
8 - 10	9	4.08×10^6	74	0.55×10^7	1.5	3.19	0.010				
> 10	15.8	4.84×10^6	74	0.65×10^7	1.8	6.60	0.020				
TOTAL	2.82	2.71×10^8	-	3.66×10^8	100	66.31	0.205	66.31	0.205	66.31	0.205

* Based on initial, unburned carbon fiber mass equal to 32.3 kg.

Table 5-20. Single Fiber Mass Released in Test D-2

FIBER LENGTH INTERVAL (mm)	AVERAGE FIBER LENGTH (mm)	MEASURED NO. OF SINGLE FIBERS	CLOUD FIBERS INTERCEPTED BY NET (%)	ESTIMATED SINGLE FIBERS IN FIBER CLOUD		SINGLE FIBER MASS RELEASED					
				(NO.)	%	gms	% *	gms	% *	gms	% *
0.5 - 1	0.75	8.85×10^7	83	10.66×10^7	23.2	5.15	0.016	5.15	0.016		
1 - 2	1.5	1.17×10^8	83	14.10×10^7	30.7	13.61	0.043	41.74	0.131		
2 - 4	3	1.21×10^8	83	14.58×10^7	31.7	28.13	0.088				
4 - 6	5	2.96×10^7	83	3.57×10^7	7.8	11.48	0.036			76.28	0.240
6 - 8	7	1.55×10^7	83	1.87×10^7	4.1	8.42	0.026	29.39	0.092		
8 - 10	0	4.86×10^6	83	0.59×10^7	1.3	3.41	0.011				
> 10	17.2	4.59×10^6	83	0.55×10^7	1.2	6.08	0.019				
TOTAL	2.58	3.81×10^8	-	4.59×10^8	100	76.28	0.240	76.28	0.240	76.28	0.240

* Based on initial, unburned carbon fiber mass equal to 31.8 kg.

Table 5-21. Single Fiber Mass Released in Test D-3

FIBER LENGTH INTERVAL (mm)	AVERAGE FIBER LENGTH (mm)	MEASURED NO. OF SINGLE FIBERS	CLOUD FIBERS INTERCEPTED BY NET (%)	ESTIMATED SINGLE FIBERS IN FIBER CLOUD		SINGLE FIBER MASS RELEASED					
				(NO.)	%	gms	% *	gms	% *	gms	% *
0.5 - 1	0.75	5.02×10^7	100	5.02×10^7	17.0	2.42	0.005	2.42	0.005		
1 - 2	1.5	1.02×10^8	100	10.20×10^7	34.6	9.84	0.020	28.21	0.057		
2 - 4	3	9.52×10^7	100	9.52×10^7	32.3	18.37	0.037			52.43	0.106
4 - 6	5	2.63×10^7	100	2.63×10^7	8.9	8.46	0.017				
6 - 8	7	1.10×10^7	100	1.10×10^7	3.7	4.95	0.010	21.80	0.044		
8 - 10	9	5.93×10^6	100	0.59×10^7	2.0	3.41	0.007				
> 10	17.6	4.37×10^6	100	0.44×10^7	1.5	4.98	0.010				
TOTAL	2.76	2.95×10^8	-	2.95×10^8	100	52.43	0.106	52.43	0.106	52.43	0.106

* Based on initial, unburned carbon fiber mass equal to 49.5 kg.

Table 5-22. Fiber Clump Mass Released in Test D-1

NUMBER FIBERS PER FIBER CLUMP	AVERAGE NO. OF FIBERS PER FIBER CLUMP	AVERAGE FIBER LENGTH (MM)	MEASURED NO. OF FIBER CLUMPS	FIBER CLUMPS INTERCEPTED BY NET (%)	ESTIMATED FIBER CLUMPS IN FIBER CLOUD		FIBER CLUMP MASS RELEASED	
					(NUMBER)	(%)	(GMS)	(%)*
2 - 5	3.5	4.1	6.5×10^6	74	8.8×10^6	60.2	8.2	0.025
6 - 10	8	3.2	1.7×10^6	74	2.3×10^6	15.7	3.8	0.012
11 - 20	15.5	4.8	6.4×10^5	74	$.9 \times 10^6$	6.2	4.3	0.013
21 - 50	35.5	7.1	8.9×10^5	74	1.2×10^6	8.2	19.5	0.060
51 - 100	75.5	3.3	4.5×10^5	74	$.6 \times 10^6$	4.1	9.6	0.030
101 - 300	200	8.6	4.8×10^5	74	$.6 \times 10^6$	4.8	66.4	0.206
301 - 500	400	5.2	9.9×10^4	74	$.1 \times 10^6$	0.7	13.4	0.041
> 500	1000	22.6	1.2×10^4	74	$.02 \times 10^6$	0.1	29.0	0.090
TOTAL	24.0	-	1.1×10^7	-	1.5×10^7	100	154.2	0.477

* Based on initial, unburned carbon fiber mass equal to 32.3 kg.

Table 5-23. Fiber Clump Mass Released in Test D-2

NUMBER FIBERS PER FIBER CLUMP	AVERAGE NO. OF FIBERS PER FIBER CLUMP	AVERAGE FIBER LENGTH (MM)	MEASURED NO. OF FIBER CLUMPS	FIBER CLUMPS INTERCEPTED BY NET (%)	ESTIMATED FIBER CLUMPS IN FIBER CLOUD		FIBER CLUMP MASS RELEASED	
					(NUMBER)	(%)	(GMS)	(%)*
2 - 5	3.5	2.9	4.7×10^6	83	5.7×10^6	41.5	3.7	0.012
6 - 10	8	3.2	2.5×10^6	83	3.0×10^6	21.9	4.9	0.015
11 - 20	15.5	4.1	1.2×10^6	83	1.4×10^6	10.2	5.7	0.018
21 - 50	35.5	4.1	1.7×10^6	83	2.0×10^6	14.6	18.7	0.059
51 - 100	75.5	4.3	8.3×10^5	83	1.0×10^6	7.3	20.9	0.066
101 - 300	200	6.5	3.7×10^5	83	0.4×10^6	3.6	33.5	0.105
301 - 500	400	11.5	1.2×10^5	83	0.1×10^6	.7	29.6	0.093
> 500	600	26	2.4×10^4	83	0.03×10^6	.1	30.1	0.095
TOTAL	26.5	-	1.1×10^7	-	1.4×10^7	100	147.1	0.463

* Based on initial, unburned carbon fiber mass equal to 31.8 kg.

Table 5-24. Fiber Clump Mass Released in Test D-3

NUMBER FIBERS PER FIBER CLUMP	AVERAGE NO. OF FIBERS PER FIBER CLUMP	AVERAGE FIBER LENGTH (MM)	MEASURED NO. OF FIBER CLUMPS	FIBER CLUMPS INTERCEPTED BY NET (%)	ESTIMATED FIBER CLUMPS IN FIBER CLOUD		FIBER CLUMP MASS RELEASED	
					(NUMBER)	(%)	(GMS)	(%)*
2 - 5	3.5	3.1	8.8×10^6	100	8.8×10^6	49.5	6.1	.012
6 - 10	8	3.9	5.0×10^6	100	5.0×10^6	28.2	10.0	.020
11 - 20	15.5	3.5	1.1×10^6	100	1.1×10^6	6.2	3.8	.008
21 - 50	35.5	4.7	1.9×10^6	100	1.9×10^6	10.7	20.4	.041
51 - 100	75.5	7.8	4.5×10^5	100	$.5 \times 10^6$	2.8	18.9	.038
101 - 300	200	8.9	3.8×10^5	100	$.4 \times 10^6$	2.2	45.7	.092
301 - 500	400	18.6	5.2×10^4	100	$.05 \times 10^6$	.3	23.9	.048
> 500	575	27.6	1.3×10^4	100	$.01 \times 10^6$	.1	10.2	.021
TOTAL	16.8	-	1.8×10^7	-	1.8×10^7	100	139.0	.281

* Based on initial, unburned carbon fiber mass equal to 49.5 kg.

Table 5-25. Single Fiber (>1 mm) Mass Summary

TEST NO.	MEASURED NO. OF SINGLE FIBERS >1 mm	CLOUD FIBER INTERCEPTED BY NET (%)	ESTIMATED NO. SINGLE FIBERS >1 mm IN FIBER CLOUD	AVERAGE FIBER LENGTH FOR FIBERS >1 mm (mm)	SINGLE FIBERS >1 mm MASS RELEASED	
					(GMS)	(%)*
D - 1	2.3×10^8	74	3.1×10^8	3.22	63.4	0.20
D - 2	2.9×10^8	83	3.5×10^8	3.14	71.1	0.22
D - 3	2.4×10^8	100	2.4×10^8	3.18	49.9	0.10

* Based on initial, unburned carbon fiber mass.

Table 5-26. Fiber Clump Mass Release Summary

TEST NO.	MEASURED NO. OF FIBER CLUMPS	CLOUD FIBER INTERCEPTED BY NET (%)	ESTIMATED NO. FIBER CLUMPS IN FIBER CLOUD	AVERAGE NO. OF FIBER PER FIBER CLUMP	FIBER CLUMP MASS RELEASED	
					(GMS)	(%)*
D - 1	1.1×10^7	74	1.5×10^7	24.0	154.2	0.48
D - 2	1.1×10^7	83	1.4×10^7	26.5	147.1	0.46
D - 3	1.8×10^7	100	1.8×10^7	16.8	139.0	0.28

* Based on initial, unburned carbon fiber mass.

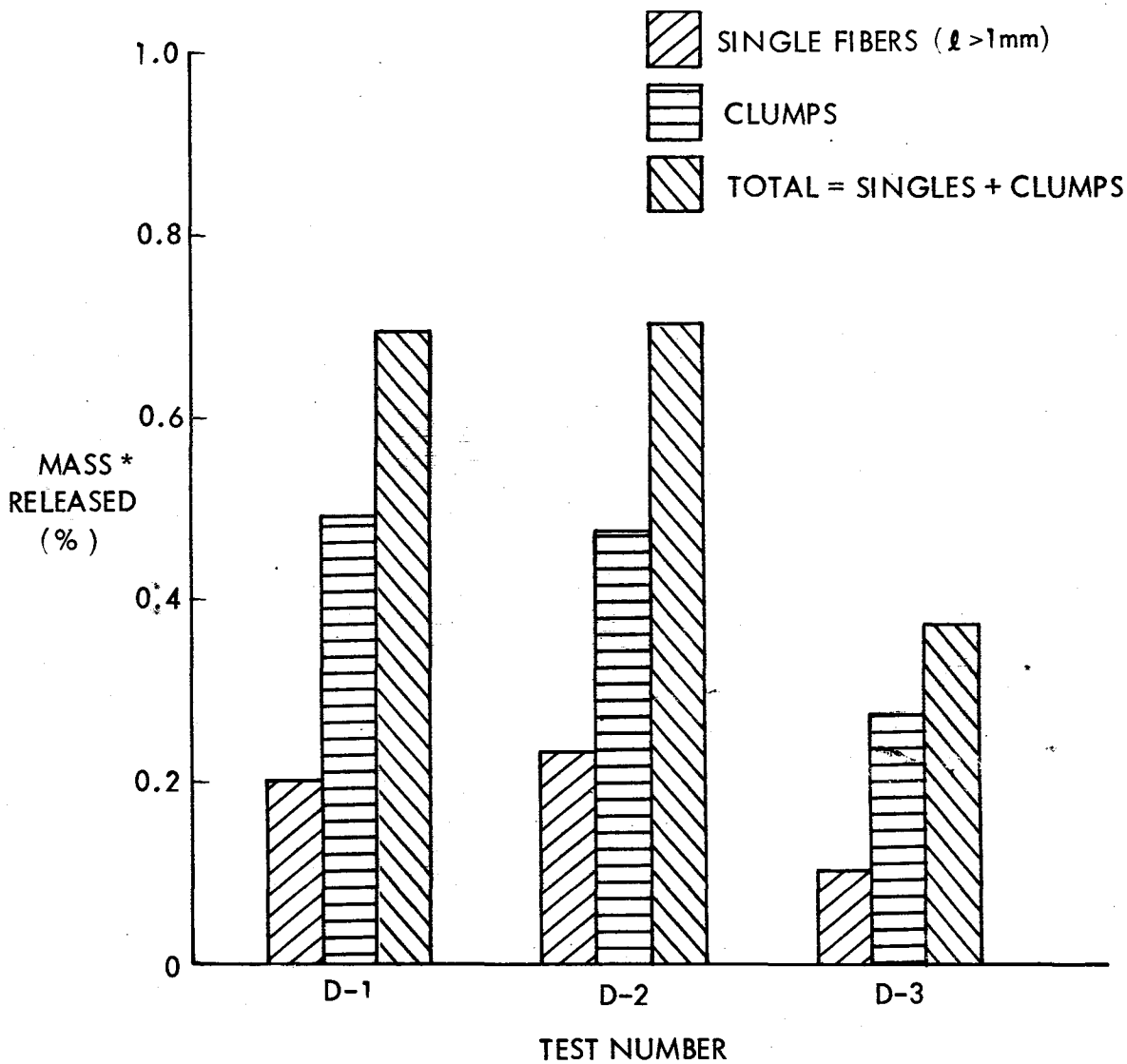

Figure 5.16. Percentage of Fiber Mass Release

Using the data in Tables 5-19, 5-20, and 5-21, it can be computed that of the mass released as single fibers of lengths greater than 1 mm, approximately 40% is released as fibers of lengths greater than 4 mm (the fiber lengths of principal concern as potential electrical hazards). This percentage varies only slightly among the three tests: 44% for tests D-1 and D-3, and 41% for test D-2.

The excellent correlation of the results obtained for mass release for the similar tests, D-1 and D-2, can be seen graphically in Figure 5.16. The data in this figure also show the excellent correlation among all three tests for the ratio of percentages of mass released as single fibers to mass released as fiber clumps.

LED FIBER DETECTOR

DATA REDUCTION TECHNIQUES

The recorded data obtained from the ground-based LED detectors were reduced by straightforward data reduction techniques. Calibrations made with the PAN 6μm dia fibers prior to each test were compared to the pulse heights of events obtained on the records. All apparent pulses, either below the general noise level or obviously representing the peaks of an oscillatory waveform, were not recorded as being fiber crossings. For all other pulses, the pulse height calibration gives a fiber "length" which is the minimum length of the single fiber associated with that pulse height. Further sophisticated analysis of the pulse height spectrum is possible at high concentrations where passive detector systems can establish a statistically significant length spectrum and multiplicity distribution for particles. However, the relatively low concentrations experienced on these tests did not permit the application of this latter analysis technique.

In general, the sensitive cross-sectional area of the detectors is not simply the geometrical cross section but is also a complex function of the fiber length, the fiber orientation with the beam axis and the pulse height threshold; however, for fibers which are small with respect to the beam diameter, where the threshold for detection above the noise level is low and where the LED beam axis is perpendicular to the air velocity vector, the geometrical cross section is a good approximation to the sensitive cross section. These criteria are met reasonably well for the ground-based LED setups for the three tests.

This geometrical cross-sectional area, as noted in a previous section, is $3.2 \times 10^{-3} m^2$ for the ground-based units, giving a sensitivity of 3.1×10^{2} fiber/m^2 per pulse.

Based on the average wind velocity experienced for each of the three tests, as reported by DPG for winds 8 metres above ground level, Table 5-27 shows the exposure represented by each pulse.

Table 5-27 Exposure Sensitivities
Ground-Based LED Units

Test	Windspeed at 8m alt. (m/s)	Exposure Sensitivity $\frac{\text{Fiber sec}}{\text{m}^3}$ per pulse
D-1	6.4	50
D-2	5.8	55
D-3	5.3	60

For the airborne units, recordings initially were read directly into an optical recorder using the tape recorder playback for each unit. It was immediately apparent that the noise levels were inordinately high, masking many of the possible short-length fiber crossings. These noise levels appeared to be oscillatory and non-random in nature, presumably due to net vibrations and possibly internal resonances in the units.

A spectrum analysis was performed on the recorded data after demodulating the 4096-Hz carrier frequency from each of the two detectors. Figure 5.17 displays results typical of all of the recordings. Unit A-2 showed resonance frequencies at about 240-, 380-, and 480-Hz which were independent of wind conditions. Unit A-1 did not exhibit these resonances at all. In the figure, the distinct frequencies at multiples of 60-Hz are due to main frequency injection at the demodulator and are not present on the recordings.

Recordings from both units exhibited vibrations of significant amplitude as a function of (presumably) wind velocity in the region below 60-Hz.

At the average wind velocities encountered during the tests, the transit time through the main part of the beam for a small fiber would be 15 mm ÷ 5 m/s = 3 ms, corresponding to fundamental frequencies of from 170-Hz to perhaps 350-Hz. Larger fiber pulses for "end-on" transit would range to somewhat less frequencies to a low of about 100-Hz.

From this analysis, it was determined that additional processing of the data would be possible by filtering out the wind-related lower frequencies and any frequencies above the maximum fundamental frequency. Notch filtering at the 240-Hz frequency would be unsuccessful, because of the wide half-width of the 240-Hz resonance and the potential loss of fiber passage data.

For all recordings, the data was accordingly processed using (a) a demodulator to remove the 4096-Hz carrier, followed by (b) a low-pass filter at 500-Hz to remove all vistages of the carrier and frequencies above those characteristic of the desired pulses, followed by (c) a high-pass filter at 60-Hz. Outputs from the tape, the filtered demodulator, and the 60-Hz filter were then displayed simultaneously on an optical recorder. Figure 5.18 shows the results for several situations on one of the tapes. The event in the left-hand trace has been cataloged as a fiber passage. The central set of traces shows a timing pulse (which

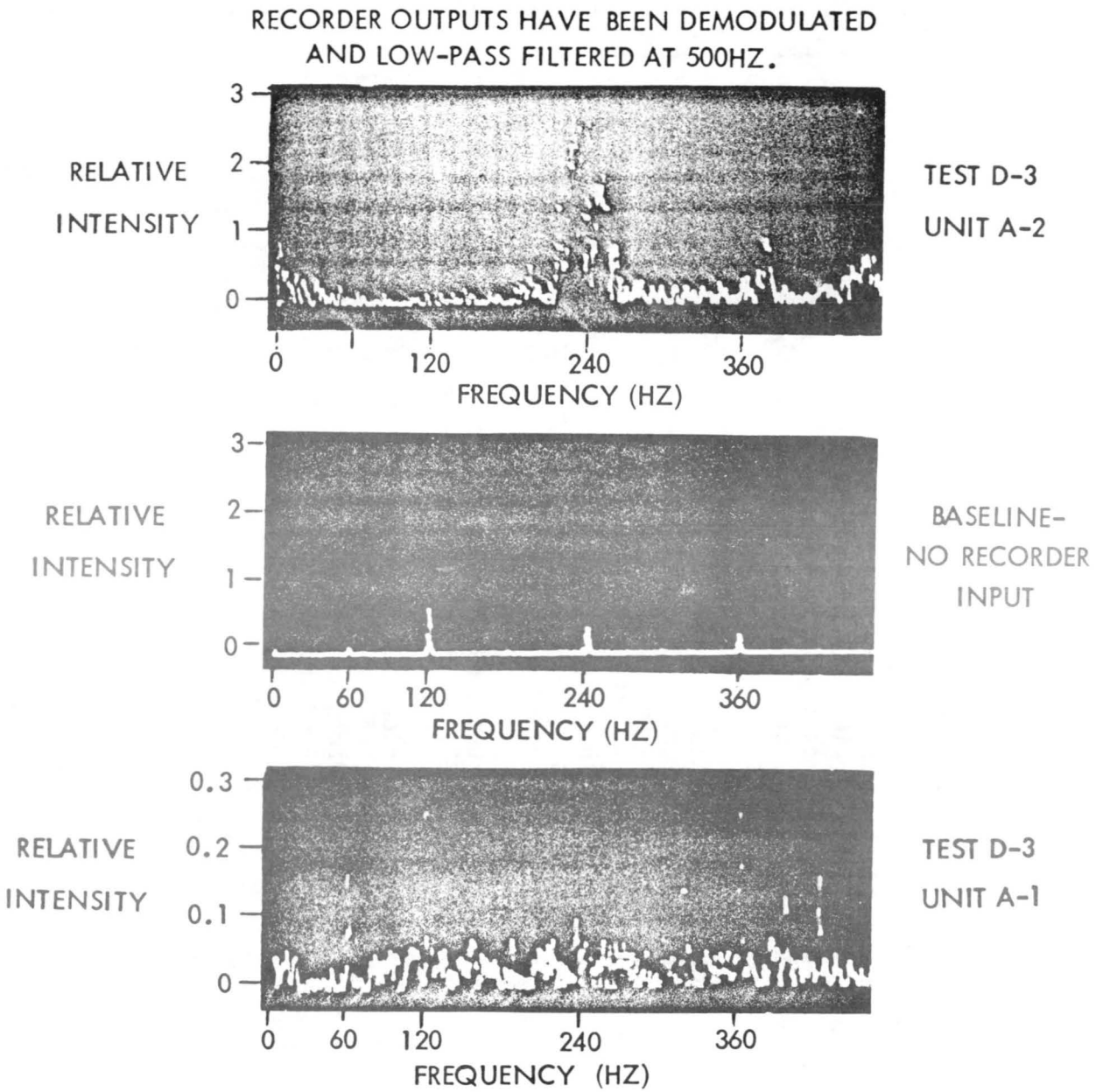

Figure 5.17. Spectrum Analysis of Recorder Tapes

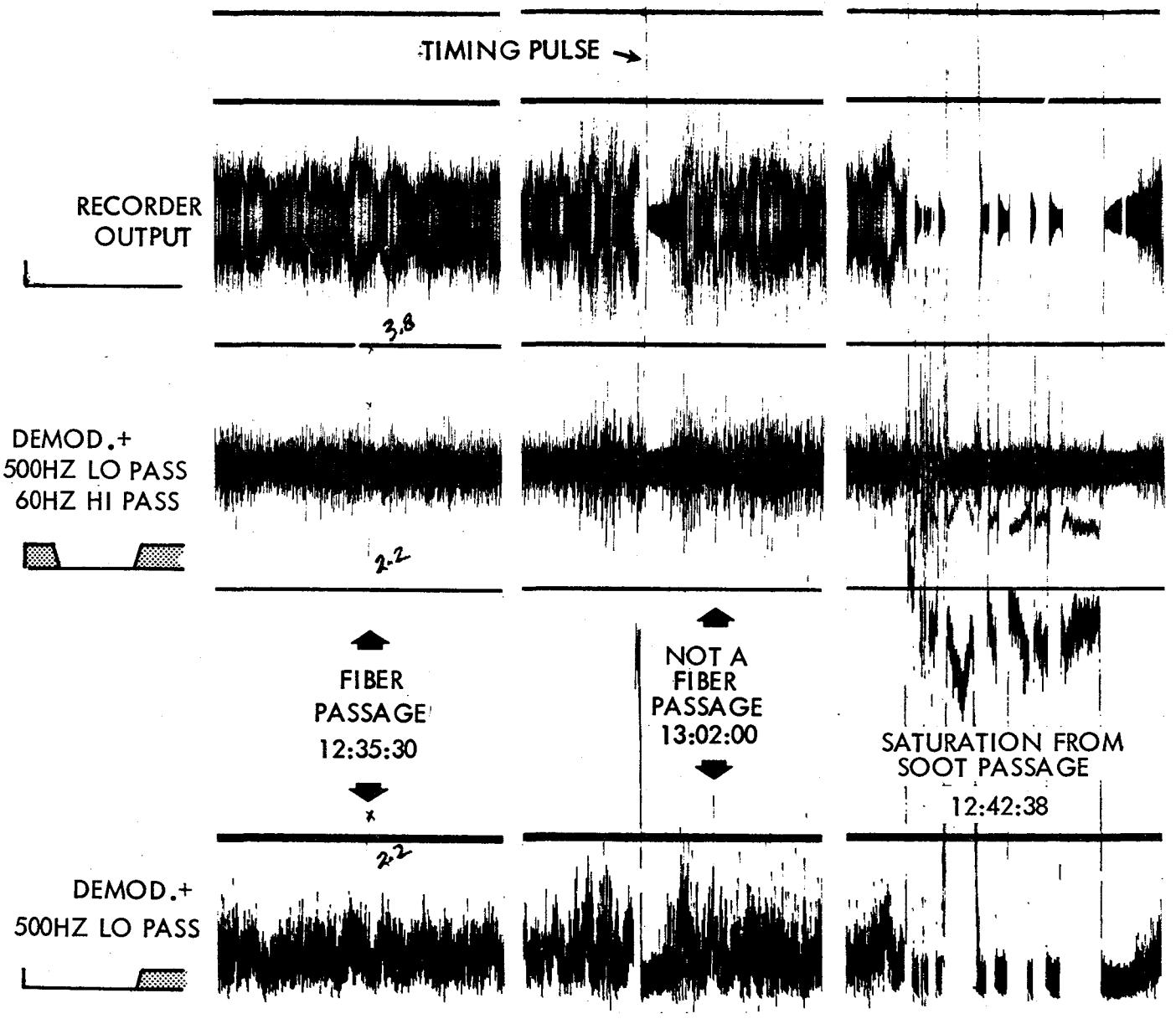

Figure 5.18. Data Analysis Test D-3 Detector A-1

has an amplitude slightly greater than passage of the 6μm PAN fiber calibrator through the 15-mm beam) and a pulse which might be assigned as a fiber passage in the undemodulated trace. But it loses its amplitude after low frequency filtering and hence, cannot be due to a fiber passage. The right-hand trace shows the signals during heavy soot passage and illustrates the impossibility of extracting fiber passage data during these dense soot periods.

The sensitivity of the airborne units - as for the ground-based units - is primarily a function of the geometrical cross section perpendicular to the beam, which is $2.64 \times 10^{-3} m^2$. The high noise levels, typically the equivalent of passage of a 5 mm fiber, reduces the effective area for observing fibers passing through the detecting volume by as much as a factor of two; hence, flux values obtained using the geometrical area can be in error by at least this much. As for the ground-based units, the exposure per observed pulse for the airborne units is obtained using the wind velocity. With due consideration of the inherent accuracy of the data and data reduction techniques, a single average value of the exposure per observed pulse was used for all three of the tests for the airborne detectors. This exposure value was based on an average windspeed of 5.8 m/s and is

$$\text{Exposure Sensitivity} = (2.6 \times 10^{-3} \times 5.8)^{-1}$$

$$\approx 70 \frac{\text{Fiber sec}}{m^3} \text{ per pulse}$$

RESULTS AND EVALUATION

The LED results for the three tests, D-1, D-2, and D-3, are displayed in Figures 5.19 to 5.22.

Test D-1 -- Approximately four hours before this test was initiated, the ground-based units and recorder were turned on to detect the presence of any fiber passage before the test. The recorder was turned off at 12:00 noon. At 3:02 pm, the T/M transmitter was activated to turn on the airborne units, and the recorder for the ground units was restarted.

Initial observations of the visible portion of the smoke plume showed that detector A-1 was generally at the bottom of the plume and detector A-2 was above and east of the plume. By 3:21 pm, the fire was starting to burn out and was almost completely out by 3:22 pm. At 3:45 pm, the T/M transmitter was reactivated to turn off the airborne units. Data was recovered from the airborne detectors at approximately 4:00 pm and the ground-based units and recorder were turned off at 5:24 pm.

In Figure 5.19, the ground-based LED results include a period of sampling prior to the initiation of the test D-1 burn. Both units recorded a significant exposure during this period. The records were closely examined to be certain that these pre-burn events were not due to spurious signals. It was verified that the events plotted were clearly due to fiber passage and that the total exposure represented during this sampling period must be at least as high as that indicated.

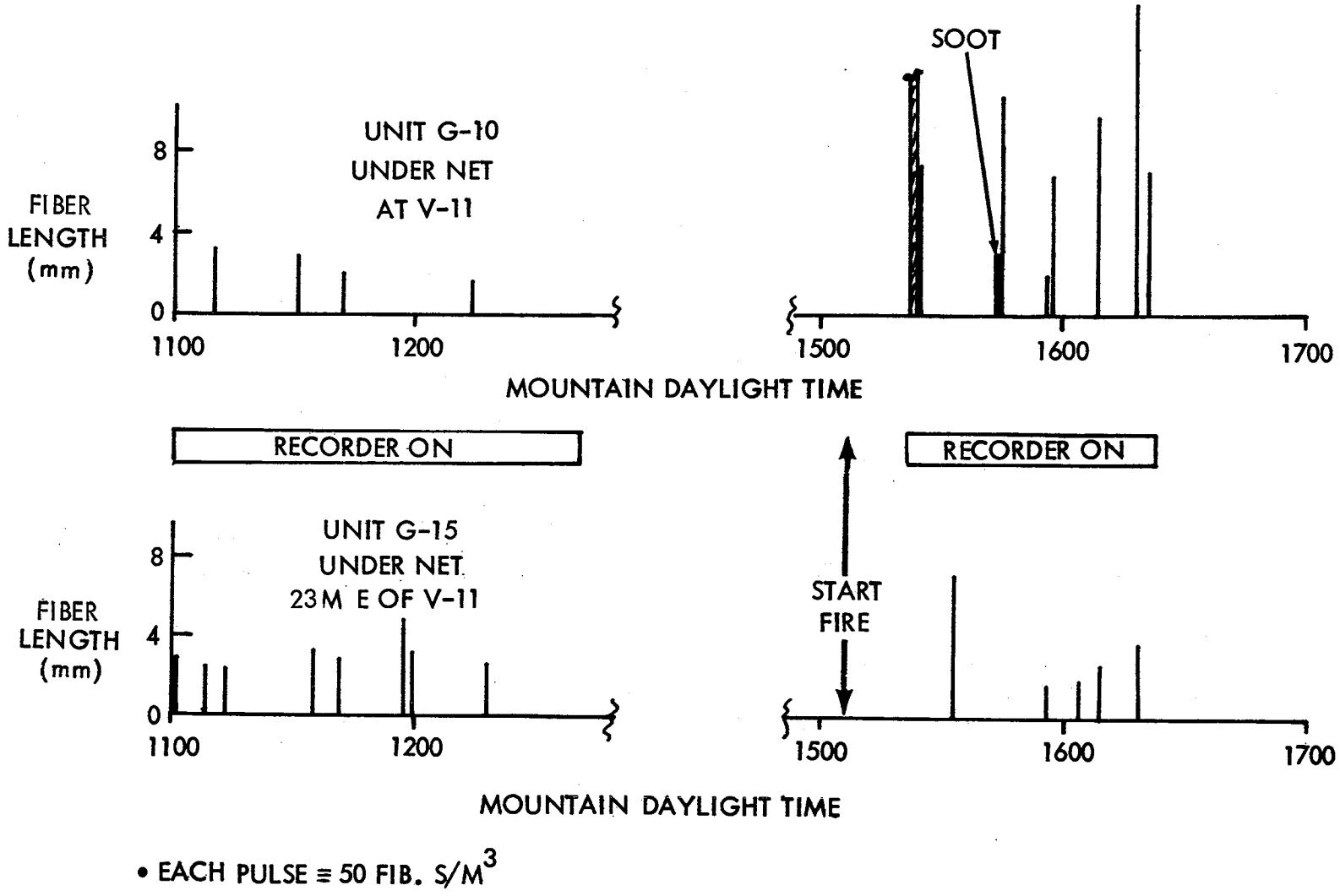

Figure 5.19. DPG Test D-1 Ground Based LED Detector Results

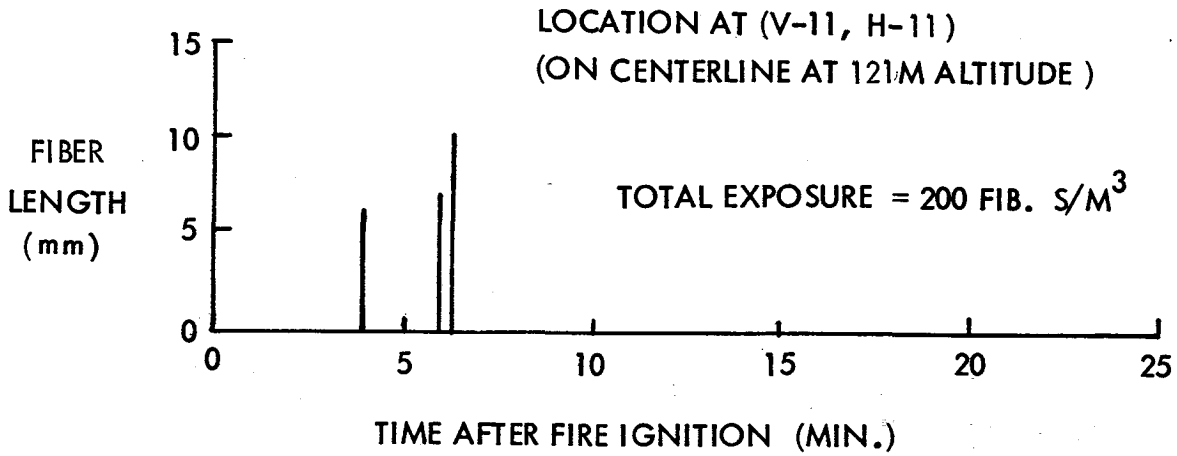

DETECTOR SENSITIVITY:

DETECTOR CROSS-SECTION, A ≅ BEAM LENGTH X BEAM DIAMETER = 26.4 CM^2

WIND VELOCITY, U = 6 M/S

EXPOSURE PER PULSE = $(U \times A)^{-1}$ ≅ 70 FIBER SECONDS/CUBIC METER

Figure 5.20. DPG Test D-1 Airborne LED Detector A-2 Results

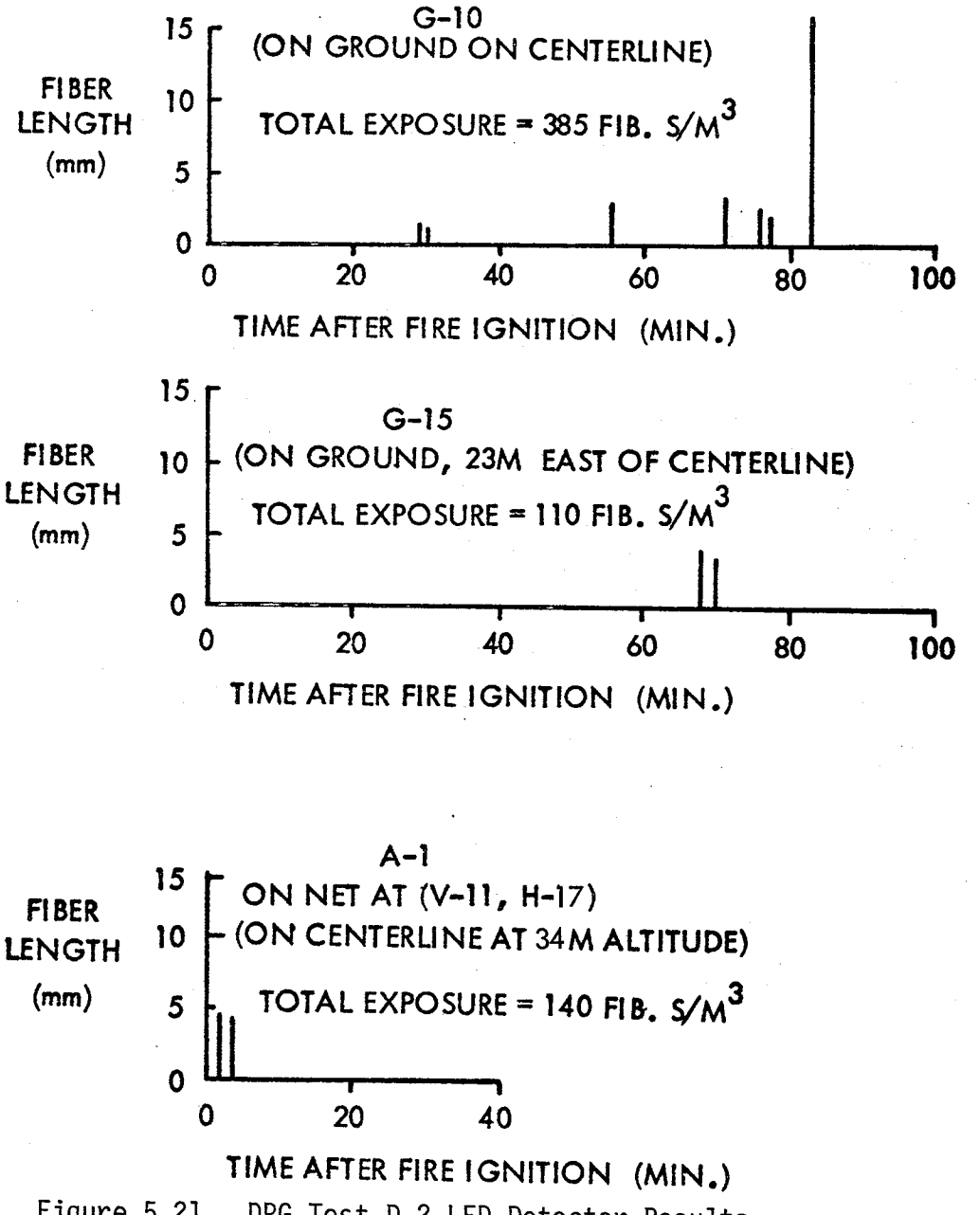

Figure 5.21. DPG Test D-2 LED Detector Results

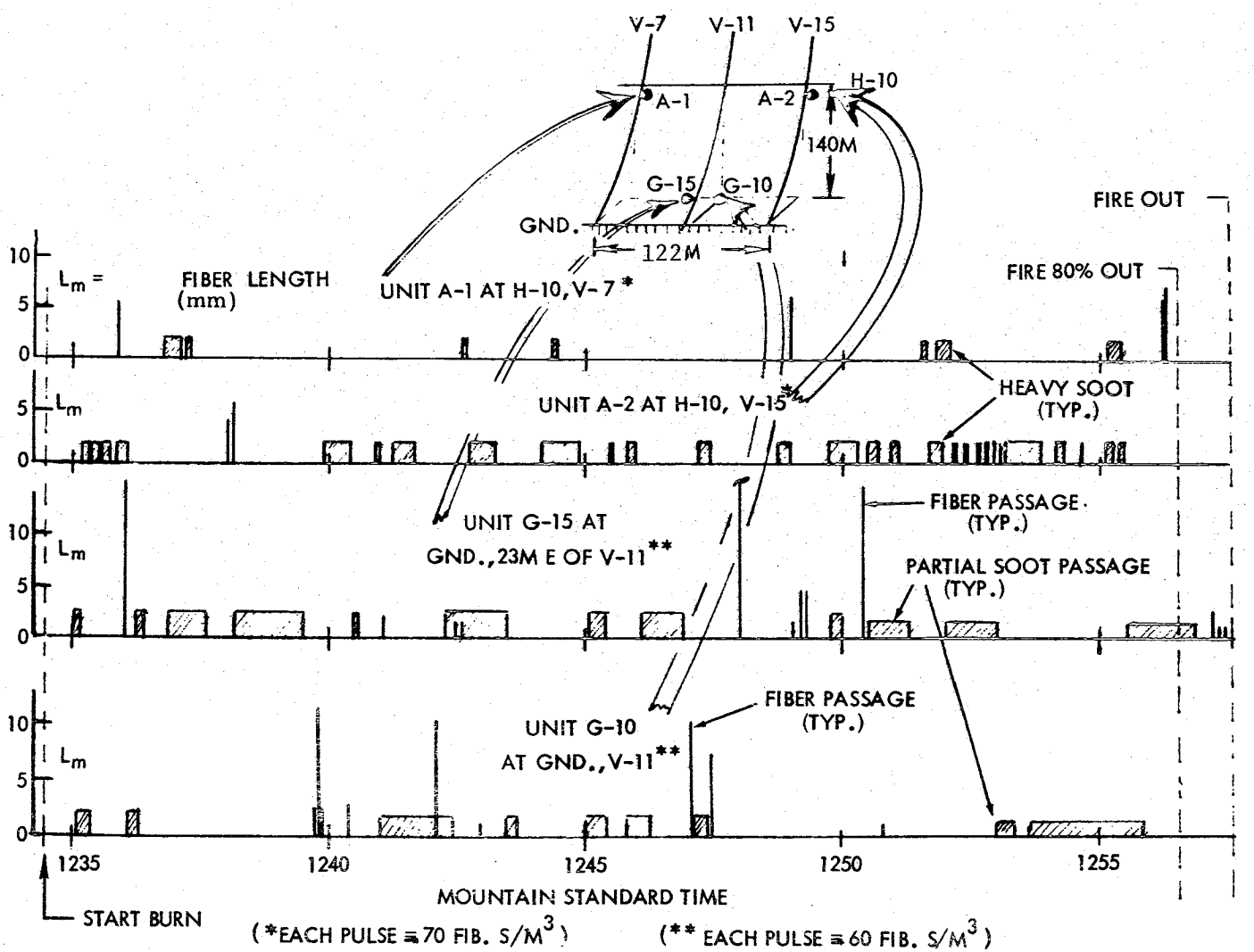

Figure 5.22. Test D-3 DPG - TRW LED Detectors Plume and Fiber Passage

Due to problems in the recorder trace, no data were recorded during the majority of the test D-1 burn period. The first receipt of soot indicated by the cross hatched area was the time both recording traces again became visible. Events were recorded considerably after the fire had burned out - to the end of the recording time - at about the time the vertical net array was lowered.

For test D-1, the recorder in the A-1 airborne unit at 35 meters altitude did not operate. The unit A-2 operated but returned very noisy data. These data were processed as described in the preceding section to give the results shown in Figure 5.20. The threshold below which pulses could not be distinguished from the noise, even with processing, was at pulse heights corresponding roughly to 4-mm length fibers.

Test D-2 -- This test was initiated at 9:41 am. The airborne detector units were activated by the T/M transmitter at 9:36 am, and the ground-based units fully activated at 9:37 am. Again, as in test D-1, the airborne detectors appeared to be completely out of the visible portion of the smoke plume. At approximately 10:01 am, the fire was starting to burn out and at 10:04 am was almost entirely out.

At about 10:20 am, the T/M transmitter was reactivated to turn off the airborne units. At approximately 11:20 am, data was recovered from the airborne detectors. It appeared that the recorder for unit A-2 did not run during the test. At 12:20 pm, the ground-based units were turned off and the recorder checked.

A malfunction of the ground based units recorder takeup reel had spoiled approximately 5 - 10 ft of paper and recordings. A previously experienced intermittent malfunction of the recorder resulting in some loss of signal on the paper track, was becoming more severe each day. The malfunction eventually forced the intensity control to be set to maximum to improve the very low signal to background contrast.

The results from test D-2 are presented in Figure 5.21. For the ground-based detectors, no pulses were received during the burn, but were received after the burn, continuing until the end of the recordings, approximately three hours after the burn (however only 100 minutes of this period is shown in Figure 5.21).

For test D-2, the recorder in the A-2 airborne unit at 125 meters altitude did not operate. The airborne unit at 34 m altitude operated and, again, the noise levels were high, but not as high as the first test. Only two events were noted by this detector and they occurred early in the burn, as shown in Figure 5.21.

Test D-3 -- The burn for this test was initiated at 12:31 pm. At 12:26 pm, the ground-based units were activated and at 12:30 pm the T/M transmitter was activated to turn on the airborne units. For this test, at least one or the other of the airborne units was within the visible portion of the smoke plume during the duration of the test. At 12:50 pm, the fire started to go out and at 12:57 pm was almost entirely out. At 1:12 pm, the T/M transmitter was reactivated to turn off the airborne units. At 2:19 pm, the optical recorder ran out of paper and a new roll was installed and recording resumed. At 3:52 pm the ground-based units were shut down. At approximately 2:30 pm, data from the airborne units was recovered.

For the third test, D-3, all four LED units operated and returned data. The results are displayed in Figure 5.22. During the test, each detector system recorded periods of heavy soot passage. During these periods, the airborne detectors were unable to distinguish fiber passage events. For the ground-based units, the soot did not appear to be as dense and the units did not go into saturation as did the airborne units. Some pulses were recorded during these periods.

For the D-3 test, as for the previous tests, very few events were identified. The data for each test was integrated over the test time to obtain exposure and the results are displayed in Table 5-28. The numbers in brackets are the exposures obtained for the vugraphs adjacent to the airborne units and the ground units.

Table 5-28 Summary of LED Detector Test Results

LED Detector	Position		Total Exposure (Fibers s/m^3)		
	Altitude (m)	East/West of Centerline (m)	Test D-1	Test D-2	Test D-3
G-10	On Gnd.	0	(50) 350 150*	(<10) 385	(770) 540
G-15	On Gnd.	23 E	(<10) 250 300*	(1660) 110	(2325) 720
A-1	34	0	No Data	(<10) 110	-
A-2	121	0	(0) 210	No Data	-
A-1	141	61 E	-	-	(90) 280**
A-2	141	61 W	-	-	(210) 140**

* Sampling for one hour, four hours before the test

** A-1 in obscuring soot for 7% of sampling time
A-2 in obscuring soot for 30% of sampling time

( ) Vugraph single fiber results

6. SUMMARY OF RESULTS

A concise restatement of the major findings of the carbon fiber investigations performed in this program is presented in this section. These findings are concerned principally with the results obtained from the analyses and evaluations of the data acquired in the large-scale fire tests conducted at Dugway Proving Ground by the Jacob's Ladder sampling net located approximately 140 m downwind from the fire.

The maximum values of single fiber depositions for fibers greater than 1 mm in length were:

Test	D-1	D-2	D-3
Deposition (Fibers/m^2)	6.5×10^4	4.0×10^4	4.3×10^4
Exposure (fiber sec/m^3)	10.2×10^3	6.9×10^3	8.1×10^3

The maximum value of single fiber and fiber clump deposition in each of the three tests was observed on a vugraph collector whose location was below 10 to 15 metres altitude. In all cases, these points of maximum deposition occurred in regions where there was no visible soot.

The deposition profiles (the distribution of the fibers along any given vertical or horizontal (crossrange) section) of the fiber cloud showed evidence of multiple peak values. As many as three or four peaks existed in the fiber distributions for some of the horizontal and vertical slices or sections through the collector array in all three tests.

The total number of single fibers greater than 1 mm in length and the total number of fiber clumps in the entire fiber cloud were estimated to be:

Test	D-1	D-2	D-3
No single fibers	3.1×10^8	3.5×10^8	2.4×10^8
No fiber clumps	1.5×10^7	1.4×10^7	1.8×10^7

The total number of single fibers greater than 1 mm in length were distributed within the entire fiber cloud approximately linearly as a function of altitude up to an 80- to 100-metre altitude. Approximately 50% of the single fibers were contained in the cloud below 50 to 70 metres. Approximately 80% of the fibers were contained in the bottom half of the cloud (below 100 metres). These results were very similar for all three tests.

The distributions of the total number of fiber clumps within the entire cloud were somewhat different for each of the tests. Approximately 50% of the fiber clumps were contained in the cloud below 20 to 75 metres depending on the test. Approximately 65 % to greater than 90% of the fiber clumps were contained in the bottom half of the cloud depending on the test.

The maximum altitude attained by the fiber cloud as it passed through, or intercepted the net, was 200 to 220 metres.

For single fibers of lengths greater than 1 mm, approximately 80% of the total number of fibers were in the length interval of 1 to 4 mm. Approximately 40% of the fibers were in the 1 to 2 mm length interval and 40% were in the 2-to 4-mm length interval. This distribution was essentially identical for all three tests.

For single fibers of lengths greater than 1 mm, 55 to 60% of the total mass of the fibers were in the length interval of 1 to 4 mm.

For tests D-1 and D-2, the number of single fibers greater than 1 mm in length was 20 to 25 times the number of fiber clumps. For test D-3, the number of single fibers greater than 1 mm in length was 13 times the number of fiber clumps.

The average length of single fibers greater than 1 mm in length was essentially identical for each of the three tests. The average lengths were:

Test	D-1	D-2	D-3
Average Length (mm)	3.22	3.14	3.18

40 to 60% of the total number of fiber clumps contained 2 to 5 fibers. 65 to 75% of the total number of fiber clumps contained 2 to 10 fibers.

Estimates of the mass of single fibers greater than 1 mm in length and the mass of fiber clumps within the entire fiber cloud is given below as a percentage of the initial, unburned carbon fiber mass for each test.

Test	D-1	D-2	D-3
$\frac{\text{Mass Single Fibers}}{\text{Initial Fiber Mass}}$ (%)	0.20	0.22	0.10
$\frac{\text{Mass Fiber Clumps}}{\text{Initial Fiber Mass}}$ (%)	0.48	0.46	0.28

The total mass of the fiber clumps was approximately 2.5 times the total mass of the single fibers greater than 1 mm in length in each of the tests.

The results obtained from the large-scale fire tests conducted at Dugway Proving Ground showed excellent correlation among all three tests.

APPENDIX A

SUMMARY OF JACOB'S LADDER STATIC LOADS

Presented in tabular format are the results of the Jacob's Ladder static load calculations performed for head-on wind conditions of 0, 6, 9, 12, 15 and 22.5 mph. The columns labeled "force/unit" and "total force" in Tables A-2 through A-7 give either the ground reactions for the tethers, net vertical cables, and mooring lines, or the free forces and dead weights acting on the system; the columns labeled "tension" give the approximate maximum tension in each cable for each specified wind condition.*

Also given are the component forces and resultant force (tension) present at the end connections of the main catenary, i.e., the point at which the main catenary attaches to the juncture plates. The loads in the main catenary are maximum at this point for any given wind condition.

It should be noted that the lifting force of the balloon increases with increasing wind velocity owing to aerodynamic lift. This incremental lift force per balloon is given in each table.

The specified ultimate breaking strengths and safe working loads (factor-of-safety equal to five) for each of the Kevlar cables used in the system is given below.

Table A-1. Kevlar Cable Specifications

Cable	Diam. (in.)	Ult. Breaking Strength (lb)	S.W.L. (lb)
Net Verticals Net Horizontals	0.13	1,450	290
Side Tethers Forward Tethers	0.25	6,000	1,200
Mooring Lines Aft Tethers Main Catenary Balloon Tethers	0.375	11,000	2,200

* In this appendix all units are given in U.S. Customary Units rather than SI units. The reason for this is that all design drawings, field layouts, load analyses, and fabrication and operational plans were developed in U.S. Customary Units. This system of units avoided confusion and errors during material procurement and field installation, checkout, and operation since all balloon, cable, hardware, and manufacturer's specifications and available tools such as measuring tapes, hand tools, load cells, and dynamometers used U.S. Customary units exclusively.

Table A-2 Load Summary for 0 mph Wind Velocity

FORCE IDENTIFICATION	FORCE/UNIT (LBS)		NO. OF UNITS	TOTAL FORCE (LBS)		TENSION (LBS)
	VERT.	HORIZ.(FWD)		VERT.	HORIZ.(FWD)	
Net Vertical	—	—	21	—	—	14
Side Tether	-79.6	—	2	-159.2	—	216
Forward Tether	—	—	2	—	—	69
Mooring Line	-823.9	—	2	-1647.8	—	899
Dead Weight	-1143.1	—	1	-1143.1	—	—
Balloon Lift	1475.0	—	2	2950.0	—	—
Wind Load on Net	—	—	1	—	—	—
Balloon Drag	—	—	2	—	—	—
Totals	—	—	—	-0.1	—	—

FORCE IDENTIFICATION	FORCES AT END CONNECTION (LBS)			
	VERT.	HORIZ.(FWD)	HORIZ.(SIDE)	TENSION
Catenary	200.6	——	157.0	255

Table A-3 Load Summary for 6 mph Wind Velocity

FORCE IDENTIFICATION	FORCE/UNIT (LBS)		NO. OF UNITS	TOTAL FORCE (LBS)		TENSION (LBS)
	VERT.	HORIZ.(FWD)		VERT.	HORIZ.(FWD)	
Net Vertical	-2.4	2.0	21	-50.4	42.0	17
Side Tether	-90.0	——	2	-180.0	——	239
Forward Tether	-19.6	38.7	2	-39.2	77.4	97
Mooring Line	-808.6	——	2	-1617.2	——	884
Dead Weight	-1143.1	——	1	-1143.1	——	——
Balloon Lift	1515.0*	——	2	3030.0*	——	——
Wind Load on Net	——	-89.8	1	——	-89.8	——
Balloon Drag	——	-15.0	2	——	-30.0	——
Totals	——	——	---	0.1	-0.4	——

* includes 40 lbs aerodynamic lift per balloon

FORCE IDENTIFICATION	FORCES AT END CONNECTION (LBS)			
	VERT.	HORIZ.(FWD)	HORIZ.(SIDE)	TENSION
Catenary	225.8	23.7	117.7	288

Table A-4 Load Summary for 9 mph Wind Velocity

FORCE IDENTIFICATION	FORCE/UNIT (LBS)		NO. OF UNITS	TOTAL FORCE (LBS)		TENSION (LBS)
	VERT.	HORIZ.(FWD)		VERT.	HORIZ.(FWD)	
Net Vertical	-5.40	4.54	21	-113.4	95.4	20
Side Tether	-104.3	—	2	-208.6	—	269
Forward Tether	-45.0	88.7	2	-90.0	117.4	145
Mooring Line	-777.4	—	2	-1554.8	—	853
Dead Weight	-1143.1	—	1	-1143.1	—	—
Balloon Lift	1555.0*	—	2	3110.0*	—	—
Wind Load on Net	—	-202.1	1	—	-202.1	—
Balloon Drag	—	-35.0	2	—	-70.0	—
Totals	—	—	—	0.1	0.7	—

* includes 80 lbs aerodynamic lift per balloon

FORCE IDENTIFICATION	FORCES AT END CONNECTION (LBS)			
	VERT.	HORIZ.(FWD)	HORIZ.(SIDE)	TENSION
Catenary	257.2	53.7	205.7	334

Table A-5 Load Summary for 12 mph Wind Velocity

FORCE IDENTIFICATION	FORCE/UNIT (LBS)		NO. OF UNITS	TOTAL FORCE (LBS)		TENSION (LBS)
	VERT.	HORIZ.(FWD)		VERT.	HORIZ.(FWD)	
Net Vertical	-9.6	8.1	21	-201.6	170.1	25
Side Tether	-125.3	—	2	-250.6	—	315
Forward Tether	-78.5	154.9	2	-157.0	309.8	214
Mooring Line	-758.9	—	2	-1517.8	—	834
Dead Weight	-1143.1	—	1	-1143.1	—	—
Balloon Lift	1635.0*	—	2	3270*	—	—
Wind Load on Net	—	-359.2	1	—	-359.2	—
Balloon Drag	—	-60.0	2	—	-120.0	—
Totals	—	—	—	-0.1	0.7	—

* includes 160 lbs aerodynamic lift per balloon

FORCE IDENTIFICATION	FORCES AT END CONNECTION (LBS)			
	VERT.	HORIZ.(FWD)	HORIZ.(SIDE)	TENSION
Catenary	301.4	94.9	247.3	401

Table A-6 Load Summary for 15 mph Wind Velocity

FORCE IDENTIFICATION	FORCE/UNIT (LBS)		NO. OF UNITS	TOTAL FORCE (LBS)		TENSION (LBS)
	VERT.	HORIZ.(FWD)		VERT.	HORIZ.(FWD)	
Net Vertical	-15.0	12.6	21	-315.0	264.6	37
Side Tether	-153.7	—	2	-307.4	—	376
Forward Tether	-123.3	243.3	2	-246.6	486.6	310
Mooring Line	-739.0	—	2	-1478.0	—	814
Dead Weight	-1143.1	—	1	-1143.1	—	—
Balloon Lift	1745.0*	—	2	3490.0*	—	—
Wind Load on Net	—	-561.3	1	—	-561.3	—
Balloon Drag	—	-95.0	2	—	-190.0	—
Totals	—	—	—	-0.1	-0.1	—

* includes 270 lbs aerodynamic lift per balloon

FORCE IDENTIFICATION	FORCES AT END CONNECTION (LBS)			
	VERT.	HORIZ.(FWD)	HORIZ.(SIDE)	TENSION
Catenary	358.1	148.3	303.3	492

Table A-7 Load Summary for 22.5 mph Wind Velocity

FORCE IDENTIFICATION	FORCE/UNIT (LBS)		NO. OF UNITS	TOTAL FORCE (LBS)		TENSION (LBS)
	VERT.	HORIZ.(FWD)		VERT.	HORIZ.(FWD)	
Net Vertical	-33.75	28.37	21	-708.8	595.8	55
Side Tether	-256.8	—	2	-513.6	—	603
Forward Tether	-275.4	543.5	2	-550.8	1087.0	643
Mooring Line	-547.0	—	2	-1094.0	—	622
Dead Weight	-1143.1	—	1	-1143.1	—	—
Balloon Lift	2005.0*	—	2	4010.0*	—	—
Wind Load on Net	—	-631.4	1	—	-1262.8	—
Balloon Drag	—	-210.0	2	—	-420.0	—
Totals	—	—	—	-0.3	0.0	—

* includes 530 lbs aerodynamic lift per balloon

FORCE IDENTIFICATION	FORCES AT END CONNECTION (LBS)			
	VERT.	HORIZ.(FWD)	HORIZ.(SIDE)	TENSION
Catenary	555.0	333.5	506.8	822

APPENDIX B

FABRICATION AND ASSEMBLY PROCEDURES

FOR

JACOB'S LADDER

Prior to the onset of the field activities, a fabrication and assembly procedures document was published, which gave the step-by-step details for assembling and installing the Jacob's Ladder system at the Dugway Proving Ground test site. This appendix is essentially the same as the fabrication and assembly document, JL79FT-100.000, developed and issued 28 August 1979 by TRW as part of the contractual effort for NASA.

In this appendix all units are given in U.S. Customary Units rather than SI units. The reason for this is that all design drawings, field layouts, load analyses, and fabrication and operational plans were developed in U.S. Customary Units. This system of units avoided confusion and errors during material procurement and field installation, checkout, and operation since all balloon, cable, hardware, and manufacturer's specifications and available tools such as measuring tapes, hand tools, load cells, and dynamometers used U.S. Customary units exclusively.

1.0 SCOPE

This appendix describes the procedures to be followed in the fabrication and assembly of the rope ladder, associated tethers, and the rope table that are to be used in the NASA carbon fiber tests at Dugway Proving Grounds.

2.0 TOOLS AND EQUIPMENT REQUIREMENTS

The tools and equipment required to fabricate and assemble the rope ladder, table and tethers are listed in Table B-1.

Table B-1 Tool and Equipment Requirements

Knives
Tyrap Tools
Tyraps
Cable Spool Support Structures
Assorted Hand Tools

3.0 MATERIAL REQUIREMENTS

3.1 ROPE LADDER AND TETHERS

The rope components of the ladder and tethers are supplied in coded lengths as listed in the cable schedule of Table B-2. Associated hardware (shackles, rings, etc.) are listed in Table B-3.

Table B-3 Rope Hardware

Item	Size	Qty.
Shackles	7/16"	54
Shackles	5/16"	6
Shackles	1/4"	70
Rings	1/2"	21
Rings	3/8"	8
Balloon Attach Plates	3/8"	2

3.2 ROPE TABLE

The rope for the rope table is 1/4" diameter dacron. Weights, to tension the rope, are to be concrete blocks 25 and 100 lbs each.

Table B-2 Cable Schedule

CABLE DIA. IN. (NOM)	CABLE LENGTH (FT)	CABLE QTY	EYE/SPLICE		NO EYE SPLICE	CODE
			ONE END	BOTH ENDS		
3/8	50	4		•		C- 1
↑	52	2		•		C- 2
	53	2		•		C- 3
	56	2		•		C- 4
	59	2		•		C- 5
	62	2		•		C- 6
	67	2		•		C- 7
	72	2		•		C- 8
	78	3		•		C- 9
	162	3		•		C-10
	150	4		•		B
	2,300	3	•			A
3/8	1,420	2		•		M
1/4	3,140	2		•		S
1/4	4,600	3	•			F
.13	1,900	4	•			SS
↑	1,000	4		•		NH- 1
	1,001	19			•	NH- 2
	110	4		•		NV- 1
	291	2		•		NV- 2
	440	4		•		NV- 3
	1,334	3		•		NV- 4
	1,111	1		•		NV- 5
	1,113	2		•		NV- 6
	1,121	2		•		NV- 7
	1,134	2		•		NV- 8
	1,152	2		•		NV- 9
	1,176	2		•		NV-10
	1,206	2		•		NV-11
	1,242	2		•		NV-12
.13	1,284	2		•		NV-13

4.0 PROCEDURES

4.1 GENERAL

The fabrication and assembly sequence will be as follows:

- Assemble the rope table
- Layout of vertical net lines
- Layout of horizontal net lines
- Tie vertical and horizontal net lines together
- Layout and assembly of catenary lines
- Connection of catenary lines to net
- Layout and connection of forward tethers
- Layout and connection of side catenary tethers
- Layout and connection of net stabilizing tethers
- Layout and connection of aft tethers
- Layout and connection of mooring lines

The rope table is assembled first to provide an area for the fabrication and assembly of the net. Next, the cables making up the net are laid out on the rope table in their relative positions, tied or connected together to form the net. The catenary which supports the net is then assembled and connected to the net. Finally, all tethers are laid out and connected at the appropriate locations.

4.2 ROPE TABLE

The rope table appears in finished form in the artist's sketch shown in Figure B.1. The rope is strung between the rows of seven-foot fence posts. Tension on each rope is maintained by tying a 100 lb weight on the end of each rope.

4.2.1 Material

The items required to assemble the rope table are:

Dacron rope	1/4" dia	18,000 ft
Concrete blocks	100 lbs	18 ea
Concrete blocks	25 lbs	64 ea
Bar	1" dia x 3' long	2 to 3 ea
Knife		2 ea

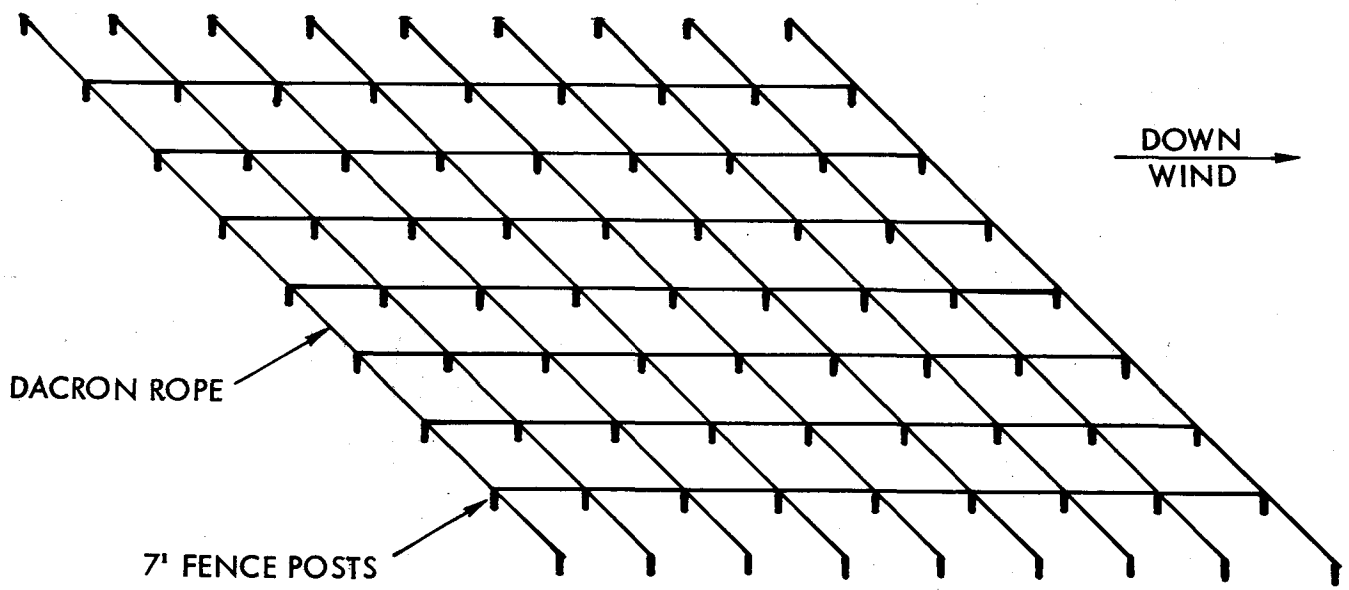

Figure B.1 Rope Table

4.2.2 Layout Procedure

a. Position one 100 lb weight at the base of each perimeter fence post along one side and one end (16 positions). Position 4 - 25 lb weights at each of the remaining perimeter fence post positions at the opposite side and end.

b. Support a spool of dacron rope using the bar as an axis for the spool so that the spool is able to rotate easily.

c. Position the spool of dacron rope at the end of a row where the 25 lb weights are located.

d. Unroll the dacron rope from the spool and thread through the eye top of each pole in the row.

e. After reaching the last fence post in the row, tie off the rope to the 100 lb weight.

f. At the spool end of the row, pull the excess rope back towards the spool. Raise and temporarily support each 25 lb weight 5 to 6 ft off the ground and while applying moderate tension to the rope, tie off th each weight. Cut the rope from the spool and remove the temporary supports from the weights.

g. Move a spool of rope to next row and repeat "c" through "f".

h. Repeat "g" for the remaining 14 rows.

4.3 NET FABRICATION

4.3.1 General

The net will be fabricated using the rope table as a bed to lay out the ropes used in the net construction.

4.3.2 Materials

Materials required to fabricate the net are:

Item	Size	Qty.	Remarks
Kevlar Cable	.13" dia	4 ea	Marked NH-1
Kevlar Cable	.13" dia	17 ea	Marked NH-2
Kevlar Cable	.13" dia	4 ea	Marked NV-1
Kevlar Cable	.13" dia	2 ea	Marked NV-2
Kevlar Cable	.13" dia	4 ea	Marked NV-3
Kevlar Cable	.13" dia	2 ea	Marked NV-4
Kevlar Cable	.13" dia	1 ea	Marked NV-5
Kevlar Cable	.13" dia	2 ea	Marked NV-6
Kevlar Cable	.13" dia	2 ea	Marked NV-7
Kevlar Cable	.13" dia	2 ea	Marked NV-8
Kevlar Cable	.13" dia	2 ea	Marked NV-9
Kevlar Cable	.13" dia	2 ea	Marked NV-10

Item	Size	Qty.	Remarks
Kevlar Cable	.13" dia	2 ea	Marked NV-11
Kevlar Cable	.13" dia	2 ea	Marked NV-12
Kevlar Cable	.13" dia	2 ea	Marked NV-13
Plastic Ties		~900 ea	
Tyrap Tool		3 ea	
Shackles	1/4" dia	66 ea	
Rings	1/2" dia	29 ea	
Bar	1" dia x 3' long	2 ea	

4.3.3 Layout of Net Verticals

a. Position Kevlar cable reels marked NV-3 through NV-13 at the designated net deadman as shown on *Figure B.2.*

b. Position Kevlar cables marked NV-1 approximately 400 ft and 900 ft downwind of net deadman as shown on Figure B.2.

c. Position remaining Kevlar cables marked NV-3 approximately 600 ft downwind of net deadman as shown on Figure B.2.

d. Position Kevlar cable marked NV-2 approximately 1000 ft downwind of net deadman as shown on Figure B.2.

e. Support one of the NV-4 through NV-13 marked Kevlar cable spools so that the cable may be unrolled from it.

f. Unroll the cable from the spool over the rope table and let the cross range rows of the table support it.

g. Connect the cable to the net deadman using a 1/4" shackle.*

h. Repeat "e", "f", and "g" for each of the remaining NV-4 through NV-13 cables.

i. Unroll and lay out the NV-3, NV-1, NV-3, NV-1 and NV-2 cables in that order for each outside net vertical over the rope table cross rows. Use a 1/4" shackle, ring, and 1/4" shackle in that order to connect between each cable segment and use a 1/4" shackle to connect the NV-3 cable to the net deadman.*

j. Attach a 1/4" shackle and a 1/2" ring to each net vertical cable at the free end. *

NOTE: It may be necessary to temporarily tie the net verticals to the rope table to prevent excessive sagging or bunching up on the rope table.

* "Lock wire"all shackle pins by manually tightening a Tyrap tie through shackle pin eye and around shackle.

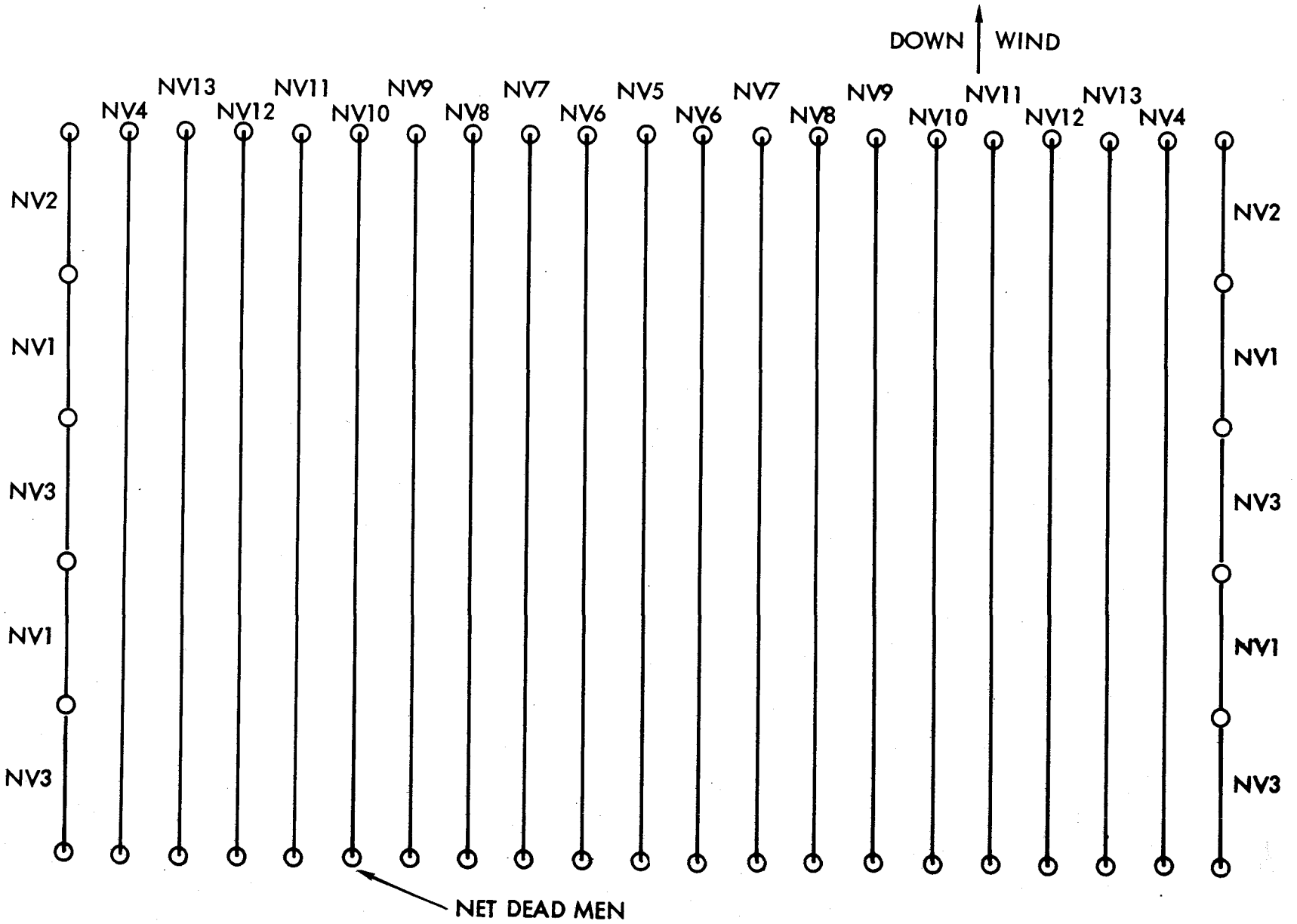

Figure B.2 Net Vertical Layout

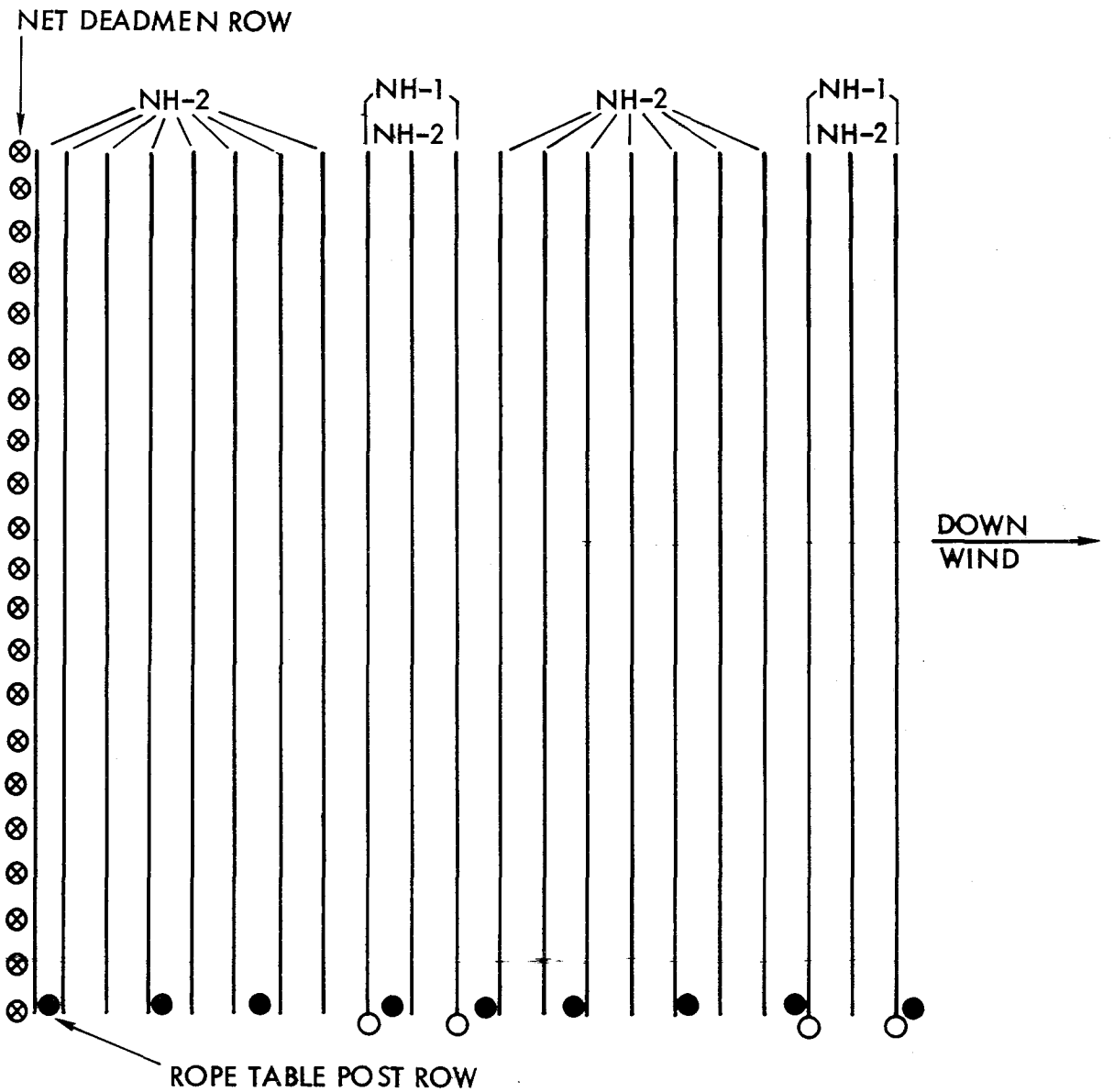

Figure B.3 Net Horizontal Layout

4.3.4 Layout of Net Horizontals

a. Position Kevlar cable reels marked NH-1 and NH-2 along one side of the rope table at approximately 50 ft intervals as shown in Figure B.3.

b. Support one of the NH-1 or NH-2 marked Kevlar cable spools so that the cable may be unrolled from it.

c. Unroll the cable from the spool over the net verticals letting the net verticals and downrange rows of the table support it.

d. Repeat step "c" for the remaining horizontal cables.

e. Connect the NH-1 cables to the rings joining the NV-1, NV-2, and NV-3 cables using 1/4" shackles. *

NOTE: It may be necessary to temporarily tie the net horizontals to the rope table to prevent excessive sagging or bunching up on the rope table.

4.3.5 Tie-Down of Cross Members

Tie down of net horizontals to net verticals will be done at each crossover point of the two sets of cables. Each cable has been pre-marked to indicate each crossover point. The crossover tie will be made using tie wraps in the manner shown in Figure B.4a for the interior crossovers and in the manner shown in Figure B.4b where the net horizontals terminate at a net vertical (all NH-2 cables). Set tension adjustment on Tyrap tool to position 2. After completing each intersection, check the integrity of the Tyrap ties by manually applying moderate force on the vertical and horizontal net cables in all opposing directions.

4.4 NET CATENARY

The net catenary is composed of 22 sections of 3/8" Kevlar cable coded C-1 through C-10 with each section located with respect to the net verticals as shown in Figure B.5.

* "Lock wire" all shackle pins by manually tightening a Tyrap tie through shackle pin eye and around shackle.

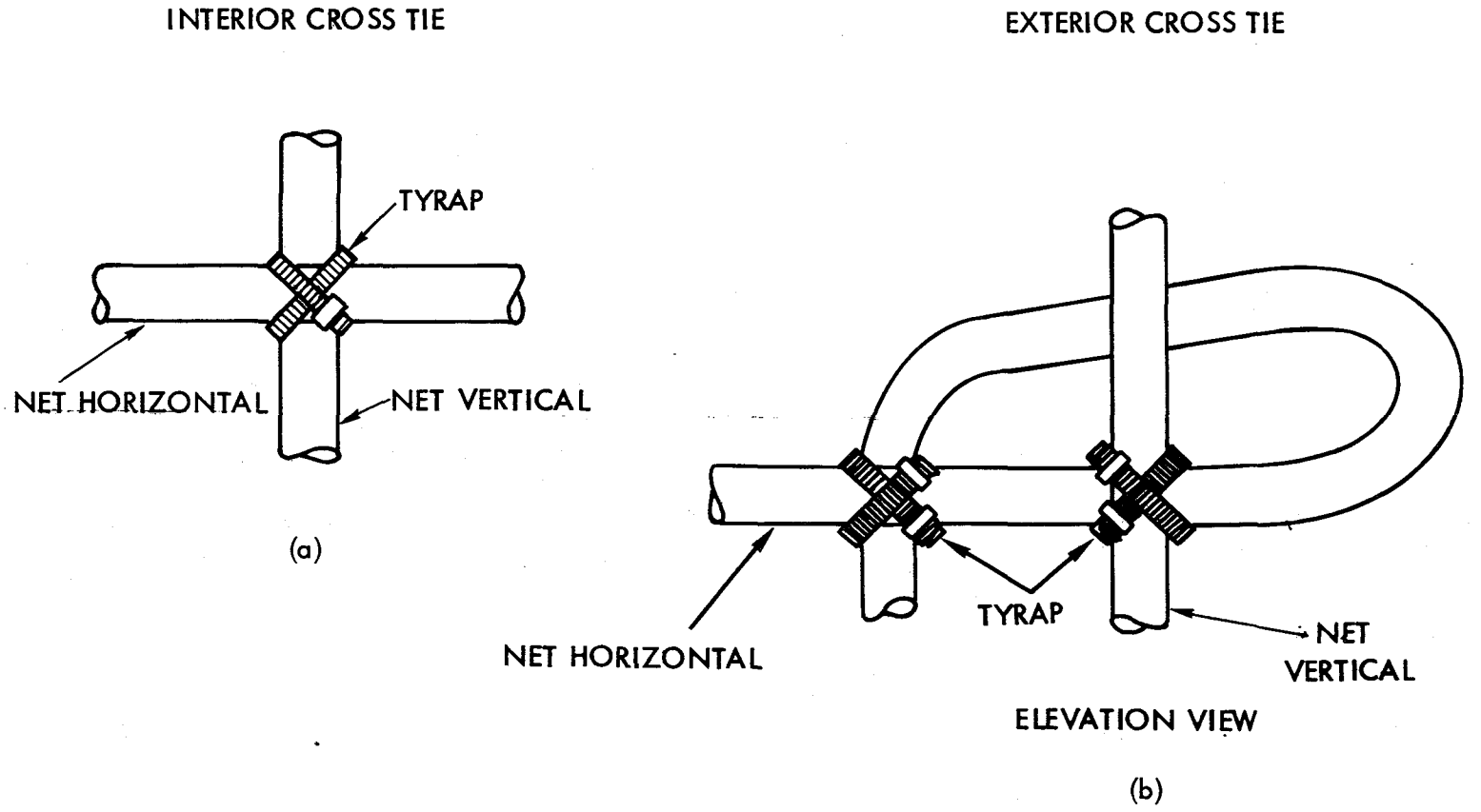

Figure B.4 Net Cross Ties

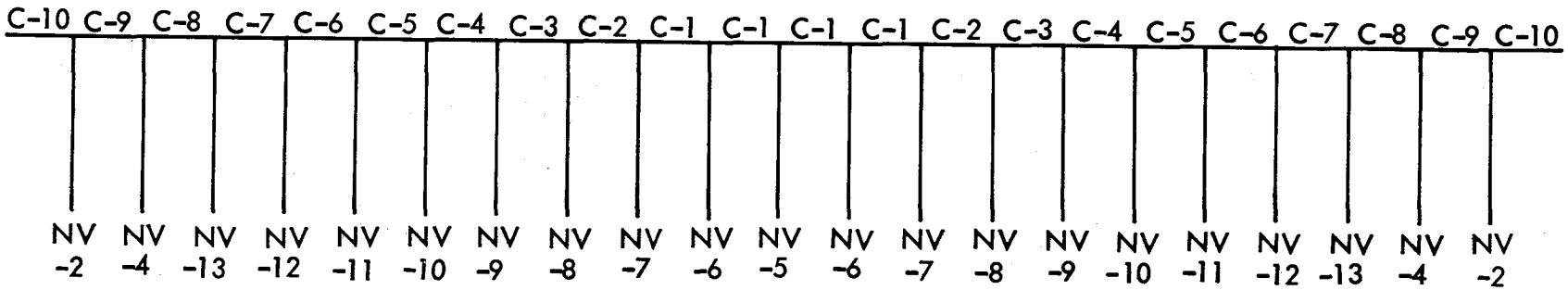

Figure B.5 Catenary Cable Locations

4.4.1 Materials Required

Item	Size	Qty.	Remarks
Kevlar Cable	3/8" dia	4 ea	Marked C-1
Kevlar Cable	3/8" dia	2 ea	Marked C-2
Kevlar Cable	3/8" dia	2 ea	Marked C-3
Kevlar Cable	3/8" dia	2 ea	Marked C-4
Kevlar Cable	3/8" dia	2 ea	Marked C-5
Kevlar Cable	3/8" dia	2 ea	Marked C-6
Kevlar Cable	3/8" dia	2 ea	Marked C-7
Kevlar Cable	3/8" dia	2 ea	Marked C-8
Kevlar Cable	3/8" dia	2 ea	Marked C-9
Kevlar Cable	3/8" dia	2 ea	Marked C-10
Shackles	7/16" dia	44 ea	
Balloon Attach Plate		2 ea	

4.4.2 Layout and Connection

a. Position the 3/8" catenary cables between the appropriate net verticals in accordance with Figure B.5.

b. Starting at one end of the net, connect the C-10 cable to the NV-2 vertical ring using a 7/16" shackle.*

c. Moving to the next position, connect one end of the cable marked C-9 to the NV-2 vertical ring using a 7/16" shackle.*

d. Unroll the C-9 cable to the next net vertical marked NV-4 and connect to the ring using a 7/16" shackle.*

e. Repeat steps "c" and "d" for each of the next 19 catenary sections.

f. Connect the last C-10 cable to NV-2 cable.

g. Connect the free terminations on the two C-10 cables to the two balloon attach plates as shown in Figure B.6 using a 7/16" shackle*, and stretch each cable to the aft tether deadman positions.

4.5 FORWARD TETHER LAYOUT

The two forward tethers, marked F, are to be laid out on either side of the net from the aft tether deadman to the forward tether deadman as shown in Figure B.7.

* "Lock wire" all shackle pins by manually tightening a Tyrap tie through shackle pin eye and around shackle.

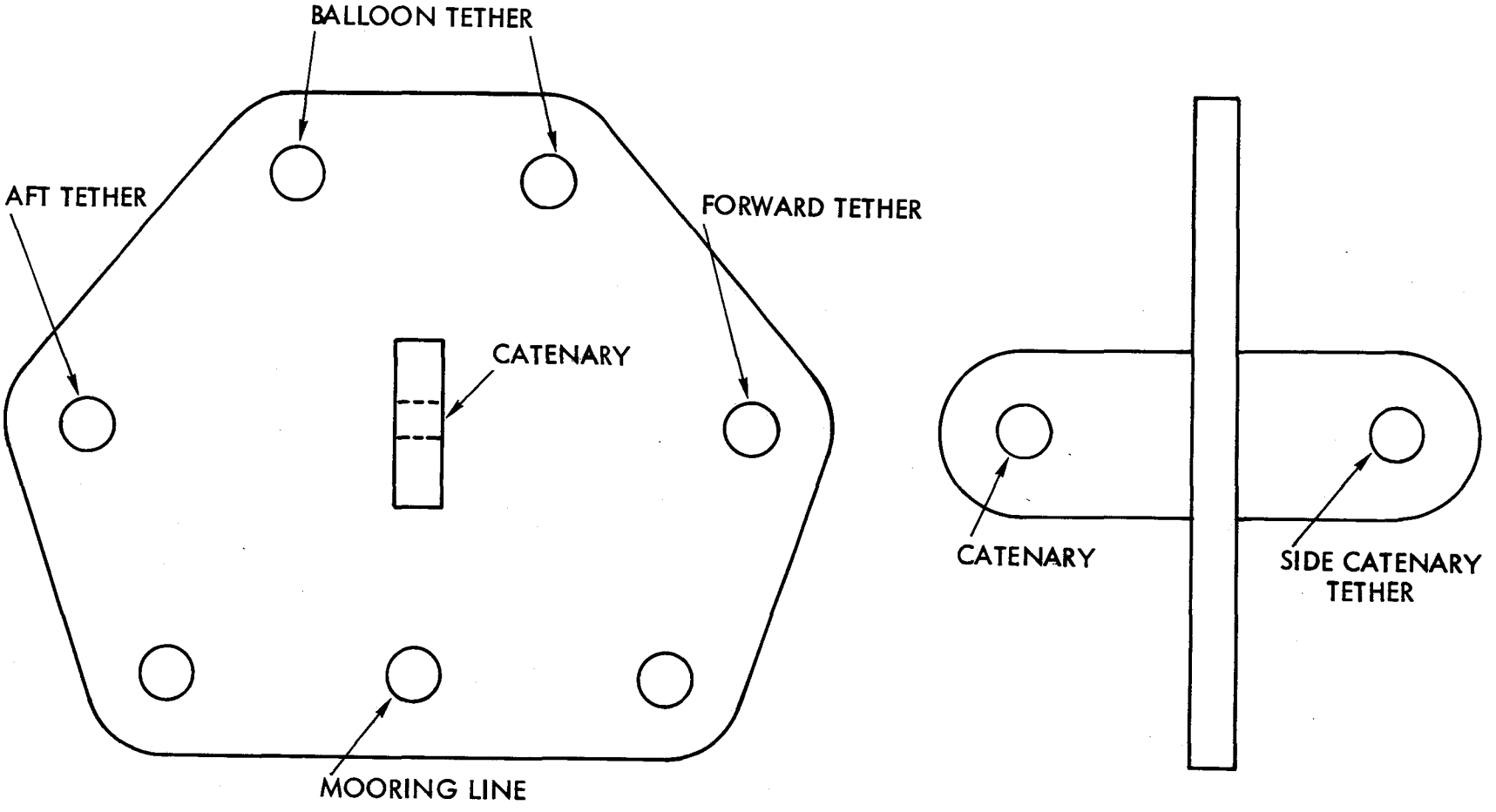

Figure B.6 Balloon Attach Plate

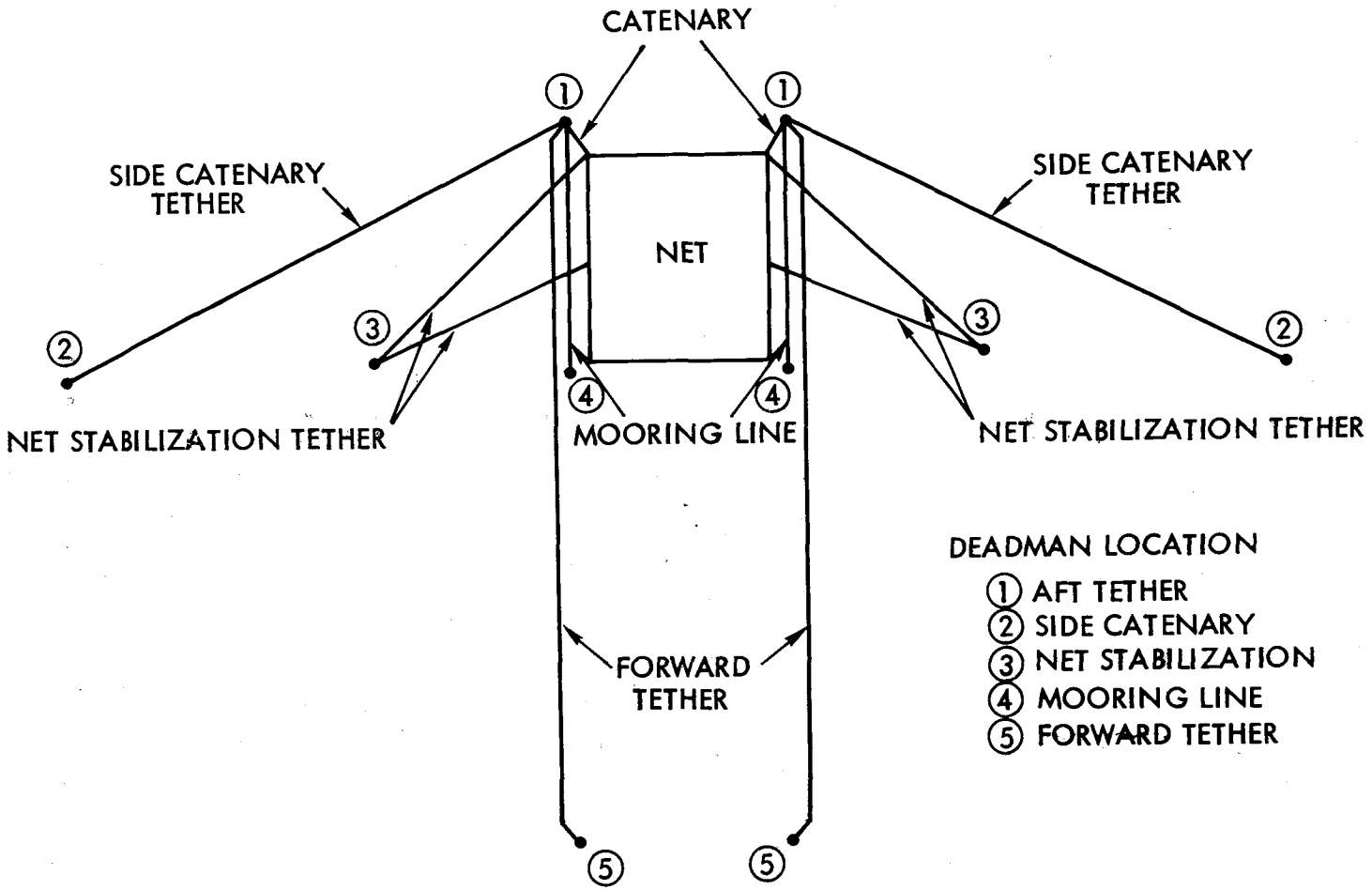

Figure B.7 Tether Lines Layout

4.5.1 Materials

Item	Size	Qty.	Remarks
Kevlar Cable	1/4"	2	Marked F
Shackles	5/16"	2	

a. The spools containing the forward tether cables are to be placed at the forward tether winch points.

b. Support one forward tether cable spool so that the spool is able to rotate freely.

c. Attach free end of cable to winch and reel in approximately 350 ft of cable on the winch drum.

d. Lay out cable to the aft tether point by unreeling the cable from the spool as the spool is moved to the aft tether point.

e. Attach the end of the cable to the balloon attach plate as shown in Figure B.6 using a 5/16" shackle.*

f. Repeat "a" through "e" for the other forward tether cable.

NOTE: Do not run vehicles over or step on any cables.

4.6 SIDE CATENARY TETHERS

The two side catenary tethers, marked S, are to be laid out on either side of the net from the side catenary tether point to the aft tether points as shown in Figure B.7.

4.6.1 Materials

Item	Size	Qty.	Remarks
Kevlar Cable	1/4" dia	2	Marked S
Shackles	5/16" dia	6	
Cable length adjustment devices		2	

* "Lock wire" all shackle pins by manually tightening a Tyrap tie through shackle pin eye and around shackle.

4.6.2 Layout Procedure

a. The spools containing the side catenary tether cables are to be placed at the aft tether point.

b. Support one of the side catenary tether cable spools so that the spool will rotate smoothly.

c. Attach the end of the side catenary tether cable to the balloon attach plate as shown in Figure B.6 using a 5/16" shackle.*

d. Lay out cable to the side catenary tether point by unreeling the cable from the spool as the spool is moved to the side catenary tether point.

e. Attach one end of the cable adjustment fixture to the end of the cable using the 5/16" shackle. *

f. Attach the other end of the cable adjustment structure to the side catenary tether deadman.using a 5/16" shackle.*

g. Repeat "b" through "f" for the other side catenary tether.

NOTE: Do not run vehicles over or step on any cables.

4.7 NET STABILIZATION TETHERS

The four net stabilization tethers are to be laid out, two on each side of the net, from the net to the net stabilization winches as shown in Figure B.7. One of the tethers is connected at the top of the net and the second is connected at the side midpoint of the net.

4.7.1 Materials

Item	Size	Qty.	Remarks
Kevlar Rope	.13" dia	4	Marked SS
Shackles	1/4" dia	4	

* "Lock wire" all shackle pins by manually tightening a Tyrap tie through shackle pin eye and around shackle.

4.7.2 Layout Procedures

a. Position two net stabilization spools at one of the net stabilization winch locations.

b. Support one cable spool so that the spool is able to rotate freely.

c. Thread the cable through one sheave and to one winch at the net stabilization winch site. Wind 300 ft of cable on winch.

NOTE: Insure that the cable winds evenly on the winch layer by layer.

d. Lay out cable to the top net horizontal by unreeling the cable from the spool as the spool is moved to the top net horizontal location.

e. Connect the net stabilization cable to the top net horizontal ring with a 1/4" shackle.*

f. At the net stabilization winch site, support the second cable spool so that the spool is able to rotate freely.

g. Thread the cable through the second sheave and wind on the second winch.

h. Lay out cable to the mid net horizontal by unreeling the cable from the spool as the spool is moved to the mid net horizontal location.

i. Connect the net stabilization cable to the mid net horizontal ring with a 1/4" shackle.*

j. Repeat "a" through "i" for the other two net stabilization cables on the opposite side of the net.

NOTE: Do not run vehicles over or step on cables.

4.8 MOORING LINE

The two mooring lines, marked M, are to be laid out on either side of the net from the mooring line deadman position to the aft tether deadman position as shown in Figure B.7.

4.8.1 Material

Item	Size	Qty.	Remarks
Kevlar Cable	3/8" dia	2	Marked M
Shackles	7/16" dia	4	

* "Lock wire" all shackle pins by manually tightening a Tyrap tie through shackle pin eye and around shackle.

4.8.2 Layout Procedure

a. The spools containing the mooring lines are to be placed at mooring line deadman.

b. Support one mooring line spool so that the spool is able to rotate freely.

c. Connect the free end of the cable to the mooring line deadman using 7/16" shackle.*

d. Lay out cable to the aft tether point position by unreeling the cable from the spool as the spool is moved to the aft tether point.

e. Connect the cable end to the balloon attach plate as shown in Figure B.6 using a 7/16" shackle.*

f. Repeat "b" through "e" for the other mooring line.

NOTE: Do not run vehicles over or step on cables.

4.9 AFT TETHER LAYOUT

The two aft tethers will be wound on the two aft winches. The thimble terminated end of the cable will be attached to the balloon attach plate.

4.9.1 Material

Item	Size	Qty.	Remarks
Kevlar Cable	3/8" dia	2	Marked A
Shackles	7/16" dia	2	

4.9.2 Winding Procedure

a. The spools containing the aft tether are to be placed at the aft tether winch locations.

b. Support one aft tether spool so that the spool is able to rotate freely.

c. Attach the free end of the spool to the winch and reel in all the cable except that length required to reach the balloon attach plate.

NOTE: Insure that the cable winds evenly on the winch drum layer by layer.

d. Connect the aft tether cable to the balloon attach plate as shown in Figure B.6 using a 7/16" shackle*, after passing cable through ground sheave that is attached to the aft tether deadman.

e. Repeat "b" through "d" for the other aft tether.

* "Lock wire" all shackle pins by manually tightening a Tyrap tie through shackle pin eye and around shackle.

5.0 ASSEMBLY CHECKOUT

A checkout of all cable attachments, winch tie downs and cable lay-outs will be made after the net system is completed. The attached check-out list will be used to perform the checkout (Table B-4).

6.0 SYSTEM CONFIGURATION

Figures B.8 through B.10 present details of the ladder system and test site layout configurations.

Figure B.8 shows two elevation views of the erected ladder.

Figures B.9 and B.10 give details of the test site layout and deadmen locations.

Table B-4 Checkout List

Flight No._____

Pre-flight Checkout ☐

Post Flight Checkout ☐

ITEM	CHECK FOR	COMPLETE	DATE	CHECKED BY
Rope Table (32 ea)	All weights securely fastened			
Net	Junctions tied (433 ea) Verticals secured to deadman (21 ea)* Verticals secured to catenary (21 ea)* Horizontals secured to end verticals (8 ea)*			
Catenary (2 ea)	Secured to balloon attach plate * No kinks, snags or abrasions			
Forward Tethers (2 ea)	Secured to winch Secured to balloon attach plate * No kinks, snags or abrasions			

Table B-4 Checkout List
(continued)

Flight No._____

Pre-flight Checkout ☐

Post Flight Checkout ☐

ITEM	CHECK FOR	COMPLETE	DATE	CHECKED BY
Side Catenary Tethers (2 ea)	Secured to balloon attach plate * Secured to line shortening device * Line shortening device secured to deadman * No kinks, snags or abrasions			
Net Stabilizing Tethers (4 ea)	Secured to net stabilizing winch Secured to top net horizontals or to mid net horizontals*			
Mooring Line (2 ea)	Secured to deadman * Secured to balloon attach plate * No kinks, snags or abrasions			

Table B-4 Checkout List
(concluded)

Flight No._____

Pre-flight Checkout ☐

Post Flight Checkout ☐

ITEM	CHECK FOR	COMPLETE	DATE	CHECKED BY
Aft Tethers (2 ea)	Secured to winch Secured to balloon attach plate *			

* All shackles should be checked for integrity of Tyrap "lock wire"

SYSTEM - ELEVATION VIEWS

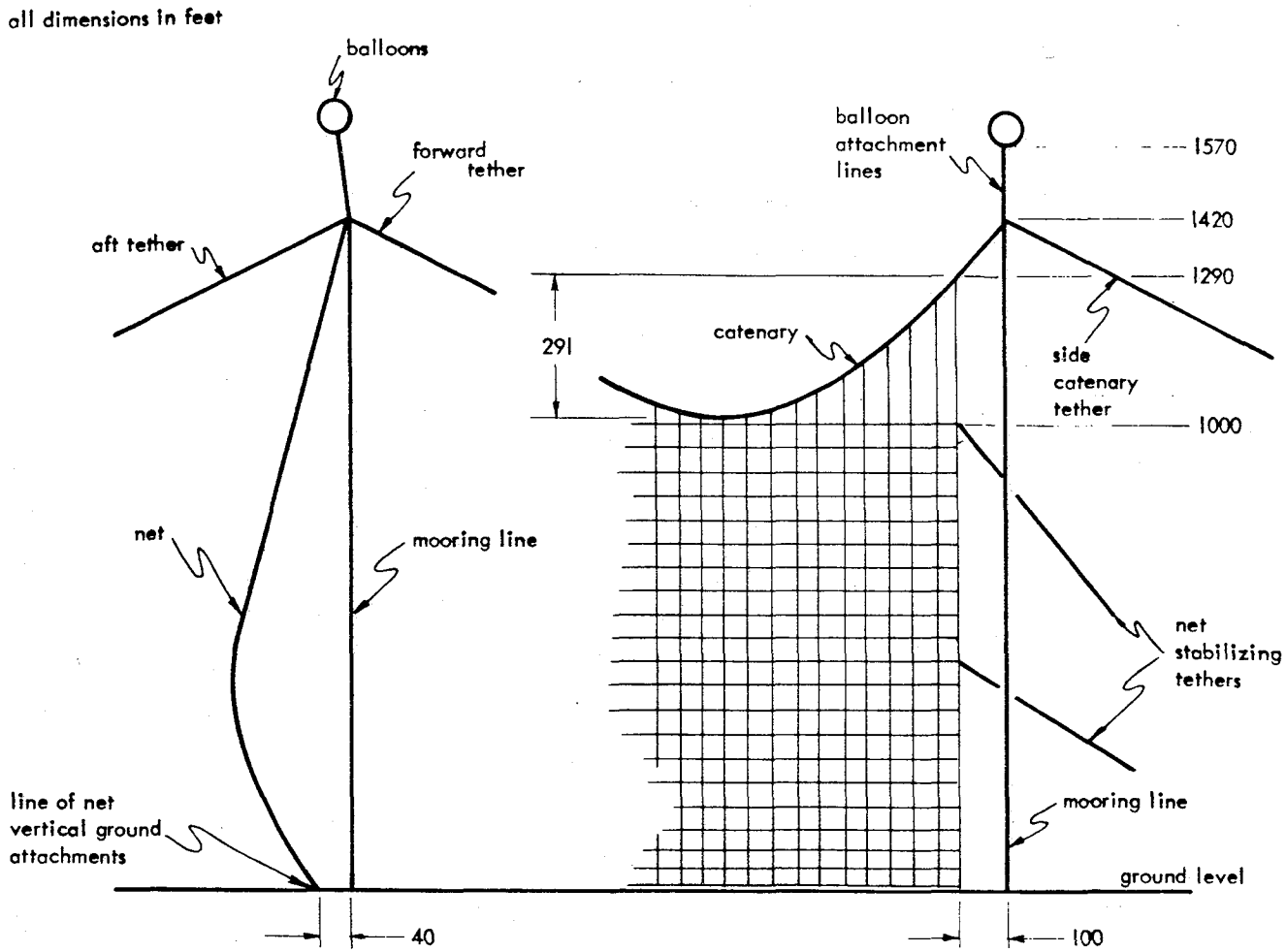

Figure B.8 Jacob's Ladder System - Elevation Views

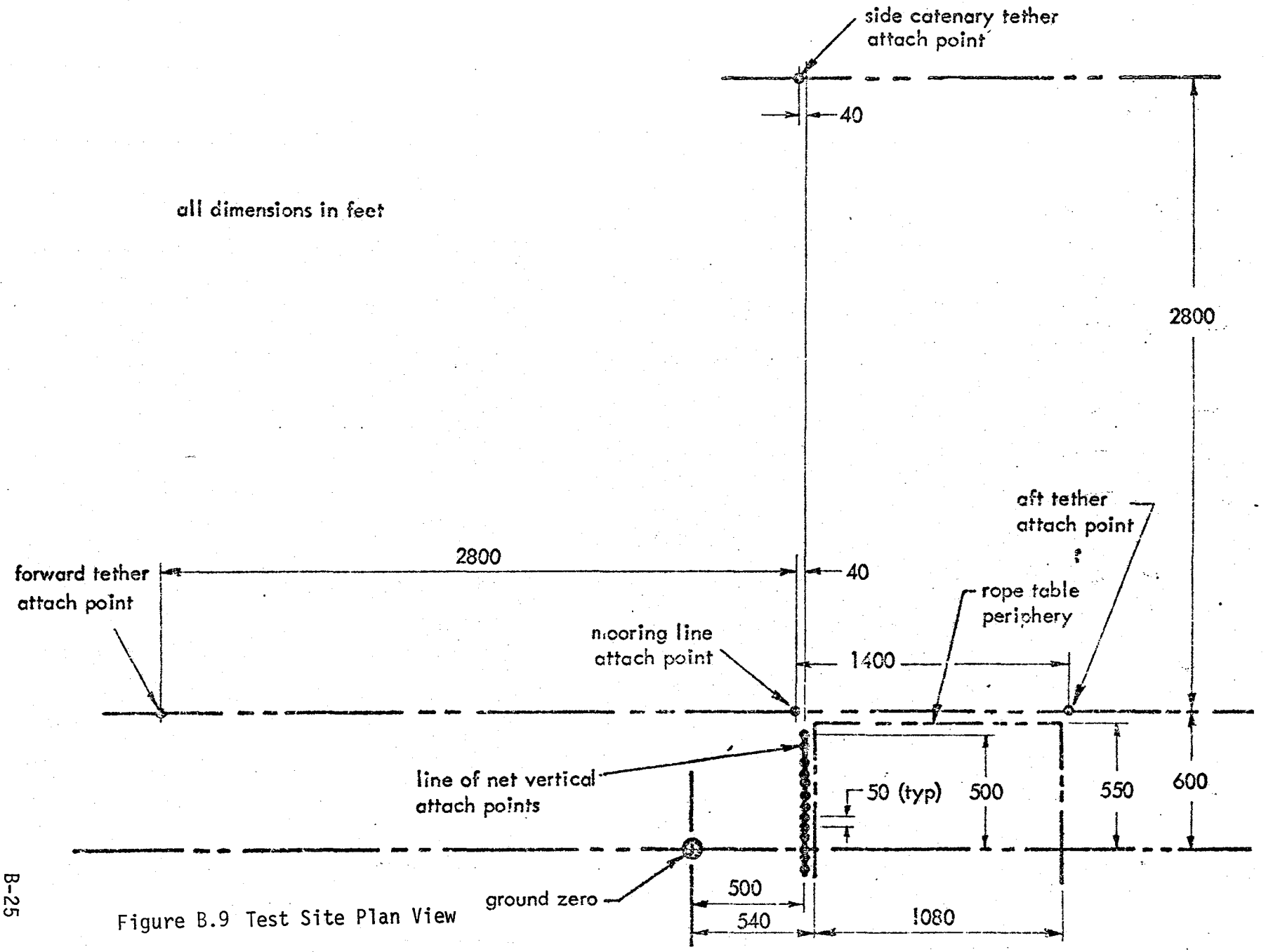

Figure B.9 Test Site Plan View

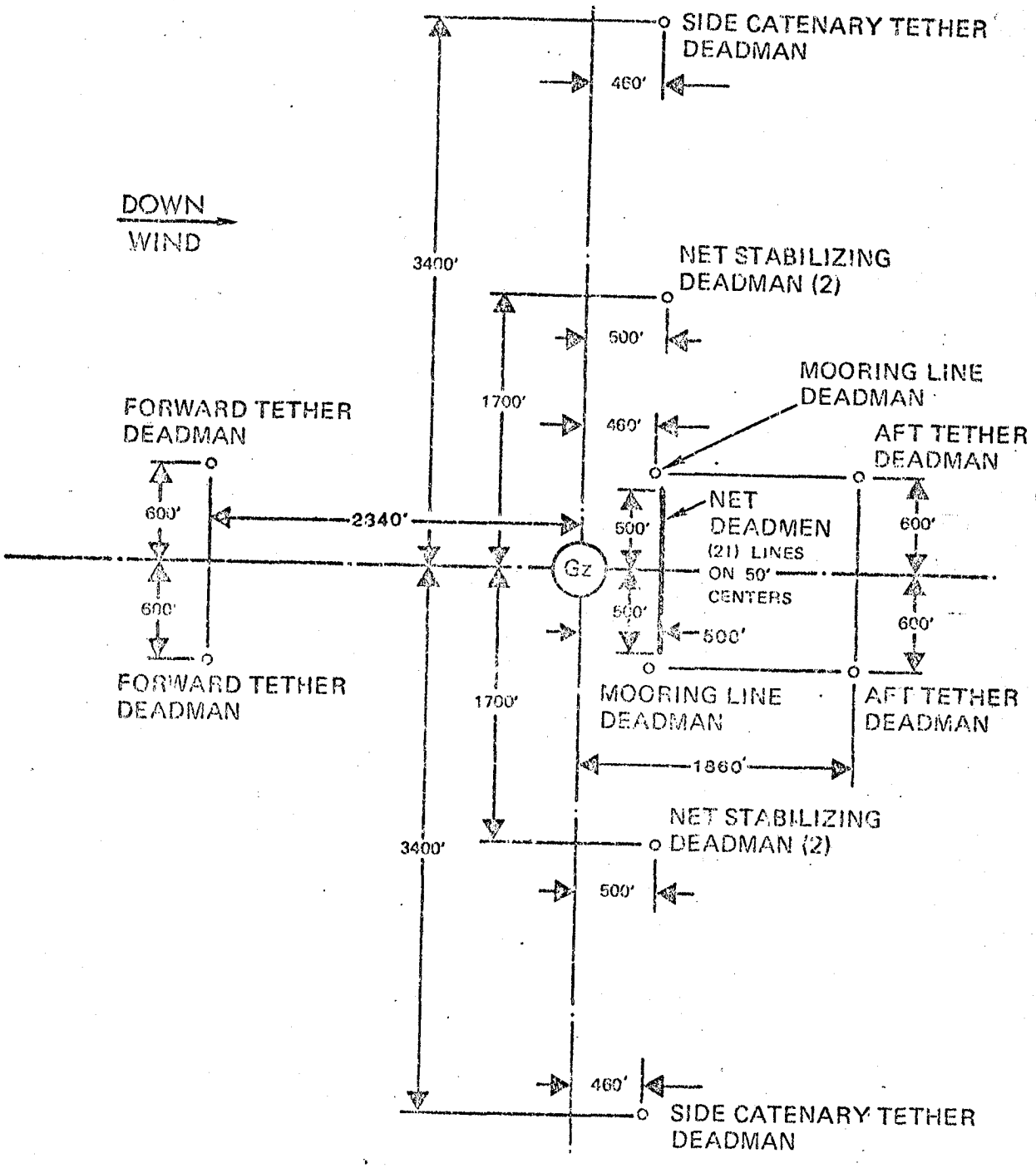

Figure B.10 Test Site Deadman Locations

APPENDIX C

OPERATIONAL PROCEDURES

FOR

JACOB'S LADDER

Prior to the conduct of the large-scale fire tests at Dugway Proving Ground, a document was published outlining the step-by-step procedures for operating the Jacob's Ladder system, including the safety and communication requirements, personnel responsibilities, and emergency operations. This appendix is essentially the same as the operational procedures document, JL79FT-101.000, developed and issued 28 August 1979 by TRW as part of the contractual effort for NASA.

In this appendix all units are given in U.S. Customary Units rather than SI units. The reason for this is that all design drawings, field layouts, load analyses, and fabrication and operational plans were developed in U.S. Costomary Units. This system of units avoided confusion and errors during material procurement and field installation, checkout, and operation since all balloon, cable, hardware, and manufacturer's specifications and available tools such as measuring tapes, hand tools, load cells, and dynamometers used U.S. Customary units exclusively.

1.0 SCOPE

This appendix delineates the procedures to be followed in storing, erecting, flying and lowering of the balloon supported net ladder to be used in support of the NASA carbon fiber tests at Dugway Proving Grounds.

2.0 PROCEDURE OVERVIEW

The general procedure that will be followed in using the net ladder in support of the NASA tests consists of 9 main steps. They are:

- Ladder storage position
- Viewgraph installation on ladder
- Balloon coupling to the ladder
- Erection of the ladder
- Flying the ladder
- Lowering the ladder
- Balloon decoupling from the ladder
- Viewgraph removal from the ladder
- Ladder storage position

3.0 SAFETY REQUIREMENTS

The following safety rules will be adhered to while in the test zone and performing the steps listed in 2.0 above.

- Safety hats will be worn at all times.
- Only authorized personnel will be allowed in the vicinity of the balloons, ladder and tethers.
- Each winch will be manned continuously during any operation involving the balloon being coupled or decoupled from the ladder, raising or lowering the ladder and flying the ladder.
- All winch operators will carry communications equipment during balloon operations and be on line with the launch director.
- Vehicles will not be driven over tether ropes unless the ropes are suitably protected.
- Personnel will be cleared from the vicinity of all ropes during the raising and lowering of the ladder.
- Personnel will wear protective gloves while handling ropes.

- An ambulance will stand by on site between the time the balloons are being coupled to the net and the time the balloons are decoupled from the ladder and are moored on their own safety line.
- There will be no smoking within a 60-foot radius of the balloon tether.
- Personnel will not step over cables which are under tension.

4.0 COMMUNICATION REQUIREMENTS

Communication between each winch operator, launch director, observers, and test director will be required during the coupling, raising, flying, lowering and decoupling operations. The distances between stations requiring communications are too great (minimum 1,000') for relying on voice or hand signals to coordinate action, so that radio communications are required.

Figure C.1 shows the stations at which radio communications are required. The winch operator, denoted by (+) will be in two-way communication with the launch director (0) at one frequency, while the observers (Δ) will be in two-way communication with the launch director at a second frequency.

5.0 PERSONNEL RESPONSIBILITIES AND COORDINATION

The organizational chart, Figure C.2, shows the manpower structure during the storing, erecting, flying and lowering of the net ladder. The responsibilities for each position during this time period are:

Test Director - Is responsible for overall test coordination. Makes decision to conduct, delay, or abort tests. Conducts countdown during test.

Launch Director - Is responsible for the raising, flying, lowering and stowage of the net ladder. Coordinates winch operator and observer operations during the times the ladder is coupled to the balloons.

Meteorology Coordinator - Is responsible for informing the test director and launch director on latest weather forecasts during all times that the balloons are coupled to the ladder.

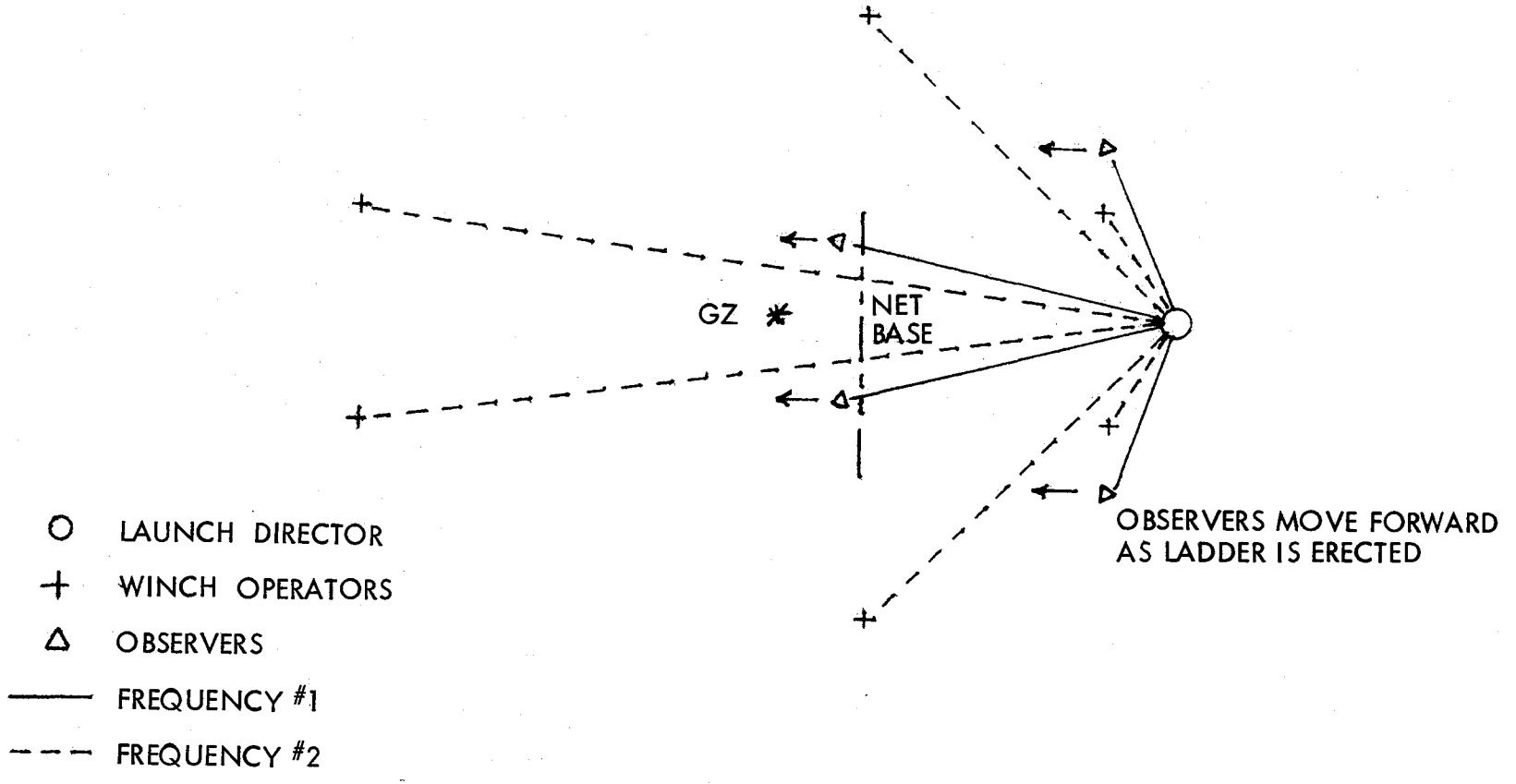

Figure C.1 Communication Requirements

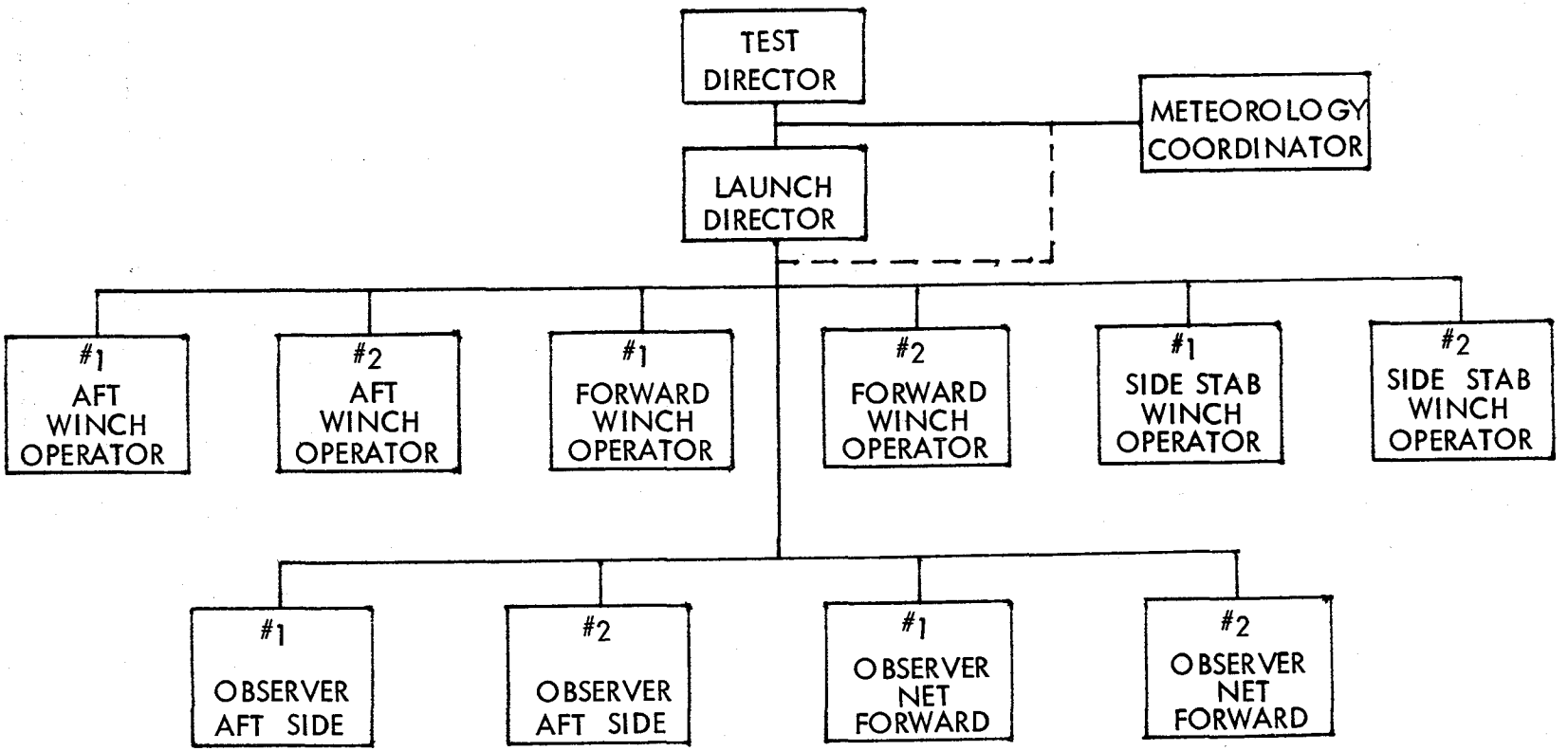

Figure C.2 Organizational Chart during Net Ladder Balloon Operations

Winch Operator - Is responsible for operating the assigned winch on the command of the launch director. Keeps launch director informed on winch and rope conditions.

Observer - Is responsible for keeping the launch director informed on net ladder and tether condition.

NOTE: During erecting and lowering of the ladder, one winch operator and one radio operator is required at each winch site (4 sites, 8 personnel).

6.0 NORMAL OPERATIONAL PROCEDURE

6.1 LADDER OPERATIONAL SPECIFICATIONS

The ladder will be coupled to the balloons and raised only when the following weather conditions exist and are forecasted during the total test period time:

wind velocity at altitudes up to 200 ft above the balloons

steady - less than 20 mph

gusty - less than 25 mph

6.2 PREFLIGHT CHECKOUT

A preflight and post flight checkout will be conducted prior to the coupling of the net ladder to the balloons and after decoupling the ladder from the balloons. This checkout will consist of

- checking all shackle-ring-plate connections
- checking all shackle-deadman connections
- checking all ties on the ladder
- checking all tether lines for kinks, snags, and abrasions.

The checklist shown in Appendix B, Table B-4, will be used and filled out for each preflight and post flight checkout and retained by the launch director.

6.3 VIEWGRAPH INSTALLATION

Viewgraphs will be installed on the ladder before the ladder is coupled to the balloon. A viewgraph will be installed at each intersection of a net vertical with a net horizontal. Each viewgraph will be attached to the

intersection as shown in Figure C.3 depending on whether the net vertical is an internal or external member. Tyrap fasteners will be used to fasten the viewgraphs to the net. The viewgraph will be placed on top of the net intersection with the sticky side of the bridal veil facing upward. The tyrap fasteners will then be placed through the holes in the viewgraph frame and connected around the vertical or horizontal net member and manually tightened. Each viewgraph will be labeled with the appropriate test number and net location information.

6.4 ERECTION OF LADDER

The ladder is ready for erection after the balloon tether lines have been transferred to the balloon attach plate and the viewgraphs installed. Upon a go-ahead signal from the test director, the launch director will direct the erection of the ladder. The procedure the launch director will follow is to

- Confirm that all preflight checkout procedures have been completed and system is in a go condition
- Request that observers take their positions
- Confirm that winch operators are ready
- Confirm that observers are placed and ready
- Request all personnel not involved in the erection of the ladder clear the area
- Confirm that the area is clear of non-essential personnel
- Confirm that all communications are operating satisfactorily
- Instruct aft winch operators to reel in on aft tether lines until safety lines holding the balloon tethered are slack
- Instruct aft winch operators to disconnect the safety lines from the balloon attach plate
- Confirm that aft safety lines have been disconnected
- Instruct aft winch operators to slowly reel out aft tether lines
- Instruct observers and aft winch operators to watch all tether lines and the ladder as the ladder raises for signs of snagging and/or kinking. Any abnormality will be reported immediately to the launch director
- Request the observers inform the launch director that the ladder is clear of the rope table
- Request the observers inform the launch director when one balloon is rising faster or moving farther forward than the other

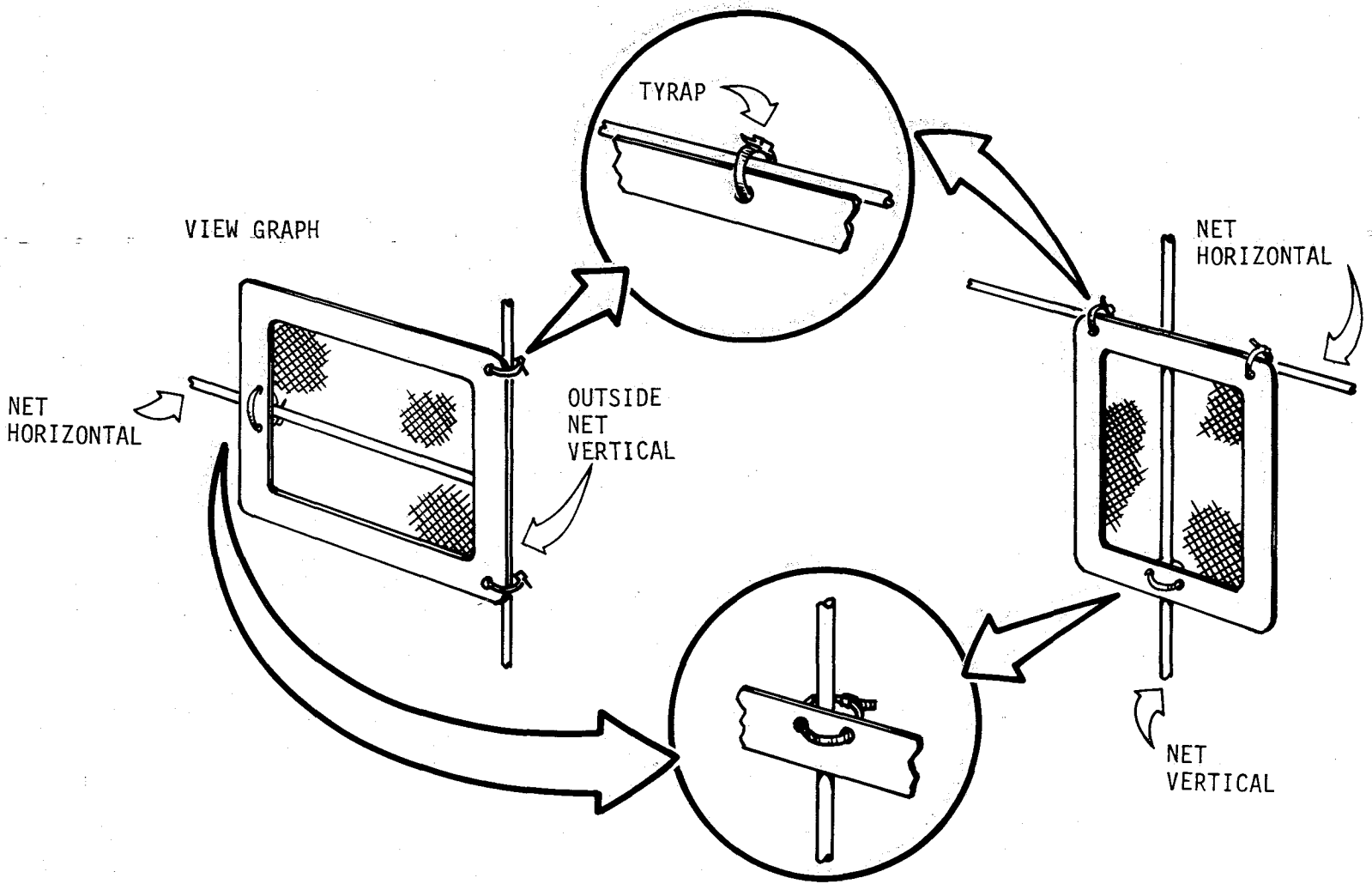

Figure C.3 Viewgraph Installation Details

- Instruct the forward winch operators to begin a slow reel in of forward tethers after the ladder clears the rope table
- Request the observers inform the launch director when the mooring lines are close to being vertical or the aft tether lines appear to be slackening
- Instruct the aft winch operators to stop reeling out of the aft tethers when the mooring line becomes vertical or when the aft tether lines start to slacken
- Instruct the forward winch operators to stop reeling in after some tension is noticed on the forward tether lines
- Instruct the side net stabilization winch operators to slowly reel in the side net stabilization tethers until some tension is noted
- Inform test director that the ladder is in position.

6.5 LOWERING OF LADDER

The ladder will be lowered following the completion of the test, when weather conditions are out of tolerance or if a malfunction of the ladder system occurs. The procedure the launch director will follow for lowering the ladder is to

- Confirm that winch operators are ready
- Confirm observers are ready
- Request that all personnel not involved with lowering of the ladder clear the area
- Confirm that the area is clear of non-essential personnel
- Instruct side net stabilizing winch operators to unreel side net stabilizing tethers to provide slack in these tethers
- Instruct forward winch operators to slowly unreel forward tethers
- Instruct aft winch operators to slowly reel in aft tethers
- Instruct forward winch operator to increase speed on forward winch to provide slack on forward tether cables
- Instruct observers to inform launch director if balloons are not descending or moving aft equally
- Instruct observers to inform the launch director when the ladder contacts the rope table
- Instruct observers to closely monitor the ladder deposition on the rope table. Observers are to inform the launch director of abnormalities
- Instruct aft winch operators to inform launch director when the balloon attach plate is within reach

- Instruct all winch operators to stop winches
- Instruct aft winch operators to attach safety cables to balloon attach plate
- Confirm safety cables are connected
- Instruct aft winch operators to unreel aft tether lines until the aft tether lines are slack
- Inform the test director that the ladder is secure and the balloons are ready for decoupling.

6.6 VIEWGRAPH REMOVAL

Personnel will be allowed to remove viewgraph records from the ladder after it is decoupled from the balloon. The procedure for removing the viewgraphs is as follows:

- Assemble the following materials
  - 9" x 11" acetate sheets ~900 ea
  - Viewgraph storage boxes 10 ea
- Cut the tyrap ties from each viewgraph and remove from the ladder
- Place a sheet of acetate on each side of the viewgraph completely covering the bridal veil
- Place the record in the viewgraph storage box after checking labeling to insure that it is correct

7.0 EMERGENCY OPERATIONAL PROCEDURES

The test will be aborted and the ladder will be lowered when the weather conditions exceed the specifications listed in paragraph 6.1 or in the event of a cable or equipment failure.

7.1 ADVERSE WEATHER CONDITIONS

Weather conditions which are out-of-tolerance with the specifications listed in paragraph 6.1 will be sufficient justification to initiate procedures to lower the ladder. Also, forecasts of weather out-of-tolerance conditions will justify lowering of the ladder in sufficient time to avoid operating in adverse weather. Lowering of the ladder will follow the procedure of paragraph 6.5.

7.2 CABLE OR EQUIPMENT FAILURE

Failure of certain cables during the flying of the ladder makes it imperative that the ladder be lowered and the balloons secured. These are:

- Catenary
- Aft Tethers
- Forward Tethers
- Side Catenary Tether
- Mooring Line
- Balloon Tether

Failure of a ladder line, a side stabilization tether, or a ladder intersection is not reason enough to abort the test, unless such failure induces such motion in the ladder that other cables will fail.

The procedure to be followed in lowering the ladder in the event of a failure of a tether depends upon which tether fails.

7.2.1 Aft Tether Failure

Failure of an aft tether means that the balloon attached to the failed tether cannot be lowered using the aft winch. To lower the ladder and balloons, it will be necessary to attach a vehicle to each mooring line and use the mooring lines to lower the ladder and balloons. The procedure is:

- Attach 18" sheaves to the mooring line deadman in the same manner the sheaves at the aft tether points are attached.
- Station a heavy vehicle downwind and within 5' of sheave at each mooring line deadman site. These vehicles will require a ring that will take a 7/16" shackle.
- Attach the mooring line pigtails through the sheaves to the attached rings on the truck.
- Move the trucks downwind slowly until the mooring line pigtails take up the balloon load and the mooring line attached to the deadman goes slack. Stop the trucks.
- Remove mooring line attachments from the deadmen.
- Slowly move the trucks downwind until the balloon attach plate is within reach.
- Maintain tension on forward tethers and remaining aft tether during this operation to keep mooring lines vertical.

- Attach safety lines between balloon attach plates and the mooring line deadman.
- Release tension on forward tethers and remaining aft tether.
- Release tension on mooring lines by moving trucks slowly upwind. Stop trucks when mooring lines become slack.
- Replace or repair faulty aft tether line.
- Increase tension on mooring lines by moving trucks slowly downwind until safety lines become slack. Stop the trucks.
- Uncouple the safety lines from the balloon attach plates.
- Slowly move trucks toward the mooring line deadmen.
- As the ladder raises, have crew insure that snags and tangles are removed from the ladder.
- Maintain slack on aft and forward tethers as the ladder raises.
- Stop the trucks when the mooring line attach loops can be coupled to the mooring line deadmen.
- Attach the mooring lines to the deadmen.
- Move the trucks toward the deadmen until the mooring line pigtail is slack.
- Remove the mooring line pigtail from the truck.
- Lower ladder in the normal way in accordance with paragraph 6.5.

7.2.2 Side Catenary Tether

A failure of a side catenary tether will allow the balloon to move towards the center of the net, and cause the catenary to form a deeper sag or more of a "U" shape. The procedure for lowering the ladder will be the same as that described in paragraph 6.5, except for the following changes and additions:

- Do not slacken the side stabilization tethers until the net is down.
- After the balloons are decoupled, reposition ladder verticals to their normal position.

7.2.3 Forward Tether

A failure of the forward tether will allow the balloon, and the upper corner of the ladder attached to that balloon, to move downwind. The procedure in lowering the ladder will be the same as that described in paragraph 6.5 except that immediately following the failure, the operator on the remaining forward tether will slack off his forward tether until the two balloons are at the same orientation.

8.0 SYSTEM CONFIGURATION

Figures C.4 and C.5 are perspectives of the ladder: Figure C.4 shows the ladder in an erected position, and Figure 5, when the ladder is in a nearly completed and completely lowered position with the net supported on the rope table.

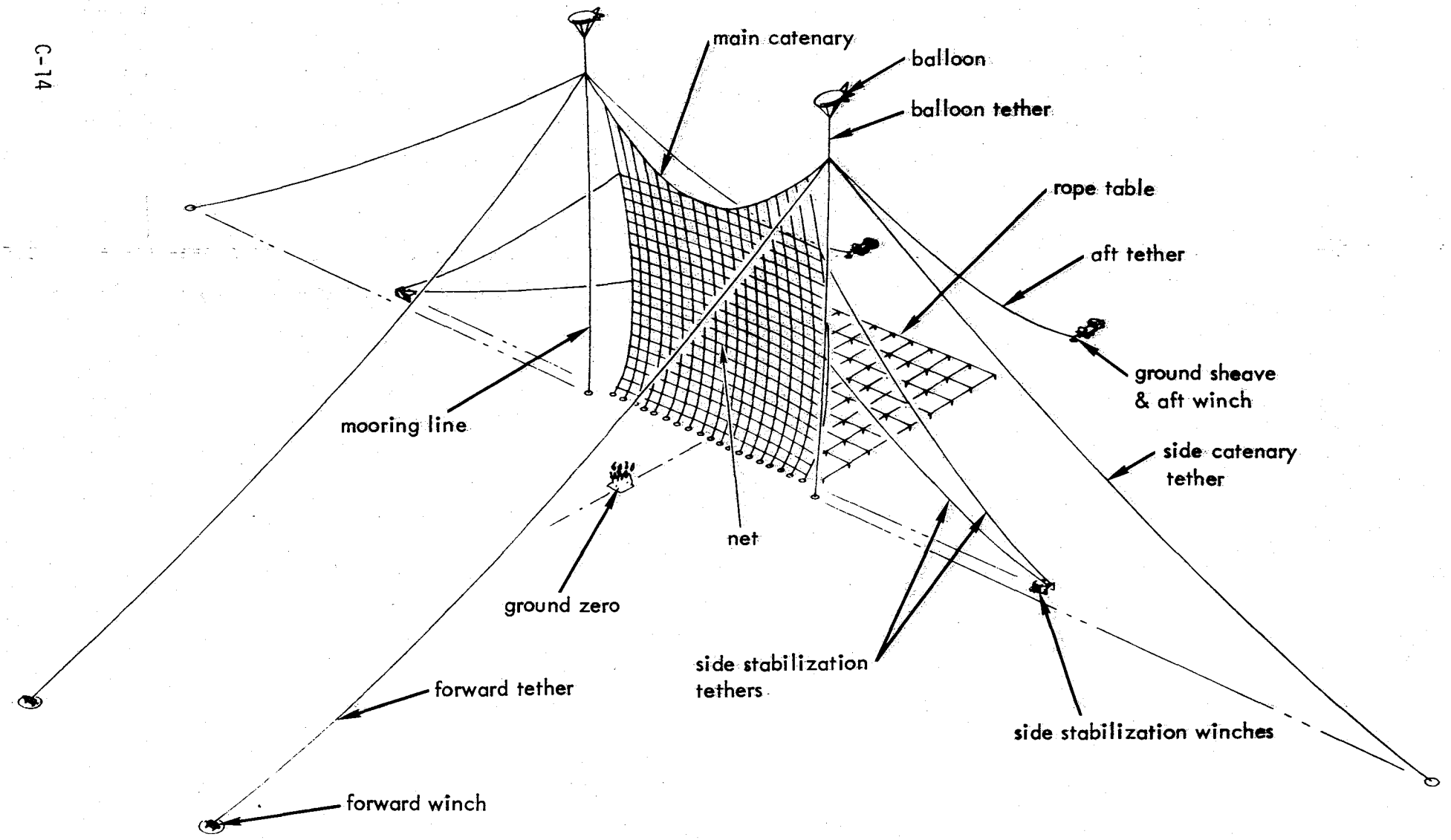

Figure C.4 Jacob's Ladder in Erected Position

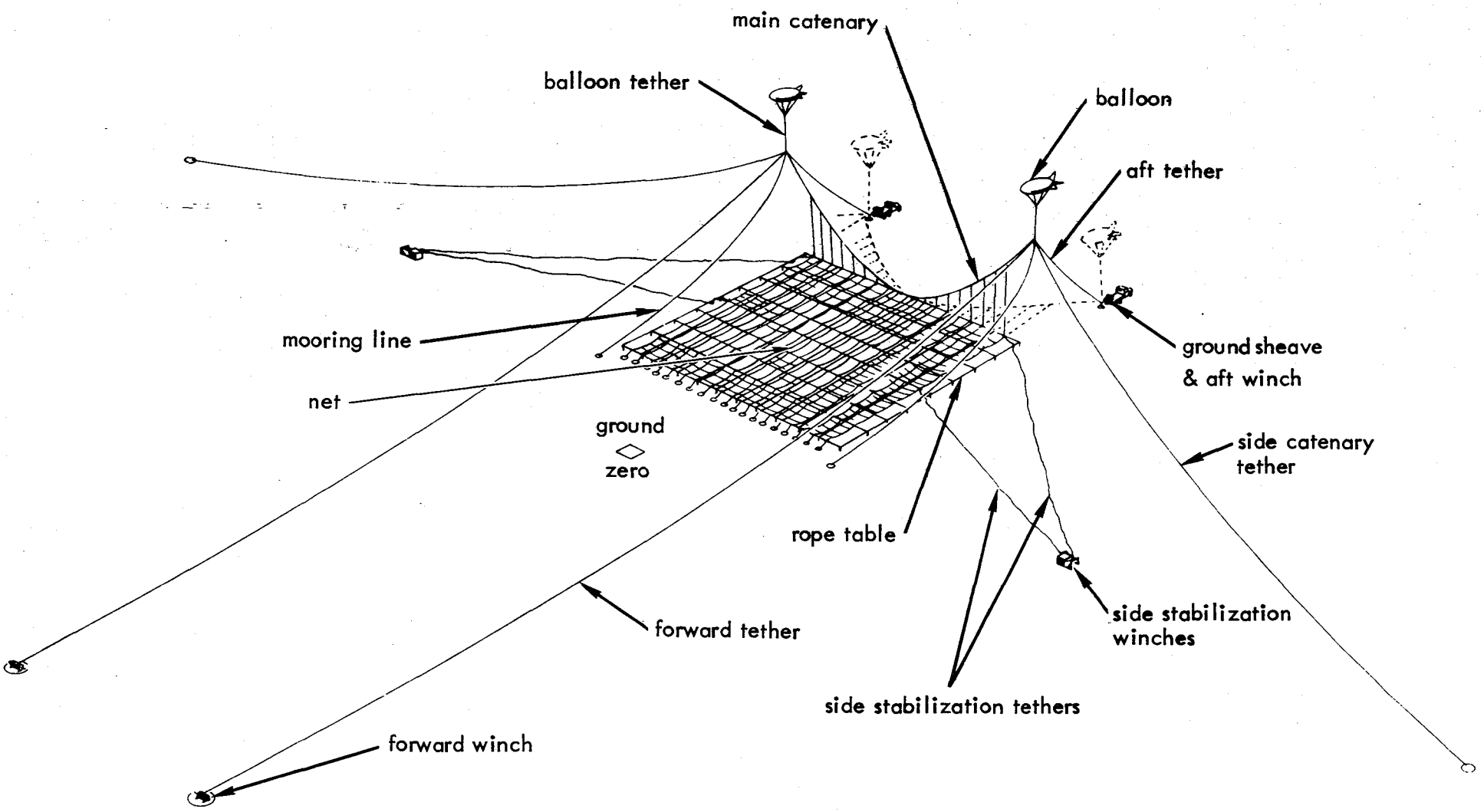

Figure C.5 Jacob's Ladder in Lowered Positions

REFERENCES

1. Whiting, John H.; Peterson, William A.; Sutton, Gary L. and Magann, Neil G: "Large-Scale Outdoor Fire-Released Carbon Fiber Tests," Dugway Proving Ground, FR-80-301, 1980.

2. Blumberg, Dorothy Rose: "Whose What?" Holt, Rinehart and Winston, 1969.

3. Lieberman, Paul; Chovit, Albert R.; Sussholz, Benjamin; and Korman, H. F.: "Data Reduction and Analysis of Graphite Fiber Release Experiments," NASA CR-159032, 1979.

4. Pride, Richard A.; McHatton, Austin D.; and Musselman, K. A.: "Electronic Equipment Vulnerability to Fire-Released Carbon Fibers," NASA TM-80219, 1980.

5. "Test Operations Procedure for NASA Fire-Released Carbon Fiber Test," U.S. Army Proving Ground, Dugway, Utah; STEDP-MT-DA-T; 26 October 1979.

6. Solomon, Luther L.; Trethewey, John D.; and Bushnell, Melvin J.: "Evaluation of Clouds of Airborne Fibers (AD 785675)," The Army Science Conference Proceedings, 18-21 June 1974, Vol. III, Principal Authors S through Z, United States Military Academy, West Point, NY.

1. Report No.	2. Government Accession No.	3. Recipient's Catalog No.
NASA CR-159215		

4. Title and Subtitle	5. Report Date
Carbon Fiber Plume Sampling for Large-Scale Fire Tests at Dugway Proving Ground	March 1980
	6. Performing Organization Code

7. Author(s)	8. Performing Organization Report No.
A. R. Chovit, P. Lieberman, D. E. Freeman, W.C. Beggs, and W. A. Millavec	NASA/TRW 80-03
	10. Work Unit No. 534-03-23-01

9. Performing Organization Name and Address	11. Contract or Grant No.
TRW DSSG 1 Space Park Redondo Beach, CA 90278	NAS 1-15465
	13. Type of Report and Period Covered
12. Sponsoring Agency Name and Address	Contractor Report
National Aeronautics and Space Administration Washington, DC 20546	14. Sponsoring Agency Code

15. Supplementary Notes

Langley technical monitor: Richard A. Pride
Langley program manager: Robert J. Huston

16. Abstract

As a participant in the NASA-sponsored large-scale fire tests at Dugway Proving Ground, TRW developed and fielded two types of carbon fiber sampling instruments, passive collectors made of sticky bridal veil mesh, and active instruments using a light-emitting diode (LED) source. These instruments measured the number or number-rate of carbon fibers released from carbon/graphite composite material when the material was burned in a 10.7 m (35-ft) dia JP-4 pool fire for approximately 20 minutes. The instruments were placed in an array suspended from a 305 m by 305 m (1000 ft by 1000 ft) "Jacob's Ladder" net held vertically aloft by balloons and oriented crosswind approximately 140 metres downwind of the pool fire. The "Jacob's Ladder" was also developed, fabricated, installed, and operated by TRW as part of this program. Three tests were conducted at Dugway Proving Ground during October and November 1979 during which released carbon fiber data was acquired. These data were reduced and analyzed to obtain the characteristics of the released fibers including their spatial and size distributions and estimates of the number and total mass of fibers released. The results of the data analyses showed that 2.5 to 3.5 x 10^8 single carbon fibers were released during the 20-minute burn of 30 to 50 kg mass of initial, unburned carbon fiber material. The mass released as single carbon fibers was estimated to be between 0.1 and 0.2% of the initial, unburned fiber mass. The average length of the released fibers was approximately 3.2 mm. Excellent correlation of the results was obtained among all three tests.

17. Key Words (Suggested by Author(s))	18. Distribution Statement
Carbon Fibers Fire Fiber Detection Balloon Lofted Systems	Unclassified - Unlimited Subject Category 24

19. Security Classif. (of this report)	20. Security Classif. (of this page)	21. No. of Pages	22. Price*
Unclassified	Unclassified	175	

For sale by the National Technical Information Service, Springfield, Virginia 22161